

Electronic Thesis and Dissertation Repository

8-14-2013 12:00 AM

Fluorescent Cytidine Analogues

Kirby J. Chicas

The University of Western Ontario

Supervisor

Robert. H.E. Hudson

The University of Western Ontario

Graduate Program in Chemistry

A thesis submitted in partial fulfillment of the requirements for the degree in Master of Science

© Kirby J. Chicas 2013

Follow this and additional works at: <https://ir.lib.uwo.ca/etd>

 Part of the [Organic Chemistry Commons](#), and the [Other Chemistry Commons](#)

Recommended Citation

Chicas, Kirby J., "Fluorescent Cytidine Analogues" (2013). *Electronic Thesis and Dissertation Repository*. 1576.

<https://ir.lib.uwo.ca/etd/1576>

This Dissertation/Thesis is brought to you for free and open access by Scholarship@Western. It has been accepted for inclusion in Electronic Thesis and Dissertation Repository by an authorized administrator of Scholarship@Western. For more information, please contact wlsadmin@uwo.ca.

FLUORESCENT CYTIDINE ANALOGUES

(Thesis format: Monograph)

by

Kirby Chicas

Graduate Program in Chemistry

A thesis submitted in partial fulfillment
of the requirements for the degree of
Master of Science

The School of Graduate and Postdoctoral Studies
The University of Western Ontario
London, Ontario, Canada

© Kirby Chicas 2013

Abstract

Two luminescent cytidine analogues have been synthesized in order to perform single nucleotide polymorphism (SNP) analysis by fluorescence spectroscopy. Herein is described the synthesis of 6-pyrenylpyrrolocytidine (PypdC), its photophysical characterization, and its subsequent incorporation into oligodeoxynucleotides (ODNs). The behavior of PypdC in ODNs is described as well as fluorescence intensity changes with respect to the match and mismatch cases. In order to obtain a greater understanding of pyrene's interaction with pyrrolocytidine, a congener, pyrenyl ethynyl cytidine (PyEtdC) was synthesized. The congener was photophysically studied and prepared for oligo synthesis

Keywords

Nucleic Acid, Cytidine, Fluorescent Nucleoside Analogue, Single Nucleotide Polymorphism, Pyrene

Table of Contents

Abstract	ii
Table of Contents	iii
List of Tables	v
List of Figures	vi
List of Schemes	viii
List of Abbreviations	ix
List of Appendices	xii
Chapter 1 - Introduction.....	1
1 Nucleic Acids	1
1.1 Modified Nucleic Acids	3
1.1.1 Therapeutics – Small Molecules and Antisense	3
1.1.2 Diagnostics – Fluorescent Nucleic Acids	5
1.2 Fluorescent C Analogues	7
1.3 Fluorescence Characterization of C Analogues	11
1.4 DNA Synthesis – Incorporation of Modified Nucleosides	14
1.5 Objective	16
1.6 References	17
Chapter 2 – Pyrenylpyrrolocytidine.....	19
2 Introduction: Precedence and Development	19
2.1 General pC Synthesis	23
2.2 Results and Discussion	25
2.2.1 Towards PypdC.....	25
2.2.2 Synthesis of PypdC.....	27
2.2.3 Incorporation into DNA.....	31

2.2.4	Nucleoside Fluorescence	34
2.2.5	Oligonucleotide Stability	38
2.2.6	ODN Fluorescence.....	40
2.3	Conclusions and Future work	41
2.4	Experimental.....	43
2.4.1	Synthetic Procedures and Characterization	43
2.5	References.....	48
Chapter 3 – Pyrenylethynylcytidine.....		50
3	Introduction – Serendipity.....	50
3.1	Results and Discussion	51
3.1.1	Towards PyEtdC in DNA	51
3.1.2	Synthesis of PyEtdC	54
3.1.3	PyEtdC Photophysics.....	55
3.1.4	Conclusions and Future Work	59
3.2	Experimental.....	60
3.2.1	Synthetic Procedures and Characterization	60
4	Summary and Conclusion	64
Appendix.....		66
Curriculum Vitae		98

List of Tables

Table 1.1 - $E_t(30)$ polarity values in comparison to dielectric constants.....	14
Table 2.1 – Coupling efficiency of the PypdC phosphoramidite.....	31
Table 2.2 – Photophysical summary of PypdC.....	36
Table 2.3 – Thermal denaturation of CFTR Mod and control.....	39
Table 2.4 – Photophysical summary of CFTR Mod.....	41
Table 3.1 – Comparison of PypdC & PyEtdC	58

List of Figures

Figure 1.1 – The central dogma of molecular biology.....	2
Figure 1.2 – Watson-Crick hybridization of the purines (G / A) and the pyrimidines (C / T) in antiparallel strands.	2
Figure 1.3 – Entecavir (left) & Clofarabine (right).....	3
Figure 1.4 – [bis- <i>o</i> -(aminoethoxy)phenyl]pyrrolocytosine, R = PNA.....	4
Figure 1.5 – Watson Crick bonding of G and C and common modification sites of C.	7
Figure 1.6 – Tricyclic cytosine (tC).....	8
Figure 1.7 - 5-(fur-2-yl)-2'-deoxycytidine (C ^{FU}).....	9
Figure 1.8 – Thiophen-2-yl pC	10
Figure 1.9 – DNA synthesis utilizing phosphoramidite chemistry.....	15
Figure 1.10 – Pyrene modified C analogues: PypdC (left), PyEtdC (right)	16
Figure 2.1 – The pyrimidines, the alkynypyrimidines, and their 5-endo dig products.....	19
Figure 2.2 – Aliphatic vs. aromatic substituted pCs and their quantum yields in ethanol.....	20
Figure 2.3 - MepdC & phenylpyrrolocytosine-N ¹ -methylene carboxylate	20
Figure 2.4 - ^{Mme} pdc & PhpdC	21
Figure 2.5 – Fluorescence intensity changes with respect to complementary base.....	22
Figure 2.6 – 6-(1-pyrenyl)pyrroloodeoxycytidine (PypdC).....	23
Figure 2.7 – The Watson Crick binding faces of a) furanouracil; b) pC; c) G	24
Figure 2.8 – Luminescence profile of PypdC at 2.2 μM in ethanol.....	35
Figure 2.9 - Luminescence profile of PypdC at 2.2 μM in water normalized to Figure 2.8...	35

Figure 2.10 – Normalized luminescence of PypdC vs. pyrene.....	37
Figure 2.11 – Normalized luminescence of PhpdC and PypdC.....	38
Figure 2.12 – Fluorescence intensity change of CFTR Mod against G,A,C,T and in the ss state at 1.5 μ M.....	40
Figure 2.13 – Possible PypdC excimer based probe.....	42
Figure 2.14 – HPLC trace of a failed synthesis towards a new PypdC probe	42
Figure 3.1 – PypdC (left) & PyEtdC (right)	51
Figure 3.2 – Luminescence profile of PyEtdC in ethanol at 1.1 μ M	55
Figure 3.3 - Luminescence profile of PyEtdC in water at 1.1 μ M normalized to the highest intensity peak in Figure 3.2.....	55
Figure 3.4 – PyEtdC luminescence profile vs. pyrene.....	56
Figure 3.5 – Normalized fluorescence of PhpdC and PyEtdC.....	57
Figure 3.6 – Brightness comparison; PypdC (2.2 μ M) vs. PyEtdC (1.1 μ M) in ethanol.....	59

List of Schemes

Scheme 2.1 – General methodologies of pC synthesis	25
Scheme 2.2 - First attempt towards PypdC.....	26
Scheme 2.3 – Second attempt towards PypdC.....	27
Scheme 2.4 – Synthesis of PypdC phosphoramidite	29
Scheme 2.5 – The trityl ON / OFF methods of ODN purification	33
Scheme 3.1 – Proposed route to PyEtdC phosphoramidite	52
Scheme 3.2 – Synthesis of PyEtdC phosphoramidite.....	53

List of Abbreviations

A – adenine

Ac – acetyl

AcOH – acetic acid

ALL – acute lymphoblastic leukemia

a.u. – arbitrary unit

BDF – base discriminating fluorophore

boPhpC – [bis-*o*-(aminoethoxy)phenyl]pyrrolocytosine

Bz - benzoyl

C – cytosine

CFTR – Cystic Fibrosis transmembrane conductance regulator

CPG – controlled-pore glass

DCM – dichloromethane

dmf – dimethylformamido

DMF - dimethylformamide

DMSO – dimethylsulfoxide

DMT – dimethoxytrityl

DMTCl – dimethoxytrityl chloride

DNA – deoxyribonucleic acid

EDTA - ethylenediaminetetraacetate acid disodium salt dihydrate

EI – electron impact

ESI – electrospray ionization

EtOH – ethanol

G – guanine

HBA – Hydrogen bond acceptor

HBD – Hydrogen bond donor

HD – Huntingtin's disease

HTT - Huntingtin

MepdC – methylpyrrolodeoxycytidine

mM – millimolar

^{Mme}pdC – methoxymethylpyrrolocytidine

mod - modification

mRNA – messenger ribonucleic acid

MS – mass spectrometer

NBS – N-bromosuccinimide

nm – nanometer

ODN – oligodeoxynucleotide

ORN - oligoribonucleotide

pC – pyrrolocytosine

PhpC - phenylpyrrolocytosine

PhpdC - phenylpyrrolodeoxycytidine

PNA – peptide nucleic acid

PyEtdC – pyrenylethynyldeoxycytidine

PypdC - pyrenylpyrrolodeoxycytidine

RNA – ribonucleic acid

R_t – retention time

S_n – excited state level n

SNP – single nucleotide polymorphism

T – thymine

tC – tricyclic cytosine

TLC – thin layer chromatography

T_m – thermal melt transition temperature

TMS – trimethylsilyl

U – uracil

UPLC – ultra performance liquid chromatography

UV – ultraviolet

Vis – visible

Å - Angstrom

ϵ – molar extinction coefficient

μ - micro

Φ – quantum yield

Φ_f – quantum yield of fluorescence

Φ_{IC} – quantum yield of internal conversion

Φ_{ISC} – quantum yield of intersystem crossing

$^{\circ}\text{C}$ – degrees celsius

λ – wavelength

λ_{ex} – excitation maximum

λ_{em} – emission maximum

List of Appendices

Appendix.....	66
---------------	----

Chapter 1 - Introduction

1 Nucleic Acids

The importance of nucleic acids is of no secret to us. We became privy when Watson and Crick famously declared, “[we] discovered the secret of life” on February 28, 1953 at The Eagle pub in Cambridge, England. Near to their place of work, the lunchtime destination would become the location in which we were gifted the structure of DNA. The elucidation however, was not solely the work of Watson and Crick. It was the culmination of work dating to the mid 19th century.

Swiss chemist Friedrich Miescher isolated a non protein substance from the nuclei of white blood cells in 1869. He would call this substance *nuclein*¹. He would isolate nuclein from white blood cells and later from salmon sperm. Despite his efforts he found the isolated substance tainted with protein. It wasn't until 1889 that Richard Altmann would isolate a protein free sample and call it *nucleic acid*¹.

Identification of the sugar, phosphate, and nitrogenous base components of nucleic acid came by way of Levene and Jacobs in 1909¹. Female scientist, Rosalind Franklin from Kings College at The University of London would later provide a key component to the mystery of nucleic acid. It was her work with Maurice Wilkins that would produce the X-ray diffraction pattern needed to lead Watson and Crick towards the double helix. The elucidation of DNA structure was recognized with a Nobel Prize in 1962 and shared amongst James Watson, Francis Crick, and Maurice Wilkins.

Francis Crick would frame the gravity of DNA through the central dogma of molecular biology. It explained in a simplified manner the flow of genetic information: transcription of DNA coding for phenotypic traits to messenger RNA (mRNA) in preparation for translation into proteins and expression of those coded phenotypes (**Figure 1.1**). By this model and still in line with our understanding, DNA is the blueprint defining our very traits.



Figure 1.1 – The central dogma of molecular biology

We are by now well aware of the antiparallel nature of the duplex (**Figure 1.2**). We know that nucleic acids are composed of a sugar phosphate backbone and of a nitrogenous base whose strand direction has been defined by its ribose moiety. Much progress has been made since 1953 and in 2003 the Human Genome Project was declared complete - the complete sequencing of the approximately 20 500 genes or three billion chemical units coding for the human being.

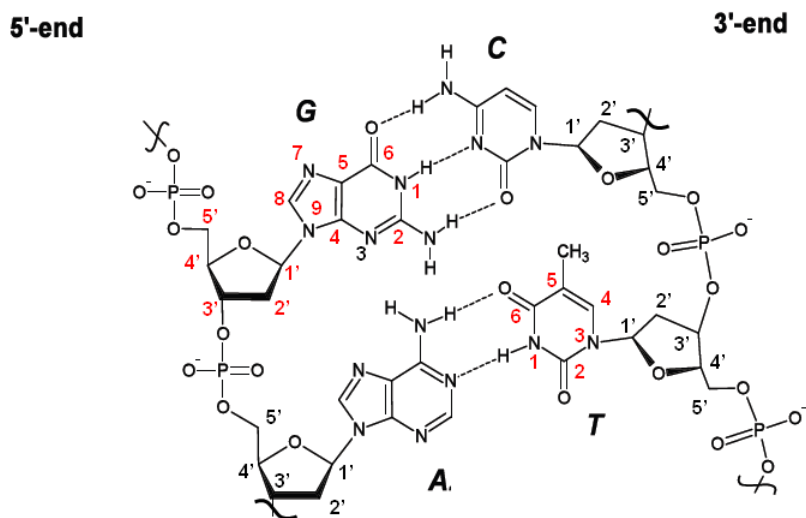


Figure 1.2 – Watson-Crick hybridization of the purines (G / A) and the pyrimidines (C / T) in antiparallel strands.

1.1 Modified Nucleic Acids

The important and complex nature of DNA and RNA has generated a great demand for tools and techniques to examine and treat nucleic acids. Modified nucleosides have been successfully applied to both therapeutic and diagnostic technologies in nucleic acids.

1.1.1 Therapeutics – Small Molecules and Antisense

Small molecule nucleosides have attracted attention due to their use in the treatment of cancer and viral diseases. These small molecules fall into one or both of the categories typically used to identify modified nucleosides: (1) ribose modified and / or (2) base modified nucleosides². Research has led to the development of Entecavir for the treatment of chronic hepatitis B virus infection and Clofarabine (**Figure 1.3**) for the treatment of refractory acute lymphoblastic leukemia (ALL) in children.

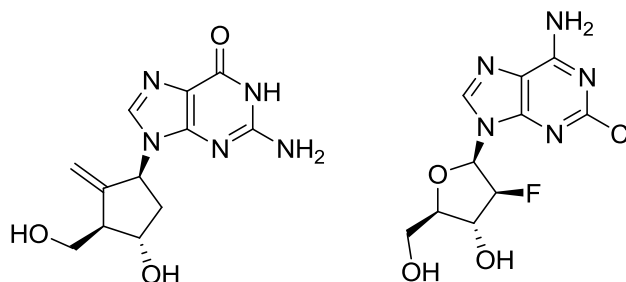


Figure 1.3 – Entecavir (left) & Clofarabine (right)

Modified nucleosides have also found success in the world of antisense therapy.

Antisense therapy is a treatment for genetic disorders or infections. If a gene is known to be responsible for a particular disease state, nucleic acids capable of binding the messenger RNA (mRNA) of the gene can be synthesized in order to prevent translation into protein. Binding of the exogenous strand with mRNA effectively silences the gene and turns it "off". The off response is brought about by the requirement for mRNA to be in single stranded state for translation³.

The synthetic nucleic acid is known as the "anti-sense" strand. The term antisense describes the nucleic acids' complementary base sequence to the gene's messenger RNA (mRNA) known as the "sense" sequence³.

Zamecnik and Stephenson⁴ first proposed the concept of antisense therapeutics in 1978. Their seminal publication detailed the synthesis of a 13 mer oligoribonucleotide (ORN), complementary to a sequence in the respiratory syncytial virus genome. They suggested that the ORN could be stabilized by terminal modifications and showed evidence of antiviral activity⁴.

The Hudson group has forayed into antisense technologies through the incorporation of boPhpC (**Figure 1.4**) into peptide nucleic acids with the help of the Corey Group at The University of Texas Dallas Southwestern Medical School. They planned to use PNA oligomers for the selective inhibition of mutant Huntington (HTT) protein. Mutant HTT is responsible for Huntington's disease (HD), an incurable neurological disorder. The Corey group reasoned that silencing of the mutant HTT protein would be a useful strategy for the treatment of Huntington's disease. When oligos containing the boPhpC moiety were added at 1 μ M concentration, selective HTT inhibition was observed⁵. The introduction of one or two boPhpC substitutions did not greatly increase the potency of inhibition of mutant HTT or improve selectivity. Alternatively, introduction of three or four boPhpC bases significantly eroded selectivity⁵. The boPhpC insert included the added advantage of intrinsic fluorescence which permitted visualization and localization of intracellular PNAs without the need for an appended fluorophore. Confocal fluorescence microscopy showed punctate intracellular PNA distribution consistent with known uptake / distribution mechanisms for PNA⁵.

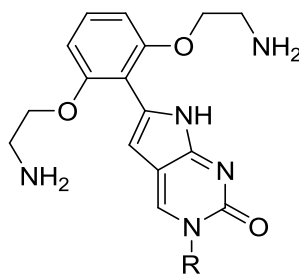


Figure 1.4 – [bis-*o*-(aminoethoxy)phenyl]pyrrolocytosine, R = PNA

1.1.2 Diagnostics – Fluorescent Nucleic Acids

Of the many diagnostic tools available for nucleic acids, none may find the ease of use and potential for broad application as readily as fluorescent nucleoside analogues.

Possessing no analytically exploitable fluorescence⁶, natural nucleosides are readily given fluorescence properties enabling them to be used for spectroscopic studies. The combination of hybridization specificity and fluorescence enables them to fulfill a number of requirements needed for an ideal detection device or assay.

Ideal detection devices and assays must offer great selectivity, excellent sensitivity, ease of use and low cost of production⁷. Nucleic acids have long been admired for their genetic coding properties but have recently emerged as important materials for molecular diagnostic technologies. Nucleic acids satisfy ideal detection device and assay requirements by a number of assets such as specific Watson-Crick base pairing, high stability (DNA), low cost of synthesis and excellent adaptability to modifications⁷.

Nucleic acids are often used in combination with fluorescence spectroscopy for a number of reasons: (1) a large selection of fluorophores for nucleic acid conjugation exists; (2) there are minimal health risks associated with fluorophore handling; (3) there is instrumentation capable of detection at ultralow concentrations; (4) portability of instrumentation for on-site detection; (5) the relatively long shelf life of fluorophores⁷.

Fluorescent nucleoside analogues have shown utility in a wide range of applications including but not limited to single nucleotide polymorphism (SNP) detection^{8a-e}, nucleic acid structure and function, and microenvironmental studies. Structure and function experiments have allowed for the resolution of hybridization events⁹, folding¹⁰, conformational change¹¹, and enzyme action¹². Microenvironmental probing studies with fluorescent nucleosides have shown nucleobase damage¹³, depurination/depyrimidation¹⁴, and base flipping¹⁰. To this day new uses for fluorescent nucleoside analogues continue to emerge broadening the utility of the technique and driving development in the field.

Numerous modifications have been explored to introduce favourable fluorescent properties to nucleic acids. Classical fluorophores such as fluorescein, rhodamine, and

their congeners such as the Alexa dyes have been appended to oligonucleotides by linkers to the sugar phosphate backbone or have been tethered to nucleobases. Modifications have also been conjugated to the base or utilize the base as the fluorophore itself. Due to the seemingly limitless possibilities for modification, numerous classifications have been assigned to the fluorescent nucleoside field. Tor has divided the field into five categories; (1) chromophoric base analogues; (2) pteridines; (3) expanded nucleobases; (4) extended nucleobases and (5) isomorphous bases¹⁵. Wilhelmson has segmented the field in terms of internal (base) and external (sugar or phosphate) modifications¹⁶. Further classifications have been offered by Asseline¹⁷ and terms such as base discriminating fluorophore (BDF) have been introduced by Saito¹⁸.

The Hudson group focuses upon modifications of *cytosine* for the fluorescent probing of nucleic acids. Typical modifications fall into two fields capable of *canonical* base pairing: base analogues possessing pendant fluorophores (extrinsic) and intrinsically fluorescent nucleoside analogues¹⁹. These terms are used frequently within the Hudson group to classify C modifications.

The pendant class often has an advantage in that higher overall brightness (defined as $\Phi \times \epsilon$) is obtained by the attachment of a well characterized fluorophore. The high brightness is due to the combination of efficient luminescence (high quantum yield, Φ) and large molar absorptivity coefficients (ϵ). Despite the usually favourable photophysical properties, this class suffers from a number of drawbacks. The use of a fluorophore covalently bound by a tether to a nucleobase can allow for the independent movement of the fluorophore making interpretation difficult. Furthermore, due to the distance of the fluorophore from the base-pairing moiety, fluorescence does not directly report on the bases' environment. Thus, observed fluorescence does not reflect hybridization at a specific base, protonation or other electronic changes at the site of interest¹⁹.

Intrinsically fluorescent base analogues are those in which fluorescence is observed from the nucleobase itself and not from an appended (extrinsic) moiety. Intrinsically fluorescent nucleosides are attractive as the base itself communicates

microenvironmental changes, thus enabling one to elucidate events occurring in close proximity to the nucleobase. Modest chemical modifications can also yield stunning photophysical properties allowing them to be competitive with traditional fluorescent probes. Historically, intrinsically fluorescent base analogues have been able to communicate hybridization change.

The Hudson group continues to work towards new fluorescent C analogues for applications in both antisense and diagnostic systems.

1.2 Fluorescent C Analogues

Described by Albrecht Kossel in 1903²⁰, the pyrimidine cytosine enjoys a three hydrogen bond Watson-Crick face for complementary pairing with guanine and shows good tolerance for chemical modifications (**Figure 1.5**).

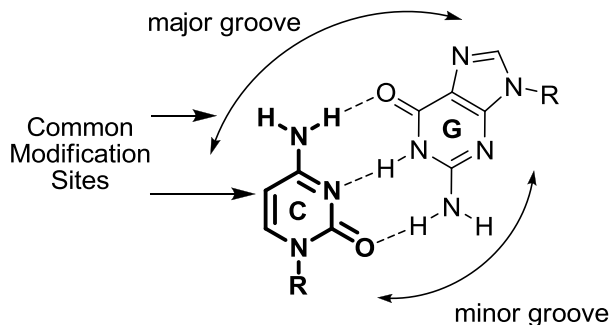


Figure 1.5 – Watson Crick bonding of G and C and common modification sites of C.

Cytosine is readily halogenated at the 5-position, providing a handle for well established carbon-carbon bond forming chemistry. Modification of the exocyclic amine also provides entry into fluorescent C analogues. Modifications of the C scaffold either by manipulation at the 5-position or of the amine generally produces a C analogue where additional substituent's or structure are found in the major groove (**Figure 1.5**). These

modifications tend to be nonperturbing in nucleic acids and in many cases increase duplex stability by favourable base stacking or additional hydrogen bond engagement of G. Modification at the 6-position is generally regarded to be detrimental due to the steric interaction of the sugar moiety in the anti-glycosidic conformer ²¹.

A wide variety of fluorescent C analogues have been developed over the years, each with their own unique characteristics and applications. The following is a brief window into the scope of fluorescent C analogues.

Tricyclic cytosine (tC, **Figure 1.6**) was first reported in 1995 for use in antisense systems.

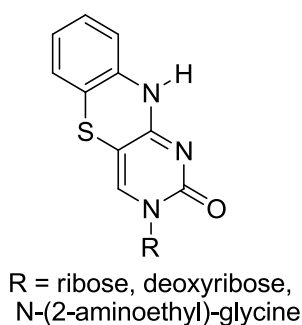


Figure 1.6 – Tricyclic cytosine (tC)

Studies on tC showed melt temperature increases with respect to 5-methylcytidine ²² and in 2001, spectrophotometric studies were undertaken ²³. Wilhelmsson showed that tC could be selectively excited over DNA ($\lambda_{\text{abs}} = 260 \text{ nm}$) at a wavelength of 375 nm with corresponding emission at 505 nm ²³. Wilhelmsson reported increased melt temperatures ²⁴ as was also reported by Matteucci in 1995. Quantum yield determinations by Albinsson *et al.* showed moderate quantum yield values for the free nucleoside ($\Phi = 0.13$) in water ²⁵. Incorporation of tC into ODNs produced slightly greater quantum yields than that of the free nucleoside. Values ranged from 0.17 – 0.24 in the ss form and 0.16 – 0.21 in the ds form. Very little change in quantum yield was observed with respect to flanking bases or incorporation into dsDNA making it a relatively insensitive analogue to microenvironment. Tricyclic cytosine has seen application in FRET ²⁶, in DNA ²⁷ and

RNA²⁸ polymerase experiments in their respective ribo and deoxy forms, and in DNA / protein interaction experiments²⁹.

The Tor group at UCSD investigated a number of conjugated five member ring systems based upon 2-phenylfuran. 2-phenylfuran is a fluorophore ($\lambda_{\text{ex}} = 280 \text{ nm}$; $\lambda_{\text{em.}} = 340 \text{ nm}$) with a desirably high molar extinction coefficient of $20\,000 \text{ M}^{-1}\text{cm}^{-1}$ and good quantum yield ($\Phi = 0.4$)³⁰. By the conjugation of a furan moiety to the six member aromatic system of cytosine (**Figure 1.6**), Tor hoped to emulate the favourable properties 2-phenylfuran. Following a previously reported synthesis³¹, Tor produced the furan labeled C analogue from 5-iodo-2-deoxyuridine.

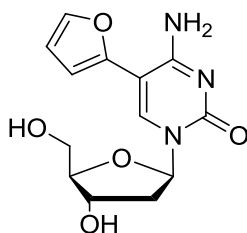


Figure 1.7 - 5-(fur-2-yl)-2'-deoxycytidine (C^{FU})

Unfortunately the quantum yield of the C^{FU} nucleoside proved to be less than ideal with a value of 0.02 in water. Although possessing a low efficiency, the C^{FU} base could still be selectively excited over DNA at $\sim 310 \text{ nm}$ with emission at $\sim 440 \text{ nm}$. The Tor group proceeded to investigate the fluorescent C analogue as a potential candidate for the detection of 8-oxoG. C^{FU} proved sensitive to 8-oxo-G and relatively insensitive to unmodified G³². Anticipating transverse mutation, fluorescence response with respect to T was also measured and determined to provide the greatest fluorescence intensity. Moreover, the emission wavelength was observed to change with complementary base. From these observations it was proposed that C^{FU} could facilitate rapid and non-destructive real time fluorescence based methods for the in vitro monitoring of oxidative stress³².

The Tor group has since sought ways to increase the efficiency of their C analogues. In looking to improve quantum yields of their furan- and thiophene-substituted pyrimidines,

the group turned their attention to the pC core which had been shown to possess favourable fluorescence characteristics in other systems.

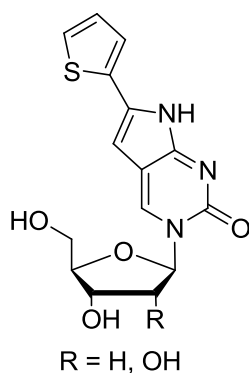


Figure 1.8 – Thiophen-2-yl pC

The group synthesized both the deoxy and ribose variants of the thiophen-2-yl pC base. Foregoing acylation of the exocyclic amino group (Discussed in Chapter 2, **Scheme 2.1**) it was observed that the intermediate nucleoside resisted annulation by copper and formation of the pyrrole ring. The intermediate nucleoside was screened against metal catalysts to induce cyclization. It was found that sodium tetrachloroaurate(III) dihydrate produced the desired cyclized product in low to moderate yield³³. Photophysical characterization of the deoxy and ribose thiophen-2-yl pC nucleosides yielded little to no difference in their photophysical properties. It was found that they underwent excitation at ~ 370 nm and emission at ~ 471 nm in water with an efficiency of ~ 0.42. A greater efficiency was observed in dioxane (~ 0.48)³³ with red shifted absorption and blue shifted emission corresponding to decreased Stokes shifts with respect to those in water. The extinction coefficients when taken into consideration with quantum yield led to brightness factors that were approximately 14 – 24 times brighter than those of the MepC or MepdC.

Characteristics of C analogues range from the insensitive (tC) to the sensitive and from the highly fluorescent to nominally fluorescent. Our work develops the scope of C analogues in the hopes of obtaining new favourable fluorescence properties or improved properties from those in literature. The archetypal structure we have studied is

phenylpyrrolocytosine developed from pyrrolocytosine and is further discussed in Chapter 2.

1.3 Fluorescence Characterization of C Analogues

Traditionally the Hudson group has obtained a particular set of values for photophysical characterization of C analogues. The values obtained allow for the comparison of fluorescent C analogues and the development or improvement of nucleic acid probes. Typically photophysical characterization includes: excitation and emission spectra in ethanol and water; fluorescence quantum yield determination in ethanol & water; molar absorptivity determinations in ethanol & water. In addition to the above mentioned values, the Hudson group has recently added the $E_t(30)$ method of polarity sensitivity measurement.

Excitation and emission spectra provide insight into the excitation and relaxation pathways used in the molecule of interest. The excitation spectra in conjunction with UV/Vis, details the excited states involved upon photon absorption. Peaks of defined structure or shoulders become clear indicators of excitement of ground state electrons into a multitude of S_n levels. Mirror image emission spectra detail a relaxation process which participates in the release of a photon from the excited S_n state. More often than not, a mirror image is not obtained as the rate of internal conversion tends to be much greater than the rate of fluorescence emission. This rate difference manifests itself as a radiationless relaxation from $S_n \rightarrow S_1$ followed by photon emission and relaxation from $S_1 \rightarrow S_0$ which we observe as a single fluorescence peak lacking significant structure. From the excitation and emission spectra we further derive Stokes shift thus determining the energy difference between the S_0 and S_1 states.

Fluorescence quantum yield (Φ_f) provides a measure of the fluorescence efficiency for a molecule. Φ_f is defined as the ratio of the numbers of photons emitted over the number of photons absorbed, it is a process that competes with internal conversion (IC); inter system crossing (ISC) and other functions of excited state decay. Excited state decay can be expressed as the sum of the possible pathways or, $1 = \Phi_f + \Phi_{IC} + \Phi_{ISC} + \Phi_n$. The higher the fluorescence quantum yield, the better the conversion of excited stated energy to

photonic emission. Vice versa, the lower the fluorescence quantum yield, the more the molecule dissipates energy by non fluorescent processes. Quantum yield (a measure of fluorescence efficiency) cannot be directly ported or compared to other molecules as it is a concentration independent value and provides little information on the luminosity of molecules at varied concentrations.

Molar absorptivity also known as the molar extinction coefficient (ϵ) is expressed by the Beer-Lambert law, $A = \epsilon l C$, where A = absorption; ϵ = molar extinction coefficient; l = path length; C = concentration. It relates the concentration of a molecule to its absorptivity making it a valuable measure for concentration determinations. More specifically, ϵ is a measure of the probability, favourability, or likelihood of a transition (absorption) at a particular wavelength. The product of epsilon taken in conjunction with fluorescence quantum yield ($\epsilon \times \Phi_f$) is a value deemed brightness. The value can be conceptualized as a measure of fluorescence efficiency per unit volume and allows for the direct comparison of two molecules that exhibit fluorescence.

Recently, the Hudson group has begun polarity sensitivity measurements in the hopes of probing duplexes and biological pockets. Microenvironmental understanding is key since intra and intermolecular forces are dependent on their immediate surroundings. In the past many methods of polarity measurement have been used. Unfortunately many of these studies utilize the dielectric constant - a bulk solvent property expressed in units of Debye (D). The value represents a molecule's ability to attenuate an electric field generated between electrodes relative to vacuum³⁴. It can be thought of as the ability of a group of molecules to respond to the applied field and reorganize to minimize the generated potential. A solvent such as water is highly capable of attenuating the generated field and would therefore have a high dielectric constant. Conversely, hydrocarbons have little or no ability to respond to an applied field and attain low dielectric constants. These bulk values do not represent the first or second solvation spheres surrounding a molecule and do not represent the environment within a small biological cavity³⁵. Microenvironmental analysis became plausible when spectroscopic studies were approached. Recently the $E_t(30)$ scale developed by Dimroth and Reichardt has gained popularity. An $E_T(30)$ value (kcal mol^{-1}) is determined by measuring a charge

transfer band of a pyridinium betaine dye in a solvent or mixture of solvents. It is thought that the $E_T(30)$ value then reflects the polarity of the immediate environment surrounding the dye as it is the first or second solvation spheres that cause changes in the measured transfer band.

The polarity sensitivity of a new molecule can be determined by plotting the stokes shift of the new molecule in varied mixtures of dioxane / water against the predetermined $E_t(30)$ value for the same mixture. It has been shown that the linear relation typically produced is of greater reliability than other spectroscopic methods and the dielectric methods for polarity determinations²³. The slope of the resultant line is termed the *polarity sensitivity* of the molecule. The greater the slope of the line, or the greater the change in stokes shift with respect to change in solvent composition, the greater the polarity sensitivity. **Table 1.1** contains $E_T(30)$ values for common solvents displaying the trend that as polarity increases the $E_t(30)$ value also increases³⁵.

Table 1.1 - $E_T(30)$ polarity values in comparison to dielectric constants.

Solvents	ϵ^a	$E_T(30)^b$
Hexane	1.889	31.0
1,4-dioxane	2.219	36.0
2-propanol	20.190	48.4
1-propanol	20.800	50.7
Ethanol	25.290	51.9
Methanol	33.520	55.4
Water	80.180	63.1

^ain units of Debye (D), ^b kcal mol⁻¹

1.4 DNA Synthesis – Incorporation of Modified Nucleosides

Currently the most popular method of oligodeoxynucleotide (ODN) synthesis is the phosphoramidite approach (**Figure 1.7**)³⁶. Construction of the DNA biopolymer follows sequential additions of the phosphoramidite monomer to an already coupled base tethered to a solid support by a succinyl arm.

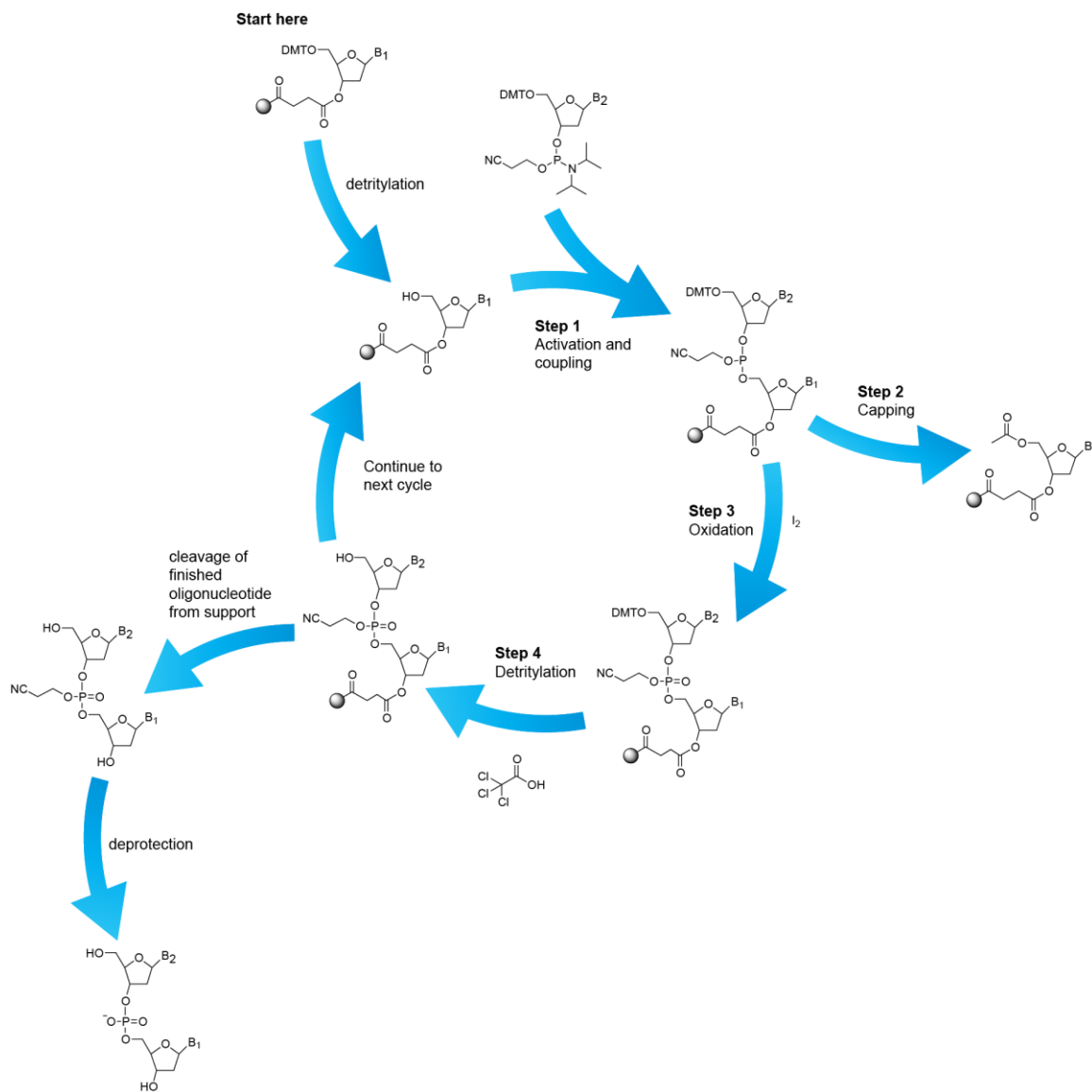


Figure 1.9 – DNA synthesis utilizing phosphoramidite chemistry.

The already present base undergoes detritylation by treatment with low percentage DCA or TCA in DCM - typically at percentages below 3% m/v. Detritylation affords the free 5' hydroxyl which reacts readily with a monomer activated by treatment with tetrazole. To ensure easy purification, a capping step is involved to minimize the ODN products by “sealing” unreacted 5' hydroxyls through acetylation. Capping is followed by oxidation of the phosphite triester to create the cyanoethyl protected phosphate. The cycle is repeated until the desired ODN length is met at which point cleavage from the solid

support and deprotection of the phosphate backbone is undertaken by heating in the presence of ammonia.

1.5 Objective

The aim of the research described herein is to expand the scope of fluorescent analogues by the synthesis and characterization of new fluorescent C analogues. We aim to test the limits of base discriminating fluorescence and duplex stability of these new analogues by the conjugation of the large and bright fluorophore pyrene.

We will describe the development of new synthetic procedures towards pyrene modified C analogues (**Figure 1.7**) as well as their incorporation or progress towards synthetic ODNs. We will then outline their ability to act as sensors in nucleic acids by the means of fluorescence spectroscopy.

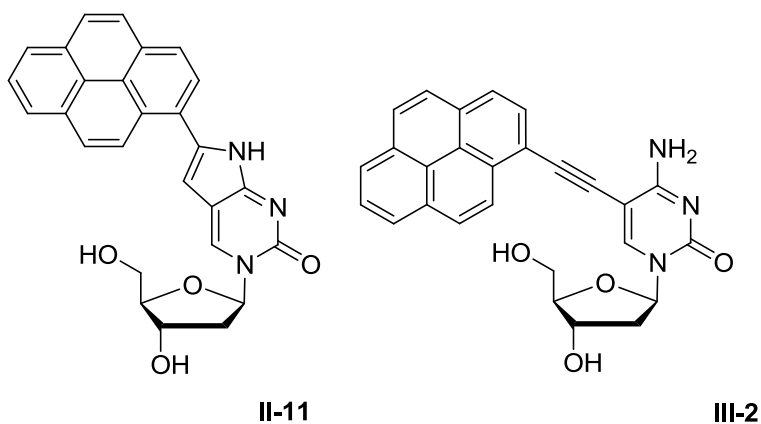


Figure 1.10 – Pyrene modified C analogues: PypdC (left), PyEtdC (right)

The analogues will have their photophysical properties studied in the nucleoside form. We will gain insight into the interactions of substituent and base electronics and the consequences that these electronics may have on the analogues as fluorescence sensors. Specifically we aim to answer whether or not the fluorescence we observe from these pyrene modified C analogues is attributed to the pyrene substituent, the base, or some combination of the two moieties.

1.6 References

1. Lagerkvist, U. *DNA Pioneers and their legacy*. Yale University Press, New Haven and London, **1998**.
2. Zhang, Li He; Xi, Zhen; Chattophaya, Jyoti; Medicinal Chemistry of Nucleic Acids. John Wiley & Sons, Hoboken, N.J., 2011.
3. Crooke, Stanley T.; *Antisense Drug Technology: Principles, Strategies, and Applications*. CRC Press, Boca Raton, **2008**.
4. Zamecnik, P.C.; Stephenson, T.C., *Proc. Natl. Acad. Sci. USA*. **1978**, 75(1), 280 – 284
5. Hua, J.X.; Dodd, David, D.W.; Hudson, R.H.E.; Corey, D.R., *Bioorg. Med. Chem. Lett.* **2009**, 19 (21), 6181 – 6184.
6. Vaya, I.; Gustavsson, T.; Mianny, F.A.; Douky, T.; Markovitsi, D.J.; *J. Am. Chem. Soc.* **2010**, 132 (34), 11834 – 11835.
7. Mayer, G.; *The Chemical Biology of Nucleic Acids*. **2010**.
8. a) Okamoto, A.; Tainaka, K.; Saito, I., *Chem. Lett.* **2003**, 32 (8), 684-685. b) Okamoto, A.; Tanaka, K.; Fukuta, T.; Saito, I., *J. Am. Chem. Soc.* **2003**, 125 (31), 9296-9297. c) Hattori, M.; Ohki, T.; Yanase, E.; Ueno, Y., *Bioorg. Med. Chem. Lett.* **2012**, 22 (1), 253-257. d) Yoshida, Y.; Niwa, K.; Yamada, K.; Tokeshi, M.; Baba, Y.; Saito, Y.; Okamoto, A.; Saito, I., *Chem. Lett.* **2010**, 39 (2), 116-117. e) Saito, Y.; Motegi, K.; Bag, S. S.; Saito, I., *Bioorg. Med. Chem.* **2008**, 16 (1), 107-113.
9. Tinsley, R. A.; Walter, N. G., *RNA-Publ. RNA Soc.* **2006**, 12 (3), 522-529.
10. Sinkeldam, R. W.; Greco, N. J.; Tor, Y., *Chem. Rev.* **2010**, 110 (5), 2579-2619.
11. Zhang, C. M.; Liu, C. P.; Christian, T.; Gamper, H.; Rozenski, J.; Pan, D. L.; Randolph, J. B.; Wickstrom, E.; Cooperman, B. S.; Hou, Y. M., *RNA-Publ. RNA Soc.* **2008**, 14 (10), 2245-2253.
12. Wahba, A. S.; Esmaili, A.; Damha, M. J.; Hudson, R. H. E., *Nucleic Acids Res.* **2010**, 38 (3), 1048-1056.
13. Greco, N. J.; Sinkeldam, R. W.; Tor, Y., *Org. Lett.* **2009**, 11 (5), 1115-1118.
14. Tanpure, A. A.; Srivatsan, S. G., *Chem.-Eur. J.* **2011**, 17 (45), 12820-12827.
15. Greco, N.J.; Tor, Y., *Tetrahedron* **2007**, 63 (17), 3515 – 3527.
16. Wilhelmsson, L.M., *Q. Rev. Biophys.* **2010**, 43 (2), 159 – 183.
17. Asseline, U., *Curr. Org. Chem.* **2006**, 10 (4), 491 – 518.
18. Okamoto, A; Saito, Y; Saito, I., *J. Photochem. Photobiol. C-photochem. Rev.* **2005**, 6 (2-3), 108 – 122
19. Dodd, D.W.; Hudson, R.H.E., *Mini-Rev. Org. Chem.* **2009**, 6 (4), 378 – 391.
20. Kossel, A.S.; *Physiol. Chem.* **1903**, 38, 49.

21. Schweize, M.P.; Kreishma, G.P., *J. Magn. Reson.* **1973**, *9* (2), 334 – 337.
22. Lin, K. Y.; Jones, R. J.; Matteucci, M., *J. Am. Chem. Soc.* **1995**, *117* (13), 3873-3874.
23. Wilhelmsson, L. M.; Holmen, A.; Lincoln, P.; Nielson, P. E.; Norden, B., *J. Am. Chem. Soc.* **2001**, *123* (10), 2434-2435.
24. Engman, K. C.; Sandin, P.; Osborne, S.; Brown, T.; Billeter, M.; Lincoln, P.; Norden, B.; Albinsson, B.; Wilhelmsson, L. M., *Nucleic Acids Res.* **2004**, *32* (17), 5087-5095.
25. Tahmassebi, D. C.; Millar, D. P., *Biochem. Biophys. Res. Commun.* **2009**, *380* (2), 277-280.
26. Stengel, G.; Gill, J. P.; Sandin, P.; Wilhelmsson, L. M.; Albinsson, B.; Norden, B.; Millar, D., *Biochemistry* **2007**, *46* (43), 12289-12297.
27. Stengel, G.; Urban, M.; Purse, B. W.; Kuchta, R. D., *Anal. Chem.* **2010**, *82* (3), 1082-1089.
28. Stengel, G.; Purse, B. W.; Wilhelmsson, L. M.; Urban, M.; Kuchta, R. D., *Biochemistry* **2009**, *48* (31), 7547-7555.
29. Greco, N. J.; Tor, Y., *Tetrahedron* **2007**, *63* (17), 3515-3527.
30. Wigerinck, P.; Pannecouque, C.; Snoeck, R.; Claes, P.; Declercq, E.; Herdewijn, P., *J. Med. Chem.* **1991**, *34* (8), 2383-2389.
31. Greco, N. J.; Sinkeldam, R. W.; Tor, Y., *Org. Lett.* **2009**, *11* (5), 1115-1118.
32. Noe, M. S.; Rios, A. C.; Tor, Y., *Org. Lett.* **2012**, *14* (12), 3150-3153.
33. Sinkeldam, R.W.; Yitzhak, T., *Org. Biomol.Chem.* **2007**, *5*, 2523 – 2528.
34. Kosower, E.M., *An Introduction to Physical Organic Chemistry*. JohnWiley & Sons, Inc., New York, **1968**, 259 – 264.
35. <http://www.atdbio.com/content/17/Solid-phase-oligonucleotide-synthesis>
accessed August 20, 2013

Chapter 2 – Pyrenylpyrrolocytidine

2 Introduction: Precedence and Development

Initially, with the intent of synthesizing 5-alkynylpyrimidines to determine their effect on the biophysical properties of PNA oligomers¹, Hudson and coworkers “rediscovered” the cyclization of *N*⁴-acyl-protected cytosine to pyrrolocytosine - an observation first made by Ohtsuka that had gone largely underappreciated². During these studies, conditions were defined for the synthesis of the simple cross-coupled products versus the annulated furanouracil and pyrrolocytosine (**Figure 2.1**). It was found that the structurally simple 5-alkynylpyrimidine derivatives were luminescent³; however, the similarly substituted pCs were determined to be better fluorophores⁴.

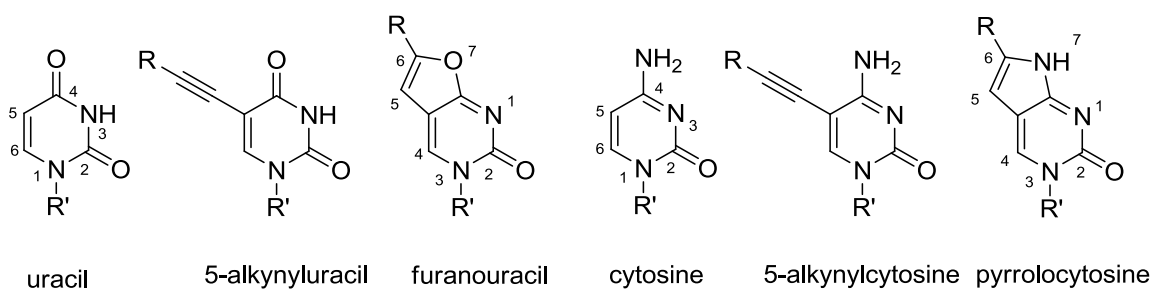


Figure 2.1 – The pyrimidines, the alkynypyrimidines, and their 5-endo dig products

Pyrrolocytosines possessing aromatic substitutions were discovered to be remarkably good fluorophores; better than those with aliphatic substitution (**Figure 2.2**). The pCs shown in **Figure 2.2** are blue fluorophores ($\lambda_{em} \sim 450$ nm) except for the *para*-(*N,N*-dimethylamino)phenyl which is bathochromically shifted ($\lambda_{em} \sim 500$ nm) and the *para*-nitrophenyl which displays weak orange fluorescence ($\lambda_{em} \sim 575$ nm). Interestingly the *p*-nitrophenyl exhibits an absorbance band that overlaps the emission of 6-phenylpyrrolocytosine (PhpC). Good luminescence is maintained in water as PhpC displays a $\Phi \sim 0.35$, approximately 10-fold greater than that of the well established MepdC (*vide infra*) analogue (**Figure 2.3**).

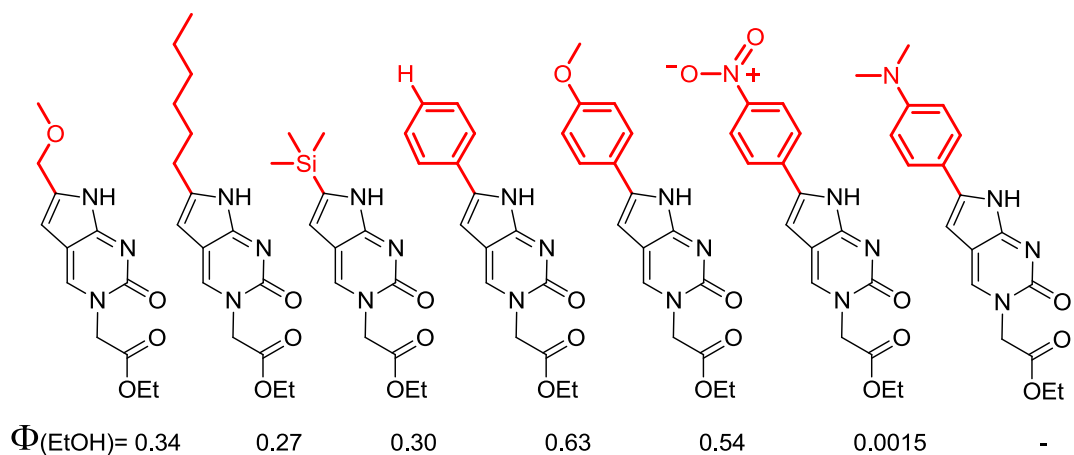


Figure 2.2 – Aliphatic vs. aromatic substituted pCs and their quantum yields in ethanol

6-Methylpyrrolo-dC (MepdC), a fluorescent C analogue dating back to the late 1980s² was a relatively unexploited modification until the turn of the century. In the early 2000s, methylpyrrolo-dC experienced a surge⁵ in use and has since become one of the more popular fluorescent C analogues. The popularity is likely due in part to its commercial availability⁶. Methylpyrrolo-dC has been shown to act similarly to C in terms of hybridization selectivity and stability⁷. MepdC has been used for the characterization of the transcription bubble of T7 RNA polymerase⁵, the kinetics of DNA repair by a human alkyl transferase⁸, and in investigations of the HIV-1-polypurine tract⁹. With methylpyrrolo-dC proving its utility in a number of experiments with considerably lesser fluorescence than PhpC, it is not surprising that PhpC garnered much excitement within the Hudson group

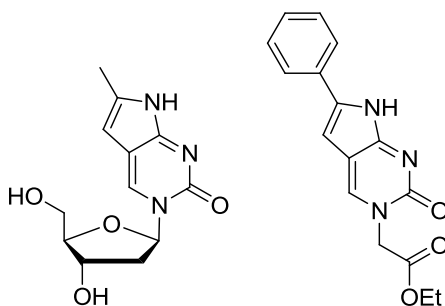


Figure 2.3 - MepdC & phenylpyrrolocytosine-N¹-methylene carboxylate

Hudson continued his investigation by converting the PhpC acetate to the Fmoc PNA monomer followed by incorporation into PNA and DNA duplexes. It was found that the PhpC containing PNA bound complementary DNA with stability on par to the corresponding unmodified PNA. The PNA oligomers also displayed excellent sequence discrimination for a complementary G versus mismatch that rival or best C⁴.

The first pC studies in DNA carried out by Hudson included the synthesis and incorporation of 6-methoxymethyl pyrrolodeoxycytidine (^{Mme}pdC) into ODNs for the purpose of selective fluorimetric detection of guanosine-containing sequences. Prior to the synthesis of the ^{Mme}pdC analogue, it had been well known from PNA systems that aromatic substitutions provided the most dramatic fluorescence response and that interesting characteristics would be observed from a phenylpyrrolodeoxycytidine (PhpdC) (**Figure 2.4**). The analogue was synthesized by the deoxyuridine route (*vide infra*). It was found that the PhpdC phosphoramidite could be synthesized in three steps with good overall yield¹⁰.

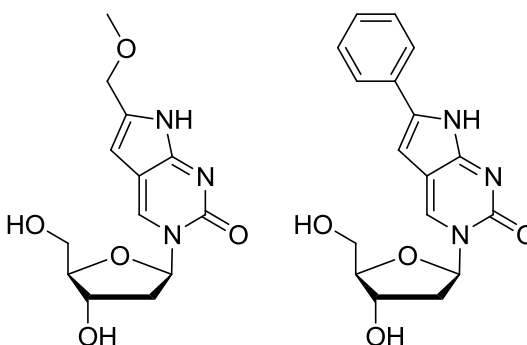


Figure 2.4 - ^{Mme}pdC & PhpdC

Thermal denaturation experiments of a centrally located PhpdC yielded a moderate increase in duplex stability (+3.3 °C)¹¹ relative to dC while maintaining excellent mismatch discrimination that was equal to or better than that of MepdC. Fluorescence emission from the PhpdC ODN was 18 times greater than that of MepdC¹¹. Additional fluorescence studies showed the ability of PhpdC to communicate the identity of the complementary base by fluorescence intensity change (**Figure 2.5**).

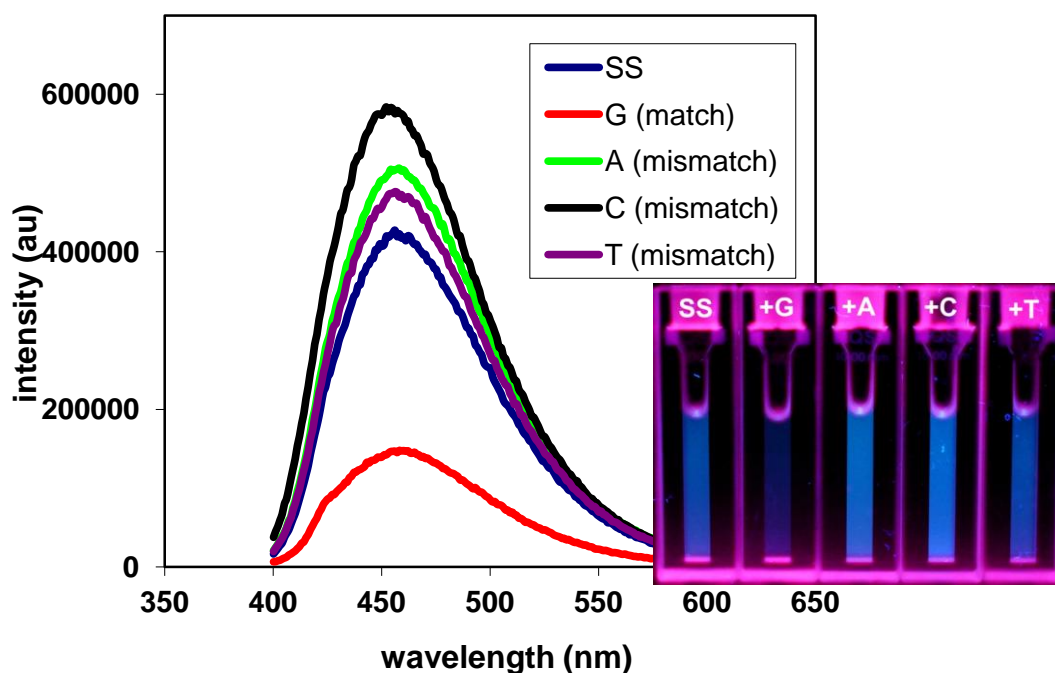


Figure 2.5 – Fluorescence intensity changes with respect to complementary base

It was proposed that modification of pyrrolocytosine with the large polycyclic aromatic hydrocarbon, pyrene, would yield interesting fluorescence properties as it is a well known fluorophore with a desirably high quantum yield (0.65) in ethanol. It was also thought that the substitution would yield insight into a number of questions important to pC understanding. We aimed to explore: (1) does conjugating highly fluorescent moieties to pC overwhelm fluorescence identification of the complementary base? (2) How large can a substitution become before it compromises duplex stability?

In regard to question (1), 6-(1-pyrenyl)pyrrolo deoxycytidine (PypdC) was suggested to behave in one of two ways. (A) It would act like PhpC as a sensitive reporter group in nucleic acid studies, or (B) the pyrene substituent would overwhelm any fluorophore-like contribution from the nucleobase. If (B) were to be true it was imagined that the hybridization dependent fluorescence would be lost.

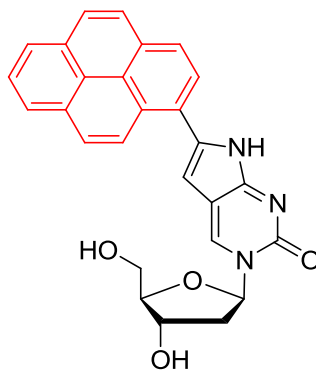


Figure 2.6 – 6-(1-pyrenyl)pyrrolo-deoxycytidine (PypdC)

In regard to question (2), duplex stability was expected to change in one of two ways: either the duplex stability would increase through greater base stacking interactions or the duplex stability would decrease due to the sheer size of the modified base. In a wild type vs. mutant case as in boPhpC (Chapter 1), these stability changes could possibly manifest themselves as such. In the case of a net stabilization for the match and mismatch cases, little to no selectivity would be observed. However if fluorescence changes were observed then a fluorimetric SNP probe would be possible. A reduction in duplex stability would either increase match strand selectivity or in the case of severe destabilization impair the target as a fluorimetric probe for G containing sequences and SNP associated disorders. In the case of increased selectivity, an antisense ODN could be developed.

2.1 General pC Synthesis

Synthetic routes towards the pC nucleoside typically follow one of two methodologies. The general features of pC synthesis are illustrated in **Scheme 2.1**. The chemistry utilized depends on the substitution desired at the 6 position of the pyrrole and the nucleic acid required. For peptide nucleic acid (PNA), the most convenient starting point is the cytosine or uracil nucleobase. For DNA / RNA structures, the deoxy- or ribonucleosides are most commonly used.

The substrates are prepared for derivatization by halogenation at the C5 position, most often iodination, in preparation for Sonogashira cross coupling chemistry. The desired,

fused bicyclic structure is achieved by the intramolecular cyclization (5-endo dig annulation) of the 5-alkynyl pyrimidine. The annulation reaction (**Scheme 2.1**, Approach 1) usually occurs under mild conditions for the uracil derivative, although there is some substrate dependence. For instance, electron rich alkynes cyclize more rapidly than those that are electron deficient. The cyclization reaction is metal ^{12a-f}, base ^{13a-b} or electrophile ¹⁴ catalyzed and is facilitated by conventional heating or microwave irradiation ¹⁵. Lewis acidic, alkynophilic metals have proven to be effective for this type of reaction ($M^+ = \text{Cu(I)}^2, \text{Zn(II)}^{12c}, \text{Au(III)}^{12a-b}, \text{Hg(II)}^{12a}, \text{Pd(0)}^{12f}$). Utilizing approach one, the final transformation is the atom exchange reaction to convert the furanouracil nucleobase to pyrrolocytosine by treatment with ammonia ¹⁶. This step is critical, of course, because furanouracil no longer pairs with any of the natural nucleobases. Complementarity to guanine is manifested once the furanouracil is converted to the pyrrolocytosine (**Figure 2.7**).

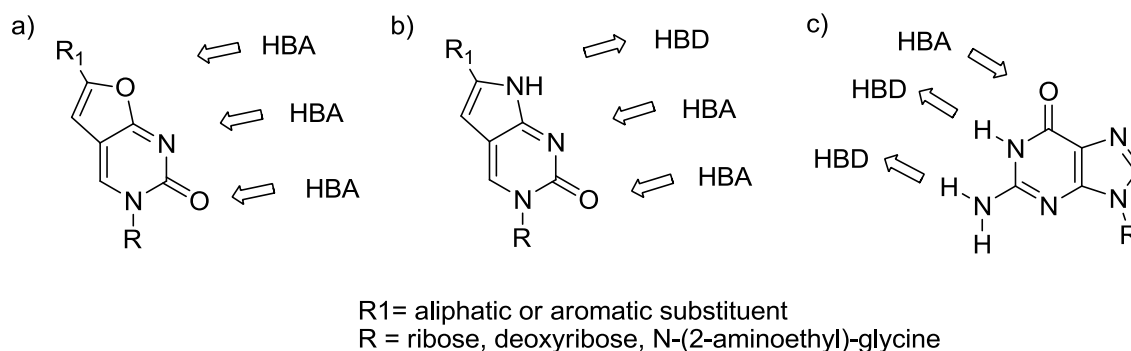
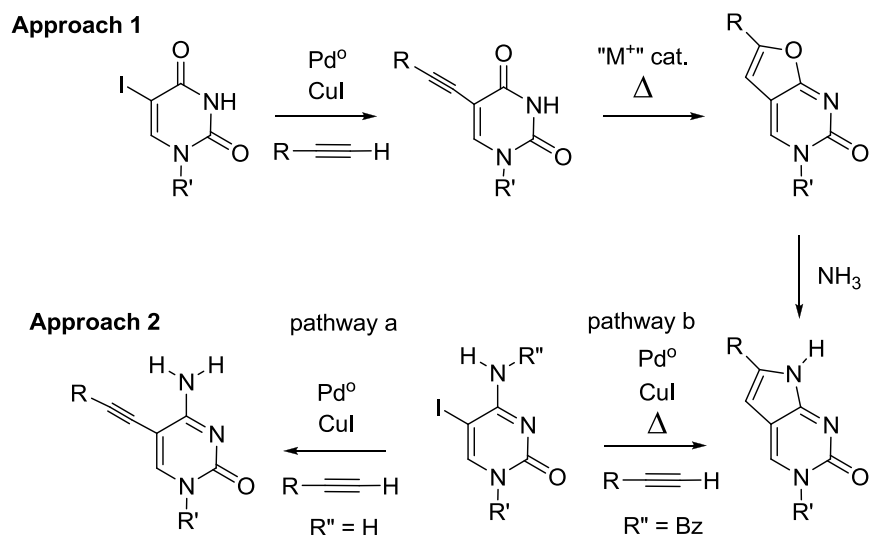


Figure 2.7 – The Watson Crick binding faces of a) furanouracil; b) pC; c) G

The second approach starts with cytosine or cytidine in preparation for cross-coupling by iodination of the base. In approach 2 (**Scheme 2.1**), partitioning of the products between the simple cross-coupled 5-alkynylcytosine and the annulated pyrrocytosine is controlled by the substrate. If the nucleobase is unprotected (pathway a), and the conditions are not forcing, then the 5-alkynylcytosine derivatives are achieved in good yield ¹⁷. For the intramolecular cyclization to occur (pathway b), acylation of the N⁴ must be undertaken prior to Sonogashira chemistry. Using this substrate and elevated temperatures (60 to 80 °C), a domino reaction sequence of cross-coupling and cyclization

occurs during which the benzoyl group is cleaved. The *N*-benzoylpyrrolocytosine is not fluorescent and not stable to silica gel column chromatography. Thus, the benzoyl group is removed to facilitate isolation and purification of the desired pyrrolocytosine.

Foregoing benzoylation of the exocyclic amine, cyclization has been reported using a gold catalyst providing low to moderate yields¹⁸.



Scheme 2.1 – General methodologies of pC synthesis

The *best* synthetic route towards a pC analogue is case specific and must be chosen appropriately as each modification to the pC scaffold will generate its own synthetic challenges.

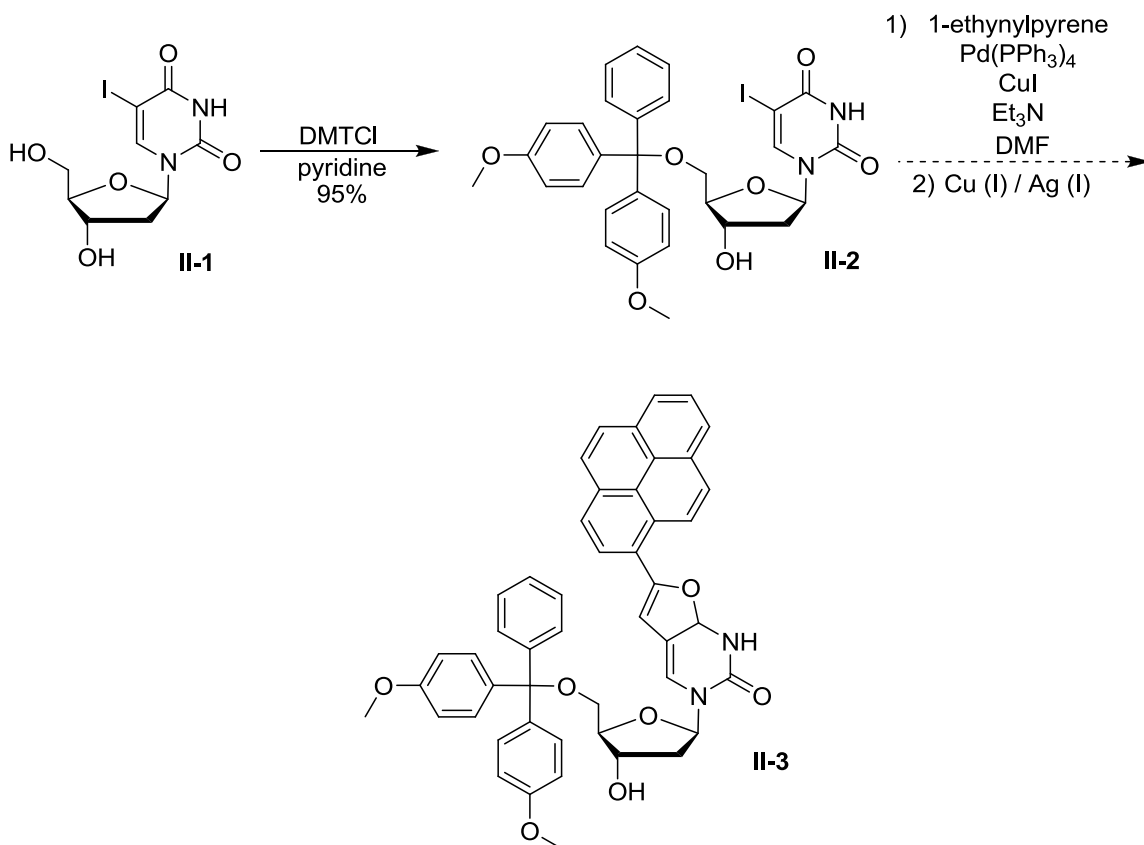
2.2 Results and Discussion

2.2.1 Towards PypdC

Our work towards a pyrene modified pC can be divided in terms of the two synthetic schemes (*vide supra*) generally utilized to synthesize pC analogues.

Initial attempts towards the target utilized the 2'-deoxy-5-iodouridine (**II-1**) starting material. The iodinated nucleoside readily underwent tritylation under standard conditions to produce the 2'-deoxy-5'-*O*-(4,4-dimethoxytrityl)-5-iodouridine (**II-2**) in high yield. Usual protocol demands a one pot conversion of (**II-2**) to produce the

furanouracil intermediate (**II-3**) that would allow ready entry into the trityl protected nucleoside via ammoniolysis. Attempts at a one pot conversion of the cross coupled product via Cu(I) and Ag(I) catalysis after Sonogashira conditions with 1-ethynyl pyrene failed to produce the furanouracil intermediate (**Figure 2.8**). Prolonged exposure to catalytic amounts of the metals at elevated temperatures produced intractable mixtures defiant of characterization

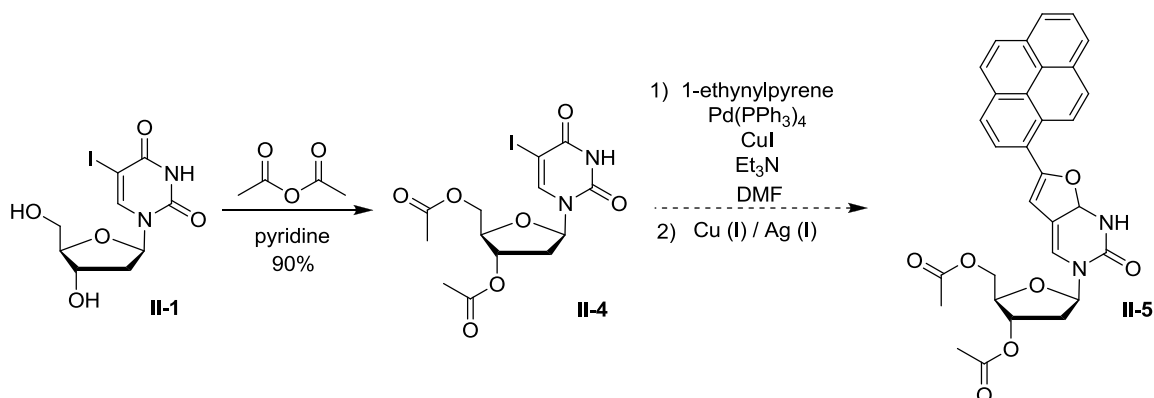


Scheme 2.2 - First attempt towards PypdC

The 4,4-dimethoxytrityl (DMT) protecting group, was thought to be the culprit for degradation as our group has known it to become labile under prolonged exposure to elevated temperatures. In order to circumvent decomposition related to protecting group loss, 5-iodouridine (**II-1**) was acetylated to afford the 3',5'-acetyl protected iodouridine (**II-4**). Treatment of the nucleoside with 1-ethynylpyrene under Sonogashira conditions and attempts at one pot cyclization (**Scheme 2.3**) failed. It was only upon isolation of the

acetyl protected cross coupled product and treatment under the aforementioned Lewis acidic conditions that the furanouracil was observed in low impure yields.

Ammoniolysis of the furanouracil afforded only intractable mixtures of non fluorescent products. This deoxyuridine route was left in favour of the deoxycytidine scheme.



Scheme 2.3 – Second attempt towards PypdC

2.2.2 Synthesis of PypdC

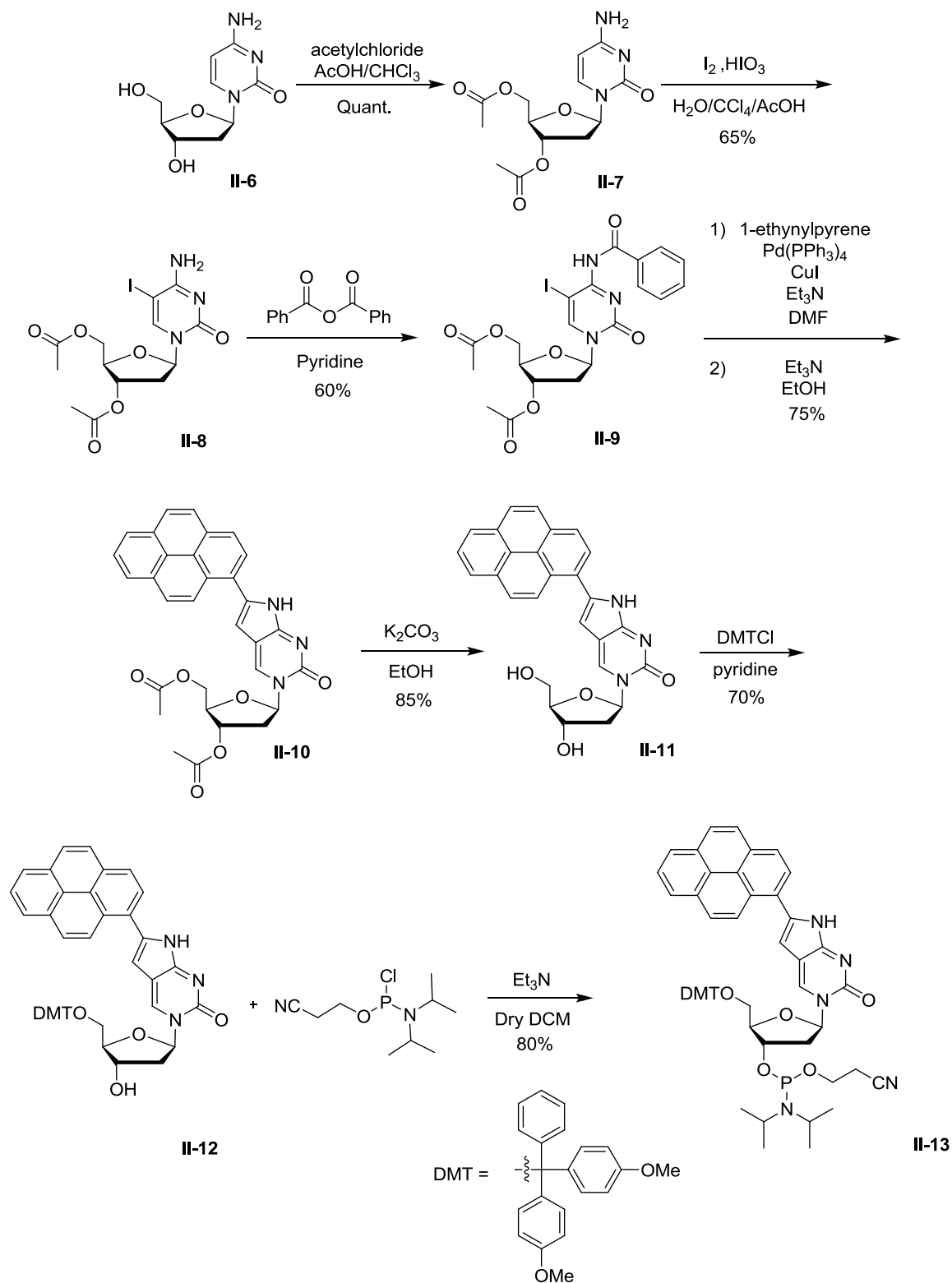
It was unfortunate that at the time of PypdC synthesis the deoxycytidine route had fallen out of favour within the Hudson group as it would prove to be the most successful and portable method of pC synthesis. The issue of contention lay within the reproducibility of the benzylation of the exocyclic amine contained within C. Seemingly attempts at benzylation of the amine led to uncontrollable bis-benzylation and a product unsuited for the required following transformations. With failure observed via the deoxyuridine route, the deoxycytidine methodology was undertaken (**Scheme 2.4**).

Deoxycytidine was treated under acidic conditions with acetyl chloride to generate the 3',5'-acetyl protected cytidine (**II-7**) in quantitative yield. The protected nucleoside proved highly amenable to iodination (**II-8**) with subsequent purification by column chromatography made possible by its increased lipophilicity.

To realize the monobenzoyl intermediate (**II-9**), microwave conditions were utilized. The reaction mixture was subjected to 120 °C at 45 s intervals and checked by TLC until completion. While facile and highly reproducible the scale to which the microwave could

be applied and the lack of constant access to a microwave lead to the exploration of thermal techniques to reach the intermediate. Treatment of **(II-8)** with benzoic anhydride in dry pyridine at 90 °C under nitrogen allowed for the selective production of monobenzoylated C **(II-9)** with little to no bis benzoylated product observed. Despite a lower yield and increased reaction time, we were able to circumvent the need for microwave chemistry and produce **(II-9)** on the gram scale.

With the selective protection and therefore access to the aforementioned acyl protected *N*⁴ cytidine possible **(II-9)**, the application of the Sonogashira tandem annulation reaction was attempted. While a number of conditions were screened, only one provided the desired result in acceptable yield. An oven dried flask charged with 1-ethynyl pyrene and **(II-9)** in dry deoxygenated DMF with subsequent addition of the metal catalysts and triethylamine in appreciable excess would allow for the eventual isolation of the acyl protected PypdC. Purification of the reaction mixture proved problematic. Initial attempts followed conditions outlined within the group led to the capture of impure acetylated PypdC. The impurities were due to excessive band broadening and rapid coelution of products. The purification process was revised. The crude reaction mixture was washed against EDTA and brine as opposed to the suggested removal of DMF by rotary evaporation. Column chromatography was then performed under a number of conditions, however, the most successful conditions were determined to be the use of toluene/methanol with gravity controlled flow. The desired fractions were taken to dryness, dissolved in DCM and added by slow drop wise addition to stirring hexanes. The slow addition was pivotal as rapid addition yielded inferior product with severe discolouration and impurity by NMR.



Scheme 2.4 – Synthesis of PypdC phosphoramidite

To reach oligonucleotide synthesis and to obtain nucleoside photophysical characterization, a deacetylation procedure was required. While conceptually simple, preliminary attempts proved only mildly fruitful. The conditions chosen called for potassium carbonate in alcoholic solvent. The conditions were based upon the idea of easy clean up (filtration of the insoluble base) as column chromatography of the unprotected nucleoside was an unattractive proposition considering the difficulty in processing the protected nucleoside. First attempts at deacetylation proved only mildly fruitful as reaction progress was difficult to obtain reliably. This was likely due to the production of a molecule that on one end contained a hydrophilic carbohydrate and on the other a hydrophobic pyrene “head”. This functionality led to difficulty in the monitoring of reaction progress by TLC as extreme streaking was observed. To take advantage of the potential clean reaction, UPLC ESI/MS was employed to follow reaction progress. UPLC allowed resolution between the three possible materials whose identities were confirmed by the in tandem mass spectrometer. Monitoring the reaction by this method allowed for complete conversion of (**II-10**) to the PypdC nucleoside (**II-11**) in high yield. First success was observed in methanol, however the reaction times proved far too long to be suitable. The alcoholic solvent was changed to ethanol and a reduction in reaction time from 4 days to 18 hours was obtained.

In order to obtain selectivity for the carbohydrate hydroxyls in preparation for phosphoramidite ODN synthesis, the bulky 4,4-dimethoxytrityl protecting group is used to protect the primary alcohol of the carbohydrate. A notoriously finicky reaction, the tritylation reaction was attempted under stringent dry conditions with firm thermal controls to allow the combination of the requisite materials under cool temperatures and reaction at room temperature. Utilizing oven dried flasks and anhydrous pyridine treated with 4 Å molecular sieves, the nucleoside (**II-11**) was dried by rotary evaporation with dry pyridine a number of times and placed under high vacuum overnight to ensure an absence of water. Both the dried nucleoside and protecting group chloride were gently dissolved in their respective dry flasks under nitrogen with pyridine at 0 °C by dropwise dissolution. Rapid dissolution had been observed to reduce yields and even cause no reactions for otherwise simple substrates. Mixing of the solutions at 0 °C under nitrogen provided the trityl protected PypdC (**II-12**) in acceptable yield. Purification, while

initially expected to be an unpleasant affair, mirrored the acetyl protected PypdC and was undramatic.

The phosphoramidite monomer for oligo synthesis contains not only the trityl protected primary hydroxyl but the phosphitylated secondary hydroxyl of the carbohydrate allowing for orthogonal deprotection and coupling steps. Entry into the PypdC monomer followed conditions outlined by Dr. Ghorbani Choghamarani ¹¹ and while allowing for facile synthesis of the monomer provided a phosphorous based impurity. The impurity carried through aqueous work up, chromatography and even precipitation from DCM/hexanes. Distillation of the phosphitylating agent removed the impurity from the reaction mixture and isolated material.

2.2.3 Incorporation into DNA

The PypdC phosphoramidite was incorporated into synthetic oligodeoxynucleotides (ODNs) utilizing the standard phosphoramidite cycle and purified by the trityl ON method (**Scheme 2.5**). All sequences synthesized utilized a T-resin. Three sequences containing PypdC were synthesized, Mano 1 Mod, Mano 2 Mod, and CFTR Mod. Incorporation of the modifications was a facile process and proceeded by acceptable yield without the modification of standard coupling time (**Table 2.1**).

Table 2.1 – Coupling efficiency of the PypdC phosphoramidite

Sequence Name	Sequence (5' → 3')	Coupling Yield (%)
Mano 1 Mod (II-14)	GTA GAT X ACT	89.2
Mano 2 Mod (II-15)	GTA GAT CXC T	94.6
CFTR Mod (II-16)	CTT TCC TXC CAC TGT	93.5

X = PypdC

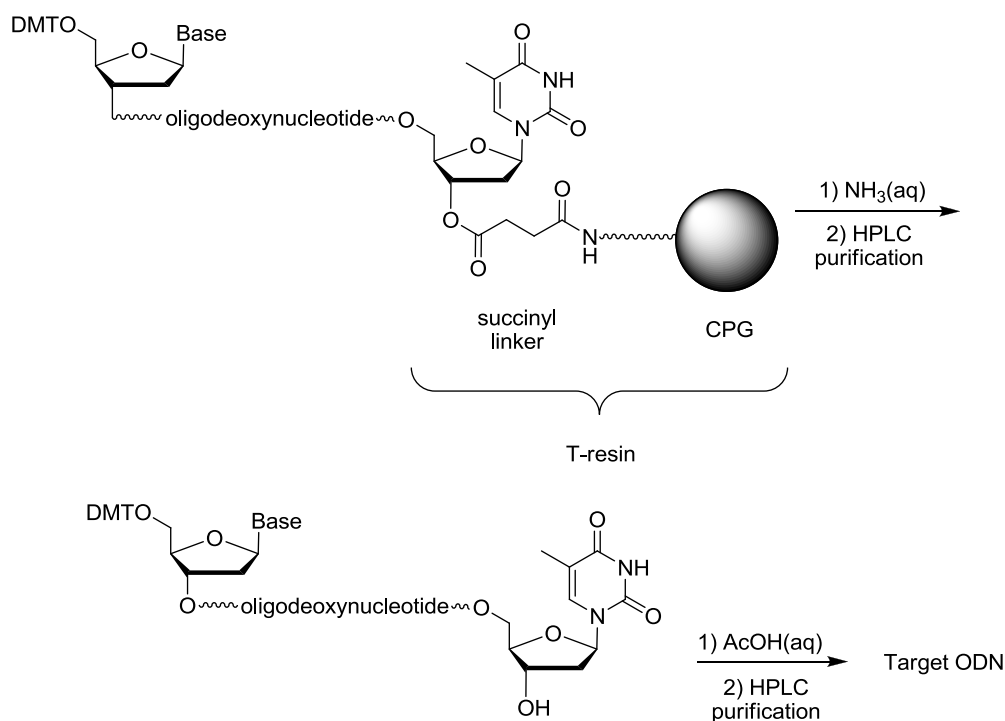
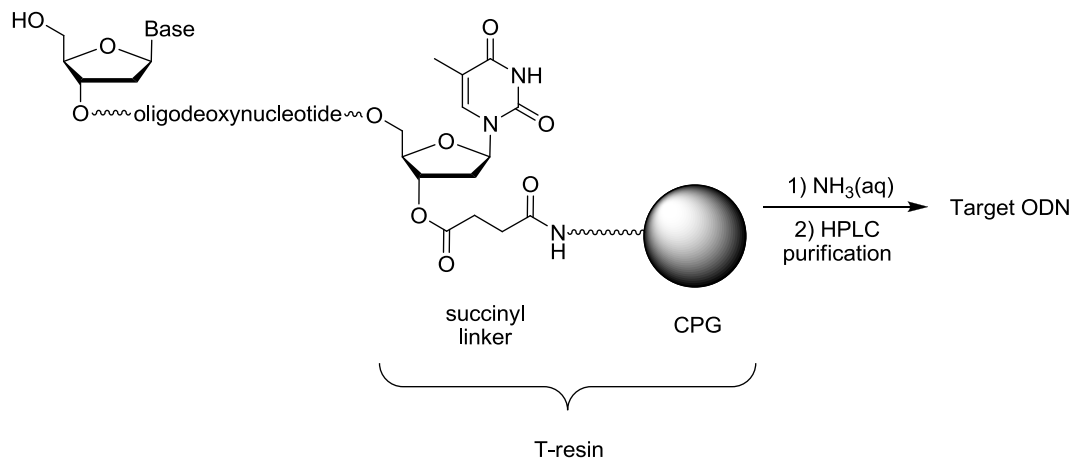
Mano 1 Mod and Mano 2 Mod were chosen as synthetic targets as they have a rich literature history first developed by Manoharan for studies on a C analogue known as “g-

clamp”¹⁹. Use of the known sequences is an attempt by the Hudson group for the standardization of initial sequences for comparison of newly synthesized analogues.

The CFTR Mod sequence was chosen as a practical application model. CFTR, an acronym for Cystic Fibrosis Transmembrane Conductance Regulator describes a particular gene susceptible to mutation leading to the disease state of Cystic Fibrosis (CF)²⁰. CF is the most frequent recessive autosomal disease in the Caucasian population and can be caused by a number of point mutations in the CFTR gene. One of these point mutations (SNP) known as W1282X²⁰ is thought to be the most common CF mutation in the Ashkenazi Jewish population where it may be present in up to 50 – 60 % of CF chromosomes²⁰.

We aimed to develop a fluorescent probe capable of seeking out and identifying the W1282X mutation. We implemented the PypdC modification in the hopes of observing fluorescence changes communicating the SNP condition.

The modified oligos were cleaved from the T-resin by treatment with ammonia in water at 50 °C overnight in small screw cap vials. After cleavage the vessels were left at the elevated temperature sans cap to remove any ammonia in preparation for HPLC purification. The vessels were heated until ammonia could not be sensed by smell.

DMT ON Method**DMT OFF Method****Scheme 2.5** – The trityl ON / OFF methods of ODN purification

Filtration of the cleaved oligo from the glass resin typically uses a 0.2 μM pore filter fed by 1 mL syringe. However, due to the viscosity of the solution and small pore size of the filter, filtration using the syringe proved impossible as excessive force was required causing the syringes to break. To prevent the loss of material by mishandling and

filtration losses, the pore size was increased to 0.45 μM . The increased pore size of the filter proved sufficient for the separation of the solvated oligo from the resin.

In order to avoid preparative scale HPLC and expedite the purification process, the solvated oligos were treated by lyophilization and taken to dryness. They were re-dissolved in 250 μL pH 7 buffer (triethylammonium acetate) in preparation for concentrated injections upon the analytical scale HPLC column. Most of the residual white solid dissolved readily, however, a fine white cloud was observed and 10 μL injections provided UV-Vis spectra with absorptions at ~ 4 minutes; a retention time too fast to be an oligonucleotide. The absorption proved so dominant that any present oligo was not observed by UV-Vis trace. Despite suspension in mixtures of up to 25% DMSO and 75% buffer, dissolution was not observed and the ODNs could not be detected. The suspensions were therefore treated by centrifugation for purification of only the mother liquor was undertaken. Removal of the mother liquor from the resulting white pellet and observation by HPLC yielded both the desired DNA and truncated sequences produced by the DNA synthesizer. The trityl ON sequences were then separated from the truncated sequences. The trityl ON sequences were deprotected by treatment with 80% acetic acid in water for 45 minutes and purified as above.

2.2.4 Nucleoside Fluorescence

Pertinent to our understanding of the interaction of the substituent pyrene with the scaffold pdC, is the fluorescence characterization of the naked nucleoside. Observation of these properties helps to explain the electronics of the molecule when incorporated into oligonucleotides or when used as a standalone probe.

Fluorescence characterization began with obtaining the normalized excitation and emission profiles in ethanol and water (**Figure 2.8 / Figure 2.9**).

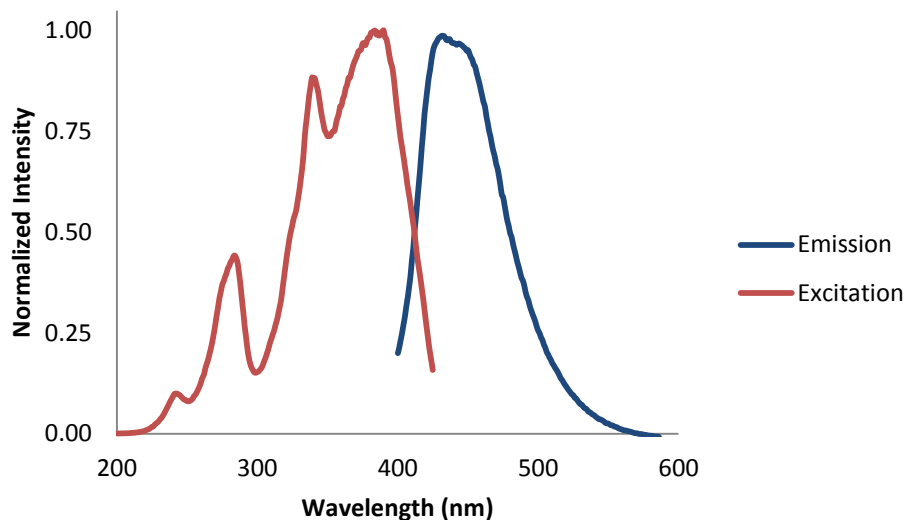


Figure 2.8 – Luminescence profile of PypdC at 2.2 μM in ethanol

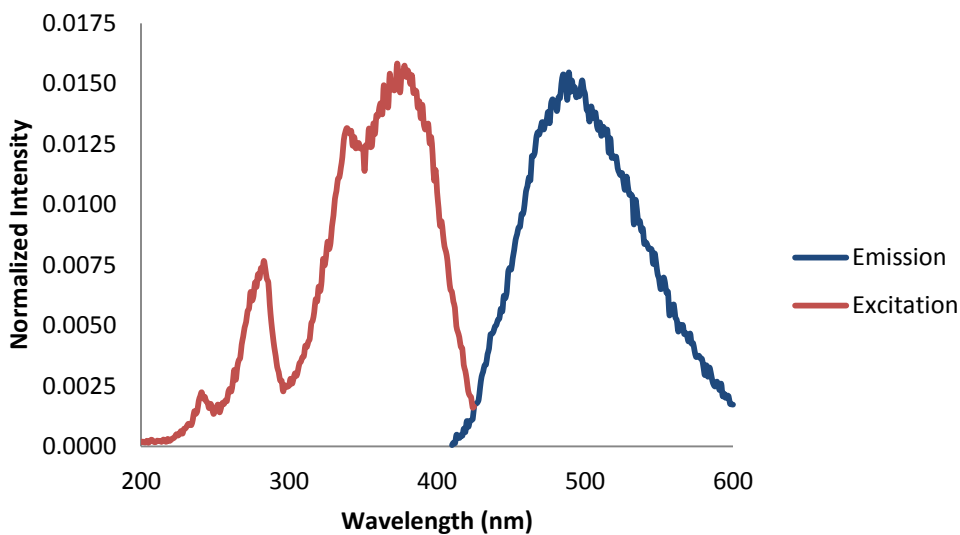


Figure 2.9 - Luminescence profile of PypdC at 2.2 μM in water normalized to **Figure 2.8**.

It is evident that equimolar concentrations of PypdC behave very differently in ethanol than in water. Likely due to polarity difference, one observes $\lambda_{\text{ex}} = 388 \text{ nm}$ and $\lambda_{\text{em}} = 443 \text{ nm}$ in ethanol in contrast to $\lambda_{\text{ex}} = 377 \text{ nm}$ and $\lambda_{\text{em}} = 485 \text{ nm}$ in water. A considerable

change in Stokes shift of 53 nm occurs when traversing between the two solvents (**Table 2.2**). Concurrent with Stokes shift change is marked decrease in fluorescence intensity.

The increased Stokes shift in water points towards a destabilization of the excited state in comparison to ethanol. The energy required to cause transition becomes larger in the more polar solvent or conversely smaller in the less polar solvent. The change in energy between the S_0 and S_1 may even go as far as to explain the decrease in fluorescence intensity. As the energy gap becomes larger (greater stokes shift), then the likelihood of non radiative processes such as internal conversion becomes more favourable. The consequence of this is that as Φ_{IC} increases, Φ_f decreases. This would manifest itself as decreased fluorescence intensity at equimolar concentration and as a decrease in quantum yield (**Table 2.2**)

Table 2.2 – Photophysical summary of PypdC

Compound	Solvent	λ_{ex}^a	λ_{em}^a	ϵ^b	Φ_f	Stokes Shift ^a	Brightness	Polarity Sensitivity
PypdC	ethanol	388	443	16.0	0.6	55	9.6	34
	water	377	485	-	0.02	108	-	

^anm, ^b $10^3 M^{-1}cm^{-1}$, ^c $cm^{-1}/(kcal \cdot mol^{-1})$

With such a drastic change in behaviour observed in fluorescence intensity (an approximate 30 fold increase in ethanol vs. water) and near doubling of stokes shift from ethanol to water, one becomes tempted to label PypdC as a solvatochromatic fluorophore. Such a fluorophore could be envisioned as a polarity reporter of enzymatic active sites, a reporter of duplex polarity, or more classically as a base discriminating fluorophore.

To test the possibility of PypdC as a microenvironmental polarity reporter, the $E_t(30)$ method was applied. Unfortunately, the polarity sensitivity determined proved to be of lesser value and less dramatic than literature molecules. The use of PypdC as a polarity reporter probe is yet to undergo further investigation.

Normalized luminescence plots of PypdC and pyrene (**Figure 2.10**) were used to understand pyrene's interaction with pdC. We observe a red shift in tandem with the retention of the S_3 , S_2 , and S_1 (left to right respectively – **Figure 2.10**) excited states indicative of pyrene in the plot of PypdC. While we see excitation structure similar to that of pyrene, we see very little in the emission that is reminiscent of the moiety. The lack of fine structure points towards a high rate of internal conversion from upper energy states to the S_1 followed by relaxation to the S_0 with the release of light. The broadening of the excitation and emission curves of PypdC with respect to that of pyrene indicates a mix of electronic character between that of pdC and pyrene and that the fluorescence emission may not be wholly attributed to the pyrene moiety itself.

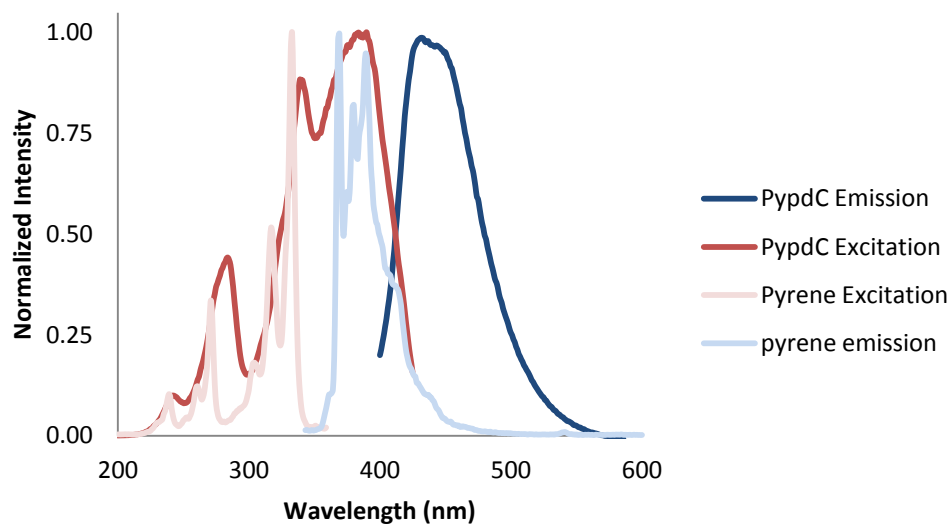


Figure 2.10 – Normalized luminescence of PypdC vs. pyrene.

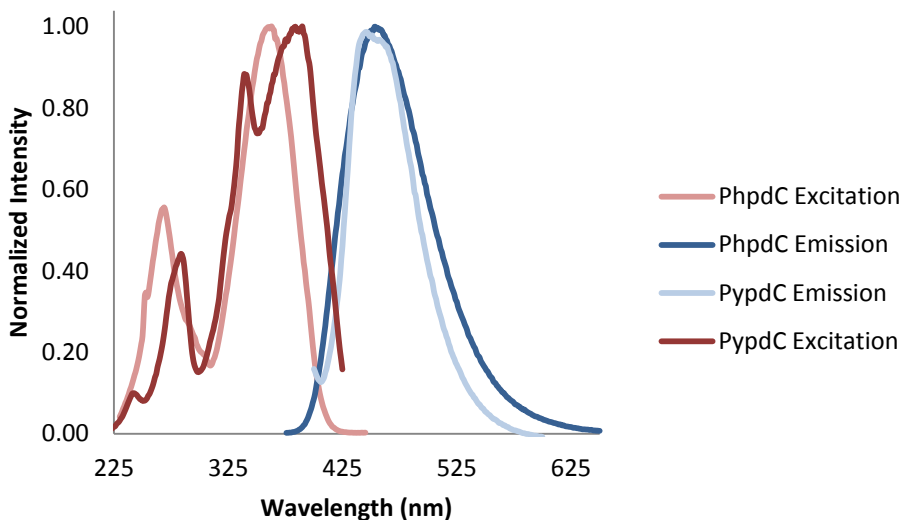


Figure 2.11 – Normalized luminescence of PhpdC and PypdC

Further bolstering the mixed electronic character hypothesis of PypdC is the comparison of normalized excitation and emission plots of PhpdC with that of PypdC (**Figure 2.11**). Both the excitation and emission plots of PypdC closely resemble those of PhpdC in structure and even wavelength emission maxima indicating that PypdC electronics more closely resemble that of PhpdC than that of pyrene.

2.2.5 Oligonucleotide Stability

When introducing a modification into DNA, one needs to consider the effect that the modification has upon the hybridization of the duplex it is forming. Hence, “how large can the substitution become before it comprises duplex stability?” is of great importance to practical application in biological samples and with respect to the tuning of fluorescence properties.

We set out to understand the effect that the large poly aromatic hydrocarbon substituted pdC might have on hybridization by performing UV-Vis thermal denaturation experiments. Of the three oligonucleotides synthesized only a partial data set of CFTR Mod could be obtained due unfortunate material shortages and instrumental errors. The CFTR Mod oligo was compared to its natural C counterpart and it was found that a

stabilization effect of + 6 °C was observed for the PypdC modified oligo vs. its C counterpart (**Table 2.3**).

Table 2.3 – Thermal denaturation of CFTR Mod and control

DNA Sequence (5'→3')	<i>T_m</i> (°C)			
	Target strand (5'→3')			
	ACA GTG GXA GGA AAG	X = G	X = A	X = C
CTT TCC T PypdC C CAC TGT (II-16)	51 ± 1	42 ± 1	46 ± 1	45 ± 1
CTT TCC TCC CAC TGT	45 ± 1	-	-	-

100 mM NaCl, 10 mM Na₂HPO₄, 0.1 mM EDTA, pH 7

The stabilization effect is reminiscent of a tricyclic cytosine analogue which was designed as a helix stabilizing modification for antisense applications in 1995 by Matteucci and coworkers²¹. Matteucci planned to use an extended aromatic face to engage greater pi stacking with neighbouring bases in order to produce irreversible binding for gene knockdown. Their studies similarly showed melt temperature increases with respect to the control in addition to good discrimination between guanine and adenine²¹.

While an incomplete data set for the CFTR Mod oligo makes interpretation difficult, if not impossible, one is able to recognize the unusually high and yet consistent *T_m* values for the mismatch cases. One would expect melt temperatures for the mismatch cases with respect to the natural C to be greatly reduced from the match case by up to 10 °C. One could postulate mismatch melts to be in the 30 – 40 °C range, which is yet lower than the temperatures observed for the mismatch cases of the CFTR Mod oligo. These early melt studies indicate that a net destabilization should not be observed for the modification but rather a net stabilization will be observed likely due to the extended aromatic face of pyrene interacting with neighbouring bases. If the net stabilization for the mismatch cases

should be true then little to no discrimination may be observed in terms of wild type vs. mutant gene selection allowing for fluorimetric signaling of matches and mismatches.

2.2.6 ODN Fluorescence

Fluorescence intensity studies of CFTR Mod were carried out to determine whether or not PypdC could be used as a classical base discriminating fluorophore reporting complementarity by fluorescence intensity (**Figure 2.11**).

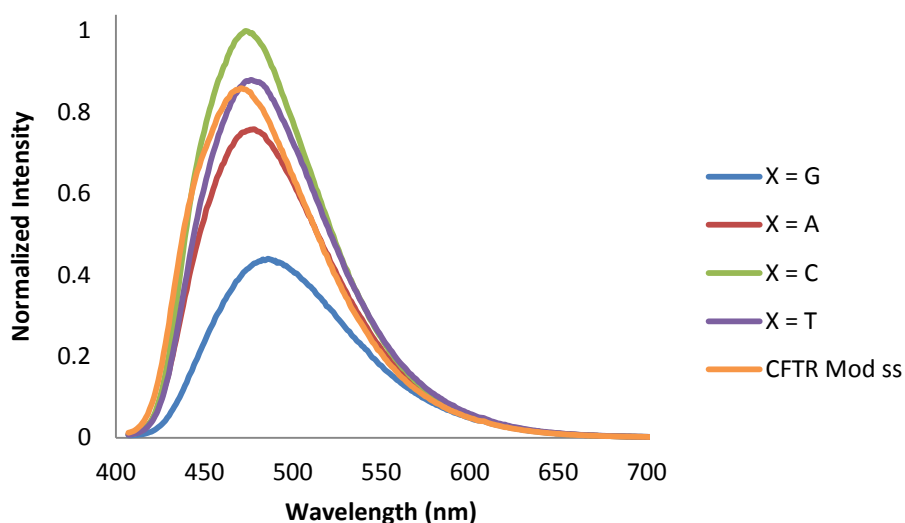


Figure 2.12 – Fluorescence intensity change of CFTR Mod against G,A,C,T and in the ss state at 1.5 μ M

Like pdC analogues before it, it seems that the PypdC modification is able to fluorimetrically respond to its base pairing partner by changes in fluorescence intensity. Arguably more interesting than the observed intensity changes, is the change in Stokes shift in the match case versus the mismatch and single strand cases (**Table 2.4**). To our knowledge, pdC analogues have yet to communicate base pairing partners by a change in Stokes shift. PypdC is the first example of such a discriminating base which in tandem with a quenching effect could readily signal a match or mismatch case by Stokes shift change

Table 2.4 – Photophysical summary of CFTR Mod

X ^a	λ_{ex} (nm)	λ_{em} (nm)	Stokes shift (nm)	Intensity change (%) ^b
G	397	487	90	-48
A	396	478	82	-12
C	397	473	76	+ 16
T	396	474	78	+ 2.0
SS ^c	396	471	75	-

^aCFTR target, ^bfrom ss intensity, ^cCFTR Mod single strand

The ability of PypdC to discriminate a match or mismatch by changes in Stokes shift as opposed to *intensity* would circumvent the need for an internal standard for ratiometric analysis of the base partner. Intensity changes may be attributed to a number of possibilities such as inner filter effect or quenching due to molecules in solution. While quenching effects are subject to a number of conditions a Stokes shift change is representative of the immediate microenvironment surrounding the base and would eliminate some uncertainty observed for previous pyrrolocytosine analogues.

2.3 Conclusions and Future work

The PypdC nucleoside was synthesized and photophysical characterization was completed. The DNA monomer was prepared and was successfully incorporated into three synthetic ODNs in acceptable coupling yields. Preliminary hybridization studies and fluorescence measurements performed upon the CFTR Mod sequence showed that a stabilization effect upon the duplex is observed in the C case if a PypdC insert is present (question 1). PypdC seems to be the first example of an intrinsic fluorophore capable of base discrimination by *Stokes shift* change rather than *intensity* change (question 2).

Due to the unique nature of the PypdC modification and because of pyrenes' ability to be involved in excimer and monomer based fluorescence we have designed (and have begun to implement) new diagnostic technologies.

In hopes of capitalizing upon the colour changing behavior of the PypdC insert, we propose a technology in which three inserts lay adjacent to each other (**Figure 2.12**).

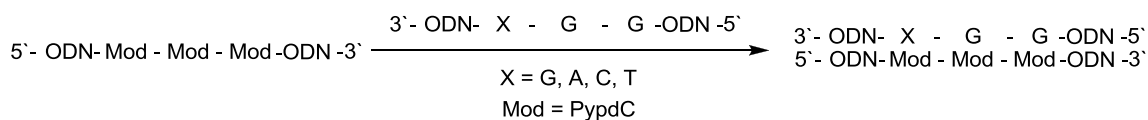


Figure 2.13 – Possible PypdC excimer based probe

We imagine that this beacon, when hybridized to a match/mismatch will cause a colour change in the excimer if not classical intensity change typical of pdC analogues.

An initial attempt at synthesizing this probe was undertaken, however, the coupling of three consecutive modifications proved problematic as three oligonucleotides were observed when cleaved from the resin (**Figure 2.13**). Each ODN is likely due to a failed coupling after each insert followed by capping. Presumably increased coupling times will lead to fewer (if no) side products.

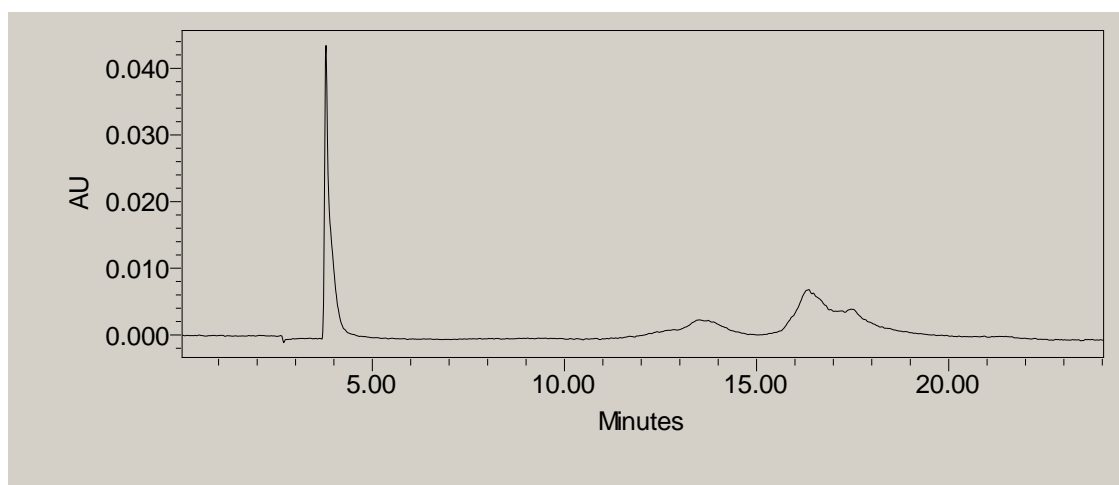


Figure 2.14 – HPLC trace of a failed synthesis towards a new PypdC probe

2.4 Experimental

2.4.1 Synthetic Procedures and Characterization

Synthesis of 3',5'-*O*-acetyl-2'-deoxycytidine (II-7)

Acetyl chloride (4.2 mL, 59.3 mmol) was taken into 10 mL chloroform and added dropwise to 2'-deoxycytidine (1.2 g, 5.39 mmol) dissolved in 10 mL acetic acid cooled to 0 °C. After stirring at r.t. for 24 h the reaction mixture was placed on ice and allowed to cool for 15 minutes. The reaction was then quenched by the dropwise addition of methanol (10 mL) and allowed to stir at r.t. for 10 minutes. After quenching, the solvent was removed by rotary evaporation yield to yield an amorphous white solid (1.86 g, quantitative). ¹H NMR (DMSO-*d*₆): δ = 9.58 (br,s, 1H), 8.62 (br,s,1H), 7.92 (d, *J*₁ = 7.82 Hz, 1H), 6.16 (m, 1H), 6.09 (t, *J*₁ = 6.84 Hz, 1H), 5.18 (m, 1H), 4.23 (br,s,3H), 2.41 (m, 2H), 2.06 (s, 3H), 2.04 (s, 3H). ¹³C NMR (DMSO-*d*₆): δ = 170.19, 170.06, 160.66, 148.30, 143.78, 94.47, 86.11, 81.88, 73.83, 63.57, 36.58, 20.78, 20.63. HRMS (ESI) *m/z* calcd for C₁₃H₁₈N₃O₆ [MH⁺] 312.1196, found 312.1198.

Synthesis of 2'-Deoxy-3',5'-*O*-acetyl-5-iodocytidine (II-8)

To 3',5'-*O*-acetyl-2'-deoxycytidine (2.0 g, 6.42 mmol) dissolved in 8 mL water was added 8 mL carbon tetrachloride, I₂ (0.98 g, 3.85 mmol), HIO₃ (0.34 g, 1.92 mmol), and 16 mL acetic acid. The mixture was heated to 40 °C and subjected to vigorous stirring. Upon completion the solvent was removed by rotary evaporation to afford a dark brown residue. The residue was taken into 50 mL DCM and washed against two 50 mL portions of 1 M sodium bicarbonate. The organic layer was dried with sodium sulphate and removed by rotovap to produce dark brown coloured foam. The foam was subjected to column chromatography. Utilizing gradient elution (DCM → 2:3 DCM / acetone) 2'-Deoxy-3',5'-*O*-acetyl-5-iodocytidine was obtained in 65 % yield (1.82 g). ¹H NMR (DMSO-*d*₆): δ = 9.14 (br, s, 1H), 8.47 (br, s, 1H), 8.17 (s, 1H), 6.06 (t, *J*₁ = 6.84 Hz, 1H), 5.18 (m, 1H), 4.26 (m, 3H), 2.47 (m, 1H), 2.37 (m, 1H), 2.09 (s, 1H), 2.06 (s, 1H). ¹³C NMR (DMSO-*d*₆): δ = 170.06, 170.01, 161.34, 149.97, 148.52, 86.18, 81.91, 73.81, 63.51, 57.31, 48.61, 36.76, 20.78. HRMS (EI) *m/z* calcd for C₁₃H₁₆I N₃O₆ [M⁺] 437.0084, found 437.0084.

Synthesis of 2'-Deoxy-3',5'-*O*-acetyl-*N*⁴-benzoyl-5-iodocytidine (II-9)

To an oven dried flask was added 2'-deoxy-3',5'-*O*-acetyl-5-iodocytidine (1.0 g, 2.28 mmol) and benzoic anhydride (0.77 g, 3.43 mmol). The solids were placed under N₂ and 10 mL dry pyridine was syringed into the reaction vessel. The stirring mixture was heated to 90 °C until completion. The reaction solvent was then removed by rotary evaporation and the subsequent residue was subjected to multiple co evaporations with toluene to produce a white solid. The solid was further purified by column chromatography and gradient elution (DCM → 95:5 DCM/acetone) to yield 2'-deoxy-3',5'-*O*-acetyl-*N*⁴-benzoyl-5-iodocytidine (0.81 g, 67 %). ¹H NMR (DMSO-*d*₆): δ = 12.83 (s, 1H), 8.24 (m, 3H), 7.62 (m, 1H), 7.53 (m, 1H), 6.12 (t, *J*_I = 6.84 Hz, 1H), 5.21 (m, 1H), 4.28 (m, 3H), 2.54 (m, 1H), 2.36 (m, 1H), 2.13 (s, 3H), 2.07 (s, 3H). ¹³C NMR (DMSO-*d*₆): δ = 178.04, 170.05, 170.00, 156.14, 147.21, 146.43, 136.19, 132.84, 129.51, 128.38, 85.96, 81.94, 73.78, 69.97, 63.50, 36.50, 20.81, 20.75. HRMS (EI) *m/z* calcd for C₂₀H₂₀I_N₃O₇ [M⁺] 541.0346, found 541.0331.

Synthesis of 2'-Deoxy-3',5'-*O*-acetyl-6-(1-pyrenylethynyl)pyrrolocytidine (II-10)

To dry DMF (5 mL) was added 2'-deoxy-3',5'-*O*-acetyl-*N*⁴-benzoyl-5-iodocytidine (0.20 g, 0.369 mmol) and 1-ethynylpyrene (0.12 g, 0.554 mmol). The stirring mixture was degassed and placed under N₂ utilizing a dry ice / acetone bath and dry line. To the degassed mixture was added Pd(PPh₃)₄ (42 mg, 0.03 mmol) and CuI (14 mg, 0.07 mmol) followed by further deoxygenation utilizing the previously described procedure. Deoxygenated triethylamine (0.18 mL, 1.4 mmol) was then added to the reaction mixture. The reaction mixture was stirred in darkness at 50 °C for 18 hrs. 10 mL anhydrous ethanol and 0.18 mL triethylamine was further added to the vessel once 18 hrs had elapsed. The reaction was kept in darkness under N₂ at 50 °C for an additional 18 hrs. Upon completion the reaction was diluted with 25 mL DCM and washed against five 50 mL portions of 5% EDTA and one 50 mL portion of brine. The organic layer was dried over sodium sulphate and removed by rotovap. The resulting orange/red solid was purified by column chromatography utilizing a toluene/methanol mobile phase (toluene → 98:2 toluene/methanol). The desired fractions were collected and dried and taken into

1 mL DCM. The DCM was then dropped by pipette into 10 mL stirring hexanes to produce a light yellow precipitate. The precipitate was gravity filtered and allowed to air dry overnight. 2'-Deoxy-3',5'-*O*-acetyl-6-(1-pyrenylethynyl)-pyrrolocytidine was collected off the filter paper as a light yellow powder (0.14 g, 75 %). ¹H NMR (DMSO-*d*₆): δ = 12.02 (s, 1H), 8.62 (s, 1H), 8.52 (d, *J*₁ = 9.38, 1H), 8.36 (m, 3H), 8.25 (m, 4H), 8.13 (m, 1H), 6.74 (s, 1H), 6.38 (t, *J*₁ = 6.64 Hz, 1H), 5.27 (d, *J*₁ = 6.25, 1H), 4.37 (br, s, 3H), 2.62 (m, 1H), 2.42 (m, 1H), 2.11 (s, 3H), 2.09 (s, 3H). ¹³C NMR (DMSO-*d*₆): δ = 170.28, 170.13, 159.87, 153.85, 138.79, 136.54, 130.92, 130.87, 130.35, 128.30, 128.10, 128.04, 127.29, 127.09, 126.64, 126.30, 125.78, 125.42, 124.86, 124.34, 124.18, 123.84, 109.72, 101.98, 87.41, 82.11, 74.23, 63.76, 38.02, 20.82, 20.69. HRMS (ESI) *m/z* calcd for C₃₁H₂₆N₃O₆ [MH⁺] 536.1822, found 536.1816.

Synthesis of 2'-Deoxy-6-(1-pyrenylethynyl)pyrrolocytidine (II-11)

To a suspension of 2'-deoxy-3',5'-*O*-acetyl-6-(1-pyrenylethynyl)pyrrolocytidine (0.10 g, 0.187 mmol) in 20 mL ethanol was added potassium carbonate (5 mg, 0.037 mmol). The reaction was stirred under ambient conditions until completion. The reaction mixture was filtered through a cotton plugged pipette and the mother liquor was removed by rotary evaporation. The remaining residue was taken into DCM and gravity filtered. A yellow solid was recovered from the filter paper and recrystallized from water/ethanol to produce the target unprotected nucleoside (0.0844 mg, 85%). ¹H NMR (DMSO-*d*₆): δ = 11.97 (s, 1H), 8.86 (s, 1H), 8.52 (d, *J*₁ = 9.38 Hz, 1H), 8.36 (m, 3H), 8.25 (m, 4H), 8.13 (m, 1H), 6.69 (s, 1H), 6.33 (t, *J*₁ = 6.25 Hz, 1H), 5.32 (d, *J*₁ = 3.91 Hz, 1H), 5.17 (t, *J*₁ = 5.08, 1H), 4.30 (m, 1H), 3.94 (q, *J*₁ = 3.91, 1H), 3.69 (m, 2H), 2.42 (ddd, *J*₁ = 13.29 Hz, *J*₂ = 5.86, *J*₃ = 3.91, 1H), 2.09 (dt, *J*₁ = 13.38 Hz, *J*₂ = 6.4 Hz). ¹³C NMR (DMSO-*d*₆): δ = 159.61, 153.99, 138.38, 136.91, 130.94, 130.82, 130.38, 128.28, 128.08, 128.04, 127.32, 127.10, 126.64, 126.43, 125.77, 125.40, 124.88, 124.11, 124.20, 123.87, 109.30, 101.92, 88.04, 87.19, 70.06, 61.12, 41.64. HRMS (ESI) *m/z* calcd for C₂₇H₂₂N₃O₄ [MH⁺] 452.1610, found 452.1601.

Synthesis of 2'-Deoxy-5'-O-(4,4'-dimethoxytrityl)-6-(1-pyrenylethynyl)pyrrolocytidine (II-12)

2'-Deoxy-6-(1-pyrenylethynyl)pyrrolocytidine (0.10 g, 0.187 mmol) was dissolved in 10 mL pyridine and dried by rotovap three times. The residue was then placed on high vacuum overnight. The dried nucleoside was placed under N₂ and dissolved in 10 mL dried pyridine and stirred with DIPEA (0.09 mL, 0.559 mmol) at 0 °C. A separate oven dried vessel was charged with dimethoxytritylchloride (0.082 g, 0.242 mmol), placed under N₂ and cooled to 0 °C. The DMTCI was then taken into 5 mL dry pyridine by slow dropwise dissolution on ice under N₂. Upon dissolution, the DMTCI solution was added dropwise to the cold nucleoside mixture. The reaction mixture was allowed to stir on ice for 15 minutes then brought to room temperature for 18 hours. The vessel was subsequently brought to 0 °C and the reaction was quenched with 5 ml methanol. After 15 minutes stirring at room temperature, the solvent was removed by rotovap and remaining pyridine was removed by co evaporation with toluene. The resulting orange/red solid was purified by column chromatography (99:2:1 toluene/methanol/triethylamine) and the fractions of interest were gathered and precipitated from DCM/hexanes (0.098 g ,70 %). ¹H NMR (DMSO-*d*₆): δ = 11.98 (s, 1H), 8.77 (s, 1H), 8.38 (m, 4H), 8.24 (m, 3H), 8.13 (m, 2H), 7.44 (d, *J*₁= 7.42 Hz, 2H), 7.32 (m, 6H), 7.25 (m, 1H) 6.90 (m, 4H), 6.34 (t, *J*₁=5.67 Hz, 1H), 5.95 (s, 1H), 5.48 (br, 1H), 4.47 (m, 1H), 4.05 (m, 1H), 3.66 (s, 3H), 3.64 (s, 3H), 3.41 (m, 1H), 3.33 (m, 1H), 2.53 (m, 1H), 2.27 (m, 1H). ¹³C NMR (DMSO-*d*₆): δ = 159.61, 158.17, 153.81, 144.72, 138.48, 136.41, 135.43, 135.18, 130.90, 130.81, 130.35, 129.82, 128.2, 127.99, 127.92, 127.75, 127.28, 127.00, 126.84, 126.63, 126.26, 125.77, 125.44, 124.84, 124.24, 124.14, 123.82, 113.30, 109.12, 101.24, 86.90, 86.11, 85.85, 69.42, 62.86, 54.96, 41.67. HRMS (ESI) *m/z* calcd for C₄₈H₄₀N₃O₆ [MH⁺] 754.2917, found 754.2902.

Synthesis of 2'-Deoxy-3'-(2-cyanoethyldiisopropylphosphoramidite)-5'-O-(4,4'-dimethoxytrityl)-6-(1-pyrenylethynyl)pyrrolocytidine (II-13)

2-Cyanoethyldiisopropylphosphoramidochloridite (0.1354 g, 0.5724 mmol) was added to a solution of 2'-deoxy-5'-O-(4,4'-dimethoxytrityl)-6-(1-pyrenylethynyl)pyrrolocytidine (0.2862 mmol) and Et₃N (0.5 mL) in dry DCM (2 mL). The reaction was allowed to stir at room temperature under N₂ for 3 hours. The reaction was quenched with MeOH (0.5 mL), washed with 0.5 M NaHCO₃ (10 mL) and the organic phase was dried with Na₂SO₄. The residue was purified by column chromatography using gradient elution (DCM/acetone/Et₃N, 99:0:1 to 94:5:1) to give a mixture of diastereomers as a yellow foam, 0.2147 g (80%). ¹H NMR (DMSO-*d*₆): δ = 11.99 (br, 1H), 8.80 and 8.76 (2 s, 1H), 8.1 – 8.40 (m, 9 H), 7.25 – 7.46 (m, 9 H), 6.88 – 6.92 (m, 4 H), 6.32 – 6.39 (2 m, 1H), 5.96 – 6.00 (2 s, 1 H), 4.69 (m, 1H), 4.17 – 4.22 (2 m, 1H), 3.69 – 3.78 (m, 1H), 3.65 – 3.67 (3 s, 6H), 3.51 – 3.60 (m, 2H), 2.78 – 2.61 (m, 2H), 2.67 – 2.70 (m, 2H), 2.59 – 2.65 (m, 1H), 2.40 – 2.45 (m, 1H), 1.02 – 1.17 (m, 14 H). ³¹P NMR (DMSO-*d*₆): δ = 147.76, 147.54. HRMS (ESI) *m/z* calcd for C₅₇H₅₇N₅O₇P [MH⁺] 955.4074, found 954.3995.

Mano 1 Mod (II-14) HRMS (ESI) calculated for C₁₁₆H₁₃₂N₃₇O₅₈P₉ [M-H]⁻¹: 3248.5995, Found: 3248.5566

Mano 2 Mod (II-15) HRMS (ESI) calculated for C₁₁₅H₁₃₂N₃₅O₅₉P₉: 3224.5965 [M-H]⁻¹, Found: 3224.5976

CFTR Mod (II-16) HRMS (ESI) for C₁₆₁H₁₉₅N₄₃O₉₃P₁₄: 4650.8100 [M-H]⁻¹, Found: 4650.6897

2.5 References

1. Hudson, R. H. E.; Li, G.; Tse, J., *Tetrahedron Lett.* **2002**, *43* (8), 1381-1386.
2. Inoue, H.; Imura, A.; Ohtsuka, E., *Nippon Kagaku Kaishi* **1987**, (7), 1214-1220.
3. Hudson, R. H. E.; Dambeniaks, A. K.; Viirre, R. D., *Synlett* **2004**, (13), 2400-2402.
4. Hudson, R. H. E.; Dambeniaks, A. K.; Moszynski, J. M., *Proc. SPIE-Int. Soc. Opt. Eng.* **2005**, *5969*, 59690J/1-59690J/10.
5. Liu, C. H.; Martin, C. T., *J. Mol. Biol.* **2001**, *308* (3), 465-475.
6. Glen Research Catalog 2012.
<http://www.glenresearch.com/Catalog/structural.html#p64> (accessed 28/08/12).
7. Berry, D. A.; Jung, K. Y.; Wise, D. S.; Sercel, A. D.; Pearson, W. H.; Mackie, H.; Randolph, J. B.; Somers, R. L., *Tetrahedron Lett.* **2004**, *45* (11), 2457-2461.
8. Zang, Z.; Fang, Q. M.; Pegg, A. E.; Guengerich, F. P., *J. Biol. Chem.* **2005**, *280* (35), 30873-30881.
9. Dash, C.; Rausch, J. W.; Le Grice, S. F. J., *Nucleic Acids Res.* **2004**, *32* (4), 1539-1547.
10. Hudson, R. H. E.; Choghamarani, A. G., *Nucleosides Nucleotides Nucleic Acids* **2007**, *26* (6-7), 533-537.
11. Hudson, R. H. E.; Ghorbani-Choghamarani, A., *Synlett* **2007**, (6), 870-873.
12. a) Iritani, K.; Matsubara, S.; Utimoto, K., *Tetrahedron Lett.* **1988**, *29* (15), 1799-1802. b) Arcadi, A.; Bianchi, G.; Marinelli, F., *Synthesis* **2004**, (4), 610-618. c) Sniady, A.; Durham, A.; Morreale, M. S.; Marcinek, A.; Szafert, S.; Lis, T.; Brzezinska, K. R.; Iwasaki, T.; Ohshima, T.; Mashima, K.; Dembinski, R., *J. Org. Chem.* **2008**, *73* (15), 5881-5889. d) Kurisaki, T.; Naniwa, T.; Yamamoto, H.; Imagawa, H.; Nishizawa, M., *Tetrahedron Lett.* **2007**, *48* (10), 1871-1874. e) Trost, B. M.; McClory, A., *Angew. Chem.-Int. Edit.* **2007**, *46* (12), 2074-2077. f) Larock, R. C., *Journal of Organometallic Chemistry* **1999**, *576* (1-2), 111-124.
13. a) Rodriguez, A. L.; Koradin, C.; Dohle, W.; Knochel, P., *Angew. Chem.-Int. Edit.* **2000**, *39* (14), 2488-2490. b) Yu, C. J.; Yowanto, H.; Wan, Y. J.; Meade, T. J.; Chong, Y.; Strong, M.; Donilon, L. H.; Kayyem, J. F.; Gozin, M.; Blackburn, G. F., *J. Am. Chem. Soc.* **2000**, *122* (28), 6767-6768.
14. Rao, M. S.; Esho, N.; Sergeant, C.; Dembinski, R., *J. Org. Chem.* **2003**, *68* (17), 6788-6790.
15. Carpita, A.; Ribecai, A., *Tetrahedron Lett.* **2009**, *50* (49), 6877-6881.
16. Woo, J. S.; Meyer, R. B.; Gamper, H. B., *Nucleic Acids Res.* **1996**, *24* (13), 2470-2475.

17. Hudson, R. H. E.; Viirre, R. D.; Liu, Y. H.; Wojciechowski, F.; Dambenieks, A. K., *Pure Appl. Chem.* **2004**, *76* (7-8), 1591-1598.
18. Noe, M. S.; Rios, A. C.; Tor, Y., *Org. Lett.* **2012**, *14* (12), 3150-3153.
19. Rajeev, K. G.; Maier, M. A.; Lesnik, E. A.; Manoharan, M., *Org. Lett.* **2002**, *4* (25), 4395-4398.
20. G. Feriotto; A. Ferlini, R. Gambari. *Human Mutation.* **2001**, *18*, 70-81.
21. Lin, K. Y.; Jones, R. J.; Matteucci, M., *J. Am. Chem. Soc.* **1995**, *117* (13), 3873-3874.

Chapter 3 – Pyrenylethynylcytidine

3 Introduction – Serendipity

Arguably, for a fluorophore there are at minimum three main components for fluorescence tuning, (1) fluorescence quantum yield; (2) molar absorptivity; (3) Stokes shift. For intrinsic fluorophores such as the pdCs to become competitive with commercially available fluorophores such as the rhodamines and alexa dyes, one needs to maximize their brightness. Brightness maximization could mean either increasing the fluorescence quantum yield or increasing the molar absorptivity of the molecule.

In Chapter 2 we discussed how pyrrolocytidines were a serendipitous discovery made by the Hudson group some years ago. The initial molecules of interest were 5-alkynylpyrimidines which only displayed modest fluorescence properties. Now as serendipity would have it that as progress was made towards PypdC, a 5-pyrenylethynyluracil was synthesized

Under ambient conditions and sunlight, the 5-pyrenylethynyluracil derivative exhibited a prominent dark purple fluorescence. Even upon serial dilutions the uracil analogue displayed a highly attractive level of fluorescence. This was attributed to a number of possibilities, one of which it was assumed that the molecule must have a high brightness factor in order to be seen in the well lit room.

We set out to synthesize a base that would take advantage of this increased brightness yet still be base pairing competent with G. The corollary of these demands was a PypdC congener, or rather a pyrenylethynylcytidine (PyEtdC) base (**Figure 3.1**).

The prospect of the new molecule opened a new set of possibilities for exploration. How do the electronics of the base change when pyrene is directly connected to the base rather than conjugated through a pyrrole? What causes the visible brightness change? Does it maintain its ability to act as a BDF? And finally, what new technologies can we develop to harvest these new discoveries?

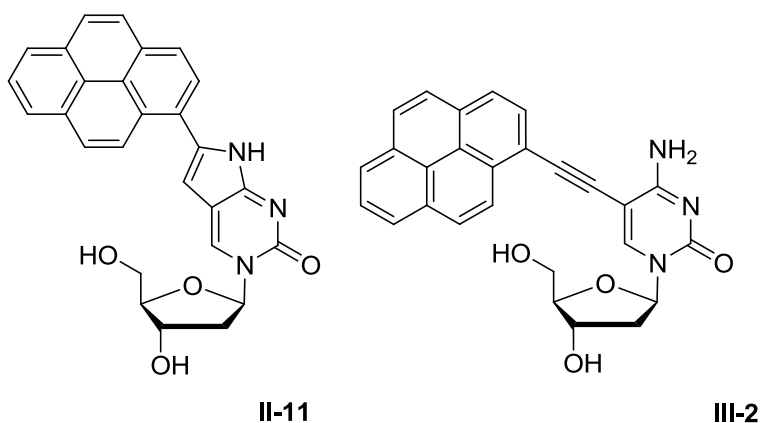


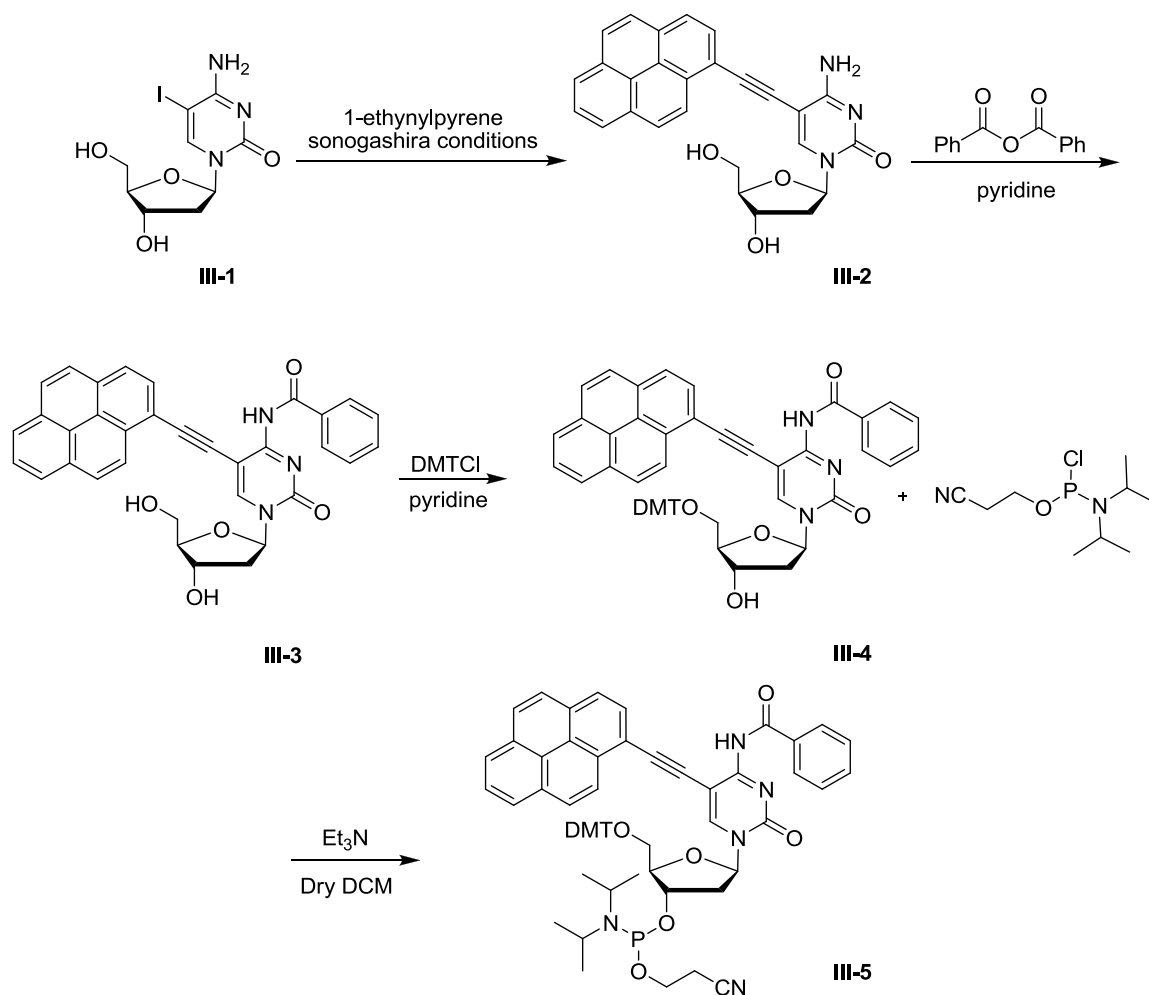
Figure 3.1 – PypdC (left) & PyEtdC (right)

3.1 Results and Discussion

3.1.1 Towards PyEtdC in DNA

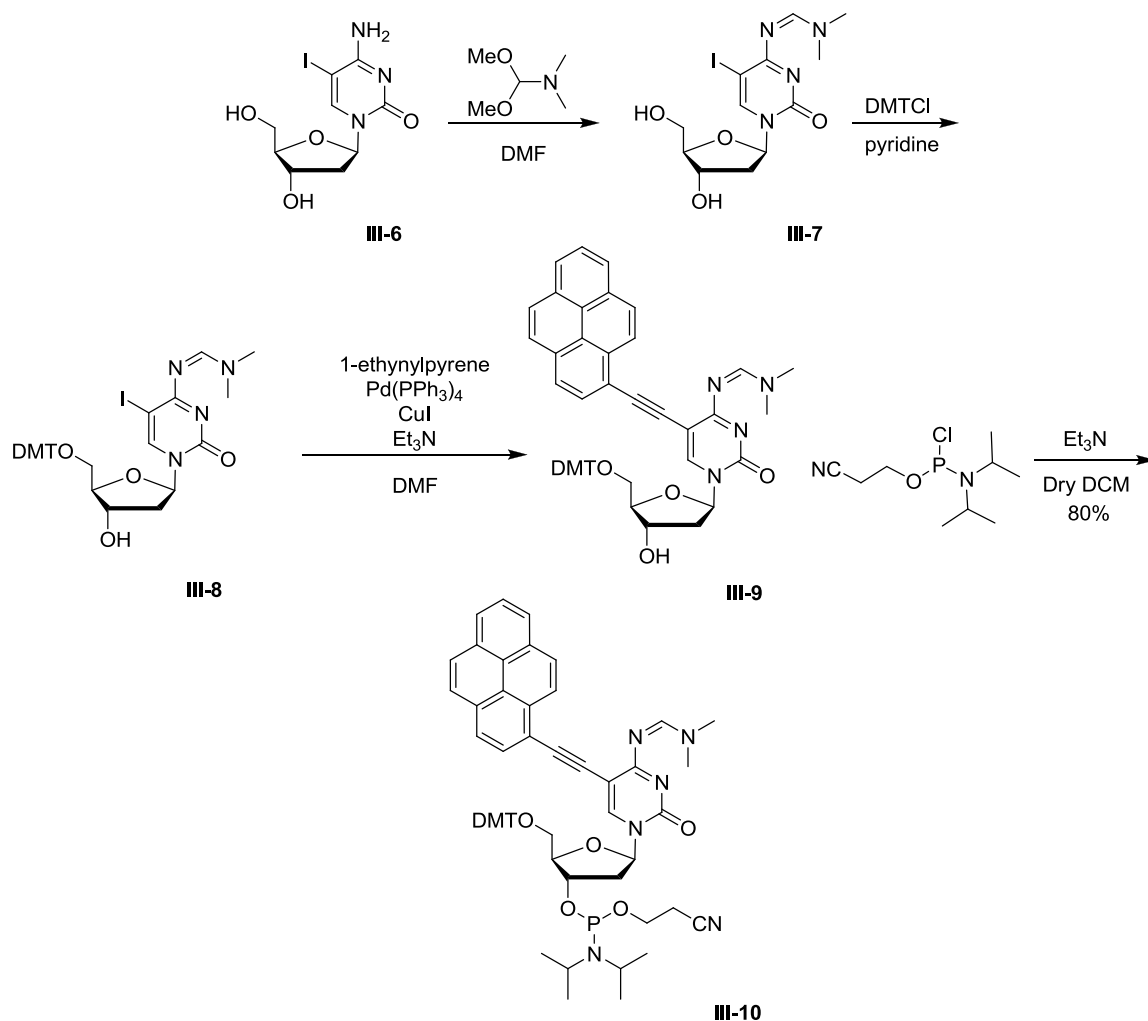
Synthesizing a pyrene cross coupled C analogue seems simple. In fact, synthesizing the nucleoside for photophysical analysis is a matter of one reaction. The goal of the project however, was not to merely synthesize the nucleoside but rather to synthesize it and incorporate it into ODNs. This requirement brought with it a host of demands.

Introduction of the benzoyl protecting group after cross coupling, while valid, drastically reduces ease of purification and increases material loss of the intermediates by purification (**Scheme 3.1**). More specifically (**III-2**) does not lend itself easily to column chromatography and unacceptably low yields are obtained during the purification process of the molecule.



Scheme 3.1 – Proposed route to PyEtdC phosphoramidite

To meet these problems we utilized the lesser known dimethylformamidino (dmf) protecting group. Dimethylformamidino was reasoned to not open the annulation pathway, introduce sufficient lipophilicity for easy column chromatography, and still allow orthogonal protection and deprotection for ODN synthesis. We further realized that unlike previous syntheses, the use of acetyl protecting groups would become unnecessary. The dmf protection would afford us chemoselective protection of the exocyclic amine, which could then be followed by regioselective protection of the primary alcohol of the carbohydrate by standard treatment with DMTCI. The fully protected and halogenated nucleoside could then undergo cross coupling with ethynyl pyrene and subsequent phosphorylation to produce the desired DNA monomer.



Scheme 3.2 – Synthesis of PyEtdC phosphoramidite

Introduction of the dimethyl formamidino group proved to be a facile process which not only proceeded in high yield but provided a substrate (**III-7**) highly amenable to trityl protection. As mentioned in Chapter 2, tritylation reactions have been known to be problematic. Presumably the issues lies with the substrate as uridine protection occurs in high yield (~ 90%) while dC protection or pdC protection requires the utmost stringency to obtain moderate success. In this case, protection of the dmf protected 5-iodo C (**III-7**) nucleoside proceeded in an unprecedented 88% yield.

Cross coupling of the pyrene moiety to the protected nucleoside (**III-8**) proved less effective than tritylation. Isolation of the title compound (**III-9**) only occurred in

moderate yield and numerous attempts at optimization proved fruitless. The yield was sufficient however for forwards progress and the nucleoside was prepared for phosphitylation.

Preparation of the DNA monomer (**III-10**) with phosphitylating agent resulted in a yellow foam that has yet to undergo complete characterization. However, preliminary analysis by ESI / MS has revealed the presence of the desired phosphoramidite.

3.1.2 Synthesis of PyEtdC

It is important to characterize the photophysical properties of the unprotected nucleoside in order to gain a better understanding of the modification in ODNs. With the importance of the bare nucleoside known, it was important to determine a facile method to synthesize the desired material.

Review of the synthesis proposed for the DNA monomer (**III-10**) showed an unnecessary number of steps to obtain the nucleoside and would consume precious material better utilized for DNA synthesis.

In order to combat wasteful chemistries, a simple one step coupling was proposed between 5-iododeoxycytidine (**III-6**) and 1-ethynyl pyrene. The reaction was performed without difficulty as the reagents proved soluble in DMF. As was expected however, purification of the resultant nucleoside (**III-11**) proved difficult. Observed by TLC was a spot to spot conversion of the limiting reagent (**III-6**). This would seemingly imply a complete consumption of material by coupling rather than degradation due to the relatively gentle Sonogashira conditions. This assumption proved difficult to corroborate as work up and purification produced only a 50% yield. The expectant difficulty in isolation was and always has been attributed to the polarity of the unprotected nucleoside. The molecule generally irreversibly binds to silica and is commonly, “lost” in column chromatography.

3.1.3 PyEtdC Photophysics

We began our photophysical survey of the PyEtdC nucleoside by examining the characteristic excitation and emission spectra in ethanol and water (**Figure 3.2** / **Figure 3.3**).

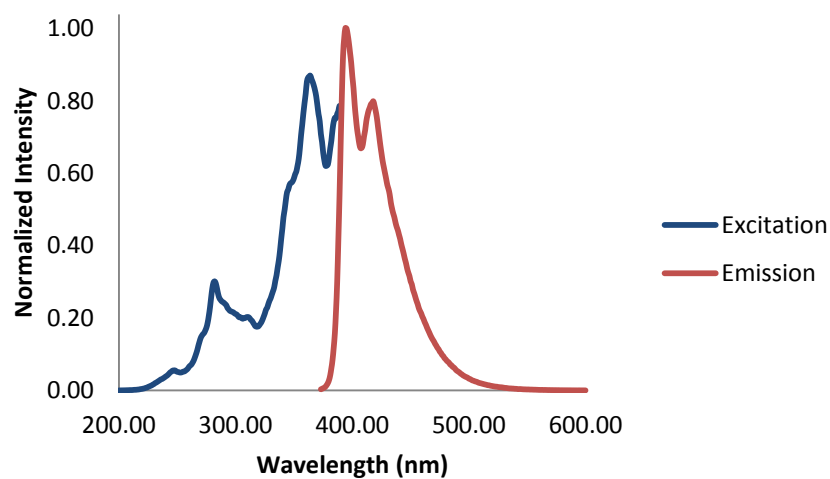


Figure 3.2 – Luminescence profile of PyEtdC in ethanol at 1.1 μM

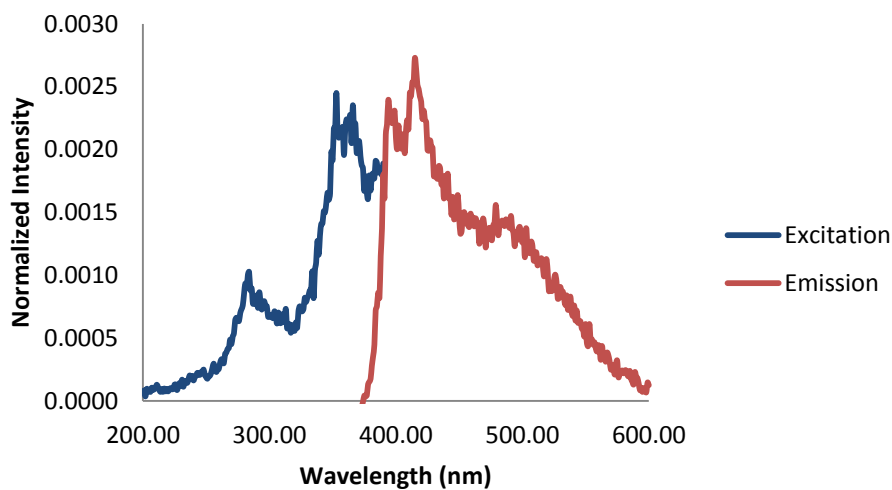


Figure 3.3 - Luminescence profile of PyEtdC in water at 1.1 μM normalized to the highest intensity peak in **Figure 3.2**

Of immediate interest is the very small Stokes shift (**Table 3.1**) not observed in pyrene (**Figure 3.4**). We further observe less dramatic red shifting of the PyEtdC profile (in comparison to PypdC) from pyrene (**Figure 3.4**). Now, as is the case in PypdC we observe the involvement of the S_3 , S_2 , and S_1 excited states in the fine structure of the excitation plot. However, unlike PypdC we observe emission reminiscent of pyrene. This may indicate that the base contributes little fluorescence character and that the molecule more closely reflects the electronics of the substituent.

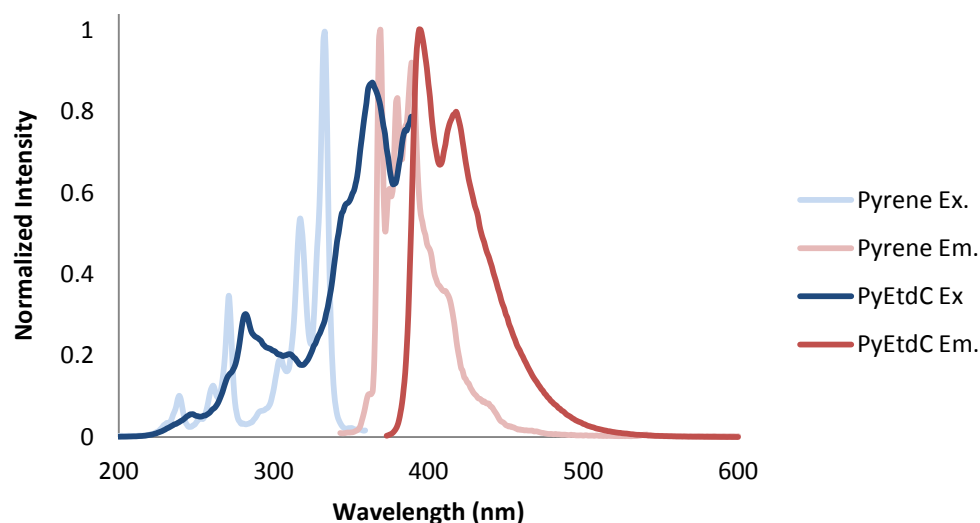


Figure 3.4 – PyEtdC luminescence profile vs. pyrene.

Further bolstering the argument, we see very little fluorescence character reminiscent of PhpdC (**Figure 3.5**) showing a drastic departure from the traditional Hudson group fluorophore. These excitation and emission spectra further provide evidence that PyEtdC is less like PhpdC and PypdC and more closely related to pyrene.

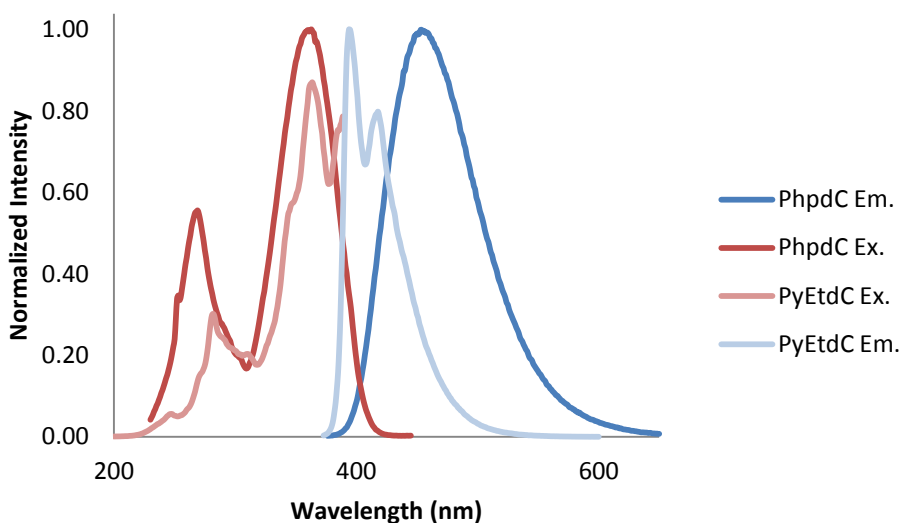


Figure 3.5 – Normalized fluorescence of PhpdC and PyEtdC

A greater ON response in ethanol is observed for that of PyEtdC nucleoside (~ 333 times more fluorescent) than that of the PypdC analogue (~ 66 times more fluorescent) in water. PyEtdC further displays aggregative behaviour in water as excimer emission is observed (**Figure 3.3**) which is not observed (**Figure 3.2**) at equimolar concentration in ethanol. The aggregative behaviour may indicate a high affinity for base stacking which may imply facile entrance into excimer technologies that may not be possible with the PypdC analogue.

A photophysical survey of PyEtdC in comparison to PypdC (**Table 3.1**) shows two very different molecules.

Table 3.1 – Comparison of PypdC & PyEtdC

Compound	Solvent	λ_{ex}^a	λ_{em}^a	ε^b	Φ_f	Stokes shift ^a	Brightness	Polarity sensitivity ^c
PypdC	Ethanol	388	443	16.0	0.6	55	9.6	34
	Water	377	485	-	0.018	108	-	
PyEtdC	Ethanol	363	393	31.0	.55	30	17	31
	water	383	394	-	0.003	11	-	

^anm, ^b $10^3 \text{ M}^{-1} \text{ cm}^{-1}$, ^c $\text{cm}^{-1}/(\text{kcal}\cdot\text{mol}^{-1})$

In terms of brightness, we clearly observe a molar absorptivity difference between PypdC and PyEtdC of nearly two fold in favour of PyEtdC. The fluorescence quantum yields are quite close, so this difference can be attributed solely to the difference in molar extinction coefficient. Thus PyEtdC is a significantly brighter fluorophore even at the mismatched molarities (**Figure 3.5**).

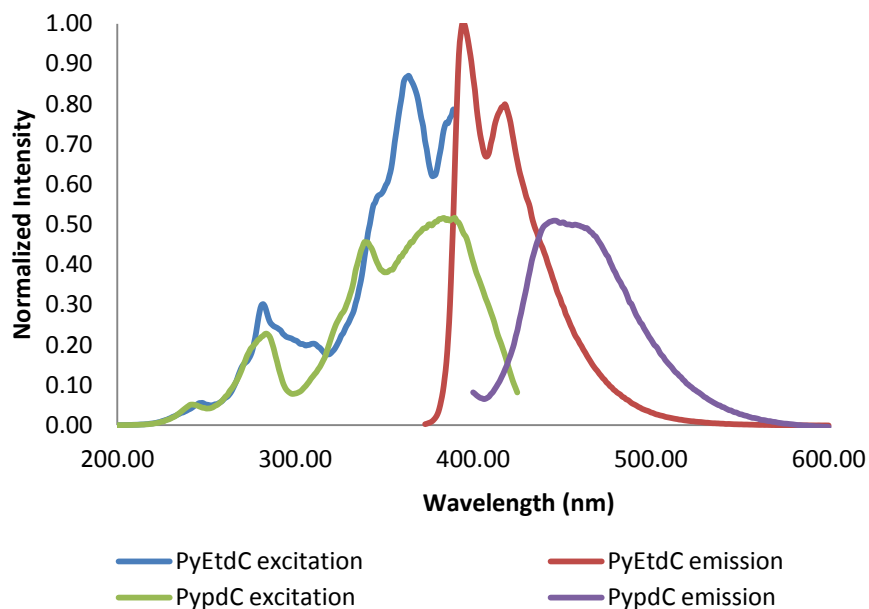


Figure 3.6 – Brightness comparison; PypdC (2.2 μM) vs. PyEtdC (1.1 μM) in ethanol

3.1.4 Conclusions and Future Work

The PyEtdC monomer for DNA synthesis has been completed in a quantity sufficient for preliminary ODN studies and photophysical studies on the nucleoside have been completed. Due to time constraints ODN synthesis has not yet been undertaken.

Future work will include incorporation of the PyEtdC nucleoside into the Mano 1 Mod, Mano 2 Mod, and CFTR Mod sequences for direct comparison to PypdC and literature pdC analogues. Once a survey of PyEtdCs qualities has been completed, it will likely find itself in use as the key component in excimer and monomer switching molecular beacons.

3.2 Experimental

3.2.1 Synthetic Procedures and Characterization

Synthesis of 2'-Deoxy-5-(1-pyrenylethynyl)cytidine (III-11)

To dry DMF (5 mL) was added 2'-deoxy-5-iodocytidine (0.50 g, 1.41 mmol) and 1-ethynylpyrene (0.41 g, 1.83 mmol). The stirring mixture was degassed and placed under N₂ utilizing a dry ice / acetone bath and dry line. To the degassed mixture was added Pd(PPh₃)₄ (0.16 g, 0.141 mmol) and CuI (53 mg, 0.282 mmol) followed by further deoxygenation utilizing the previously described procedure. Deoxygenated triethylamine (0.72 mL, 5.64 mmol) was then added to the reaction mixture. The reaction mixture was stirred in darkness at r.t. for 18 hrs. Upon completion the reaction solvent was removed by reduced pressure and dried overnight by high vacuum. The resulting orange/red solid was purified by column chromatography utilizing a DCM/methanol mobile phase (95:5 DCM/MeOH). The desired fractions were collected and dried to produce 2'-deoxy-5-(1-pyrenylethynyl)-cytidine (0.31 g, 50%). ¹H NMR (DMSO-*d*₆): δ = 8.63 (s, 1H), 8.57 (d, *J*₁=9.38 Hz, 1H), 8.43 (d, *J*₁= 7.82 Hz, 1H), 8.35 (m, 4H), 8.23 (q, *J*₁= 8.99, 2H), 8.12 (m, 1H), 7.91 (br, s, 1H), 7.25 (br, s, 1H), 6.19 (t, *J*₁=6.25, 1H), 5.28 (m, 2H), 4.30 (m, 1H), 3.85 (m, 1H), 3.69 (m, 2H), 2.19 (m, 2H). HRMS (ESI) *m/z* calcd for C₂₇H₂₂N₃O₄ [MH⁺] 452.1610, found 452.1590.

Synthesis of 2'-Deoxy-*N*⁴-dimethylformamidino-5-iodocytidine (III-7)

An oven dried flask was charged with 2'-deoxy-5-iodo-cytidine (0.50 g, 1.41 mmol) and placed under nitrogen. To the flask was syringed 5 mL dry DMF and N,N-dimethylformamide dimethyl acetal (0.94 mL, 7.07 mmol). The reaction was heated to 50 °C and stirred for 24 hrs. The reaction solvent was removed by rotovap and the remaining solid was subjected to column chromatography (95:5 DCM/MeOH) and the desired dmf protected nucleoside was isolated as white foam (0.52 g, 90 %). ¹H NMR (DMSO-*d*₆): δ = 8.58 (s, 1H), 8.46 (s, 1H), 6.08 (t, *J*₁= 6.25 Hz, 1H), 5.22 (d, *J*₁= 4.3 Hz, 1H), 5.13 (t, *J*₁=4.88 Hz, 1H), 4.21 (dd, *J*₁=5.86 Hz, *J*₂=3.91 Hz, 1H), 3.80 (q, *J*₁= 3.52 Hz, 1H), 3.64 (m, 1H), 3.55 (m, 1H), 3.20 (s, 3H), 3.12 (s, 3H), 2.18 (ddd, *J*₁=13.19 Hz, *J*₂ = 5.96, *J*₃ = 3.91), 2.01 (dt, *J*₁= 13.19 Hz, *J*₂ = 6.5 Hz, 1H). ¹³C NMR (DMSO-*d*₆): δ =

168.02, 158.29, 154.18, 147.33, 87.49, 85.68, 69.80, 68.71, 60.74, 40.97, 40.90, 34.92.
HRMS (ESI) m/z calcd for $C_{12}H_{18}N_4O_4I$ $[MH^+]$ 409.0373, found 409.0385.

Synthesis of 2'-Deoxy-5'-*O*-(4,4'-dimethoxytrityl)-*N*⁴-dimethylformamidino-5-cytidine (III-8)

2'-Deoxy-*N*⁴-dimethylformamidino-5-iodocytidine (0.33 g, 0.809 mmol) was dissolved in 10 mL dry pyridine and taken to dryness by reduced pressure three times and subjected to high vacuum for a period of 12 hours. The dried nucleoside was dissolved in 5 mL pyridine under an inert atmosphere of nitrogen and placed on an ice bath. In a separate oven dried flask, DMTCI (0.41 g, 1.21 mmol) was placed under nitrogen and brought to 0 °C. The DMTCI was dissolved by the dropwise addition of 5 mL dry pyridine and was transferred to the reaction vessel containing the dried nucleoside by syringe and slow addition on ice. Upon completion, the reaction mixture was placed in an ice bath for 15 minutes, 5 mL methanol was added, and the reaction was allowed to stir at r.t. for 10 minutes. The solvent was removed by rotary evaporation and the crude mixture was purified by column chromatography (89:10:1 DCM/MeOH/Et₃N). 2'-Deoxy-5'-*O*-(4,4'-dimethoxytrityl)-*N*⁴-dimethylformamidino-5-iodocytidine was isolated as a white foam (0.50 g, 88%). ¹H NMR (DMSO-*d*₆): δ = 8.58 (s, 1H), 8.13 (s, 2H), 7.40 (d, $J_1 = 7.42$, 2H), 7.30 (m, 6H), 7.23 (m, 1H), 6.91 (s, 2H), 6.89 (m, 2H), 6.11 (t, $J_1 = 6.64$, 1H), 5.30 (br, 1H), 4.20 (m, 1H), 3.93 (m, 1H), 3.73 (br, s, 6H), 3.21 (s, 3H), 3.12 (s, 3H), 2.25 (m, 1H), 2.12 (m, 1H). ¹³C NMR (DMSO-*d*₆): δ = 168.17, 158.37, 158.08, 154.08, 146.32, 144.75, 135.46, 135.41, 129.73, 127.96, 127.65, 126.71, 113.31, 85.91, 85.86, 70.67, 69.14, 63.65, 55.07, 40.92, 34.94. HRMS (ESI) m/z calcd for $C_{33}H_{36}N_4O_6I$ $[MH^+]$ 711.1680, found 711.1655.

Synthesis of 2'-Deoxy-5'-*O*-(4,4'-dimethoxytrityl)-*N*⁴-dimethylformamidino-5-(1-pyrenylethynyl)cytidine (III-9)

To dry DMF (5 mL) was added 2'-deoxy-5'-*O*-(4,4-dimethoxytrityl)-*N*⁴-dimethylformamidino-5-iodocytidine (0.50 g, 1.22 mmol) and 1-ethynylpyrene (0.41 g, 1.83 mmol). The stirring mixture was degassed and placed under N₂ utilizing a dry ice / acetone bath and dry line. To the degassed mixture was added Pd(PPh₃)₄ (0.14 g, 0.12

mmol) and CuI (46 mg, 0.244 mmol) followed by further deoxygenation utilizing the previously described procedure. Deoxygenated triethylamine (0.62 mL, 4.88 mmol) was then added to the reaction mixture. The reaction mixture was stirred in darkness at r.t. for 18 hrs. Upon completion the reaction was diluted with 25 mL DCM and washed against five 50 mL portions of 5% EDTA and one 50 mL portion of brine. The organic layer was dried over sodium sulphate and removed by rotovap. The resulting orange/red solid was purified by column chromatography utilizing a DCM/methanol mobile phase (DCM \rightarrow 97:2:1 DCM/methanol/Et₃N). The desired fractions were collected and dried and taken into 1 mL DCM. The DCM was then dropped by pipette into 10 mL stirring hexanes to produce a light yellow precipitate. The precipitate was gravity filtered and allowed to air dry overnight. 2'-Deoxy-5'-O-(4,4'-dimethoxytrityl)-N^d-dimethylformamidino-5-(1 pyrenylethynyl)cytidine was collected off the filter paper as a light yellow powder (0.59 g, 60 %). ¹H NMR (DMSO-*d*₆): δ = 8.81 (s, 1H), 8.73 (d, $J_1=8.99$, 1H), 8.41 (s, 1H), 8.32 (d, $J_1=7.82$ Hz, 2H), 8.15 (m, 5H), 7.49 (m, 3H), 7.38 (dd, $J_1=8.99$ Hz, $J_2=2.34$ Hz, 4H), 7.30 (t, $J_1=7.82$ Hz, 2H), 7.13 (m, 1H), 6.84 (m, 4H), 6.21 (t, $J_1=6.45$ Hz, 1H), 5.37 (d, $J_1=4.3$ Hz, 1H), 4.32 (dd, $J_1=5.86$ Hz, $J_2=3.52$ Hz, 1H), 4.05 (m, 1H), 3.55 (s, 3H), 3.54 (s, 3H), 3.38 (s, 3H), 3.31 (s, 3H), 3.23 (m, 2H), 2.40 (ddd, $J_1=13.38$ Hz, $J_2=6.15$ Hz, $J_3=3.13$ Hz, 1H), 2.23 (m, 1H). HRMS (ESI) *m/z* calcd for C₅₁H₄₅N₄O₆ [MH⁺] 809.3339, found 809.3303.

Synthesis of 2'-Deoxy-3'-(-cyanoethyl)diisopropylphosphoramidite-5'-O-(4,4'-dimethoxytrityl)-N^d-dimethylformamidino-5-(1 pyrenylethynyl)-cytidine (III-10)

2-Cyanoethyl diisopropylphosphoramidochloridite (0.0998 g, 0.4219 mmol) was added to a solution of 2'-Deoxy-5'-O-(4,4'-dimethoxytrityl)-N^d-dimethylformamidino-5-(1 pyrenylethynyl)cytidine (III-9) (0.1705 g, 0.2109 mmol) and Et₃N (0.4 mL) in dry DCM (2 mL). The reaction was allowed to stir at room temperature under N₂ for 3 hours. The reaction was quenched with MeOH (0.5 mL), washed with 0.5 M NaHCO₃ (10 mL) and the organic phase was dried with Na₂SO₄. The residue was purified by column chromatography using gradient elution (DCM/acetone/Et₃N, 99:0:1 to 94:5:1) to give a yellow foam (0.16 g, 80%).

HRMS (ESI) m/z calcd for $C_{60}H_{62}N_6O_7P$ $[MH^+]$ 1009.4418, found 1009.4417

4 Summary and Conclusion

We successfully developed a synthetic route leading to the PypdC phosphoramidite for DNA synthesis (**Scheme 2.4**). We incorporated the phosphoramidite into ODNs in acceptable yield without the modification of coupling time or changing of the standard synthetic cycle. Attempts at coupling three adjacent modifications failed and requires further work to make contiguous synthesis possible.

Thermal denaturation studies on duplexes of PypdC containing oligos showed a possible stabilization effect due to the presence of the modified insert with respect to natural C. This is attributed to a favourable pi stacking interaction due to the presence of pyrene allowing greater overlap with adjacent bases.

The PypdC nucleoside underwent photophysical characterization to understand the effects of the pyrene substituent on the fluorescent nature of the C analogue. It was found that the PypdC nucleoside exhibited excitation character similar to that of pyrene with a featureless emission similar to that of previous pdC analogues. It was determined that PypdC fluorescence is less characteristic of pyrene and more indicative of pyrrolocytosine.

Spectroscopic studies on PypdC containing oligos showed fluorescence intensity change with respect to the complementary base as has been previously observed for pyrrolocytosine analogues. In addition to intensity change a Stokes shift change was observed for the match case which was not observed for the mismatch and ss cases. The intrinsically fluorescent nature of the pyrene substituent would then seem inconsequential to the base discriminating nature of the C analogue.

Future work will include thermal denaturation experiments on the remaining PypdC containing oligos. Characterization of the ODNs fluorescence response with respect to base complement will be conducted confirming or disproving the base discriminating nature and stabilizing effect thought to be attributed to PypdC.

In addition to the PypdC analogue we further reported the synthesis of the PyEtdC monomer (**Scheme 3.2**). The phosphoramidite was not incorporated into ODNs however photophysical studies on the nucleoside were completed.

It was determined that PyEtdC excitation and emission is closely related to that of pyrene. This may indicate that the fluorescent C analogue may act more like a base with a pendant pyrene fluorophore rather than a traditional base discriminating fluorophore.

To further understand the electronics of the analogue it will be incorporated into ODNs for stabilization and fluorescence study.

Appendix

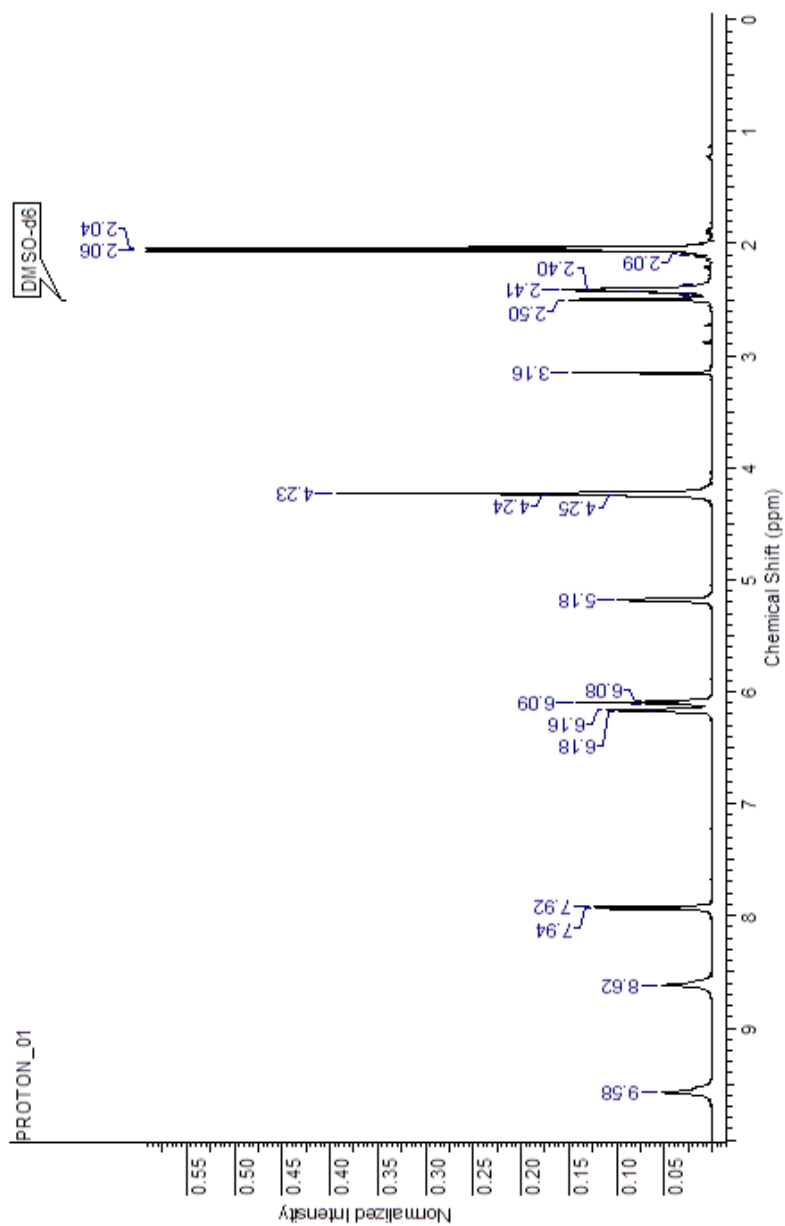
Table of Contents

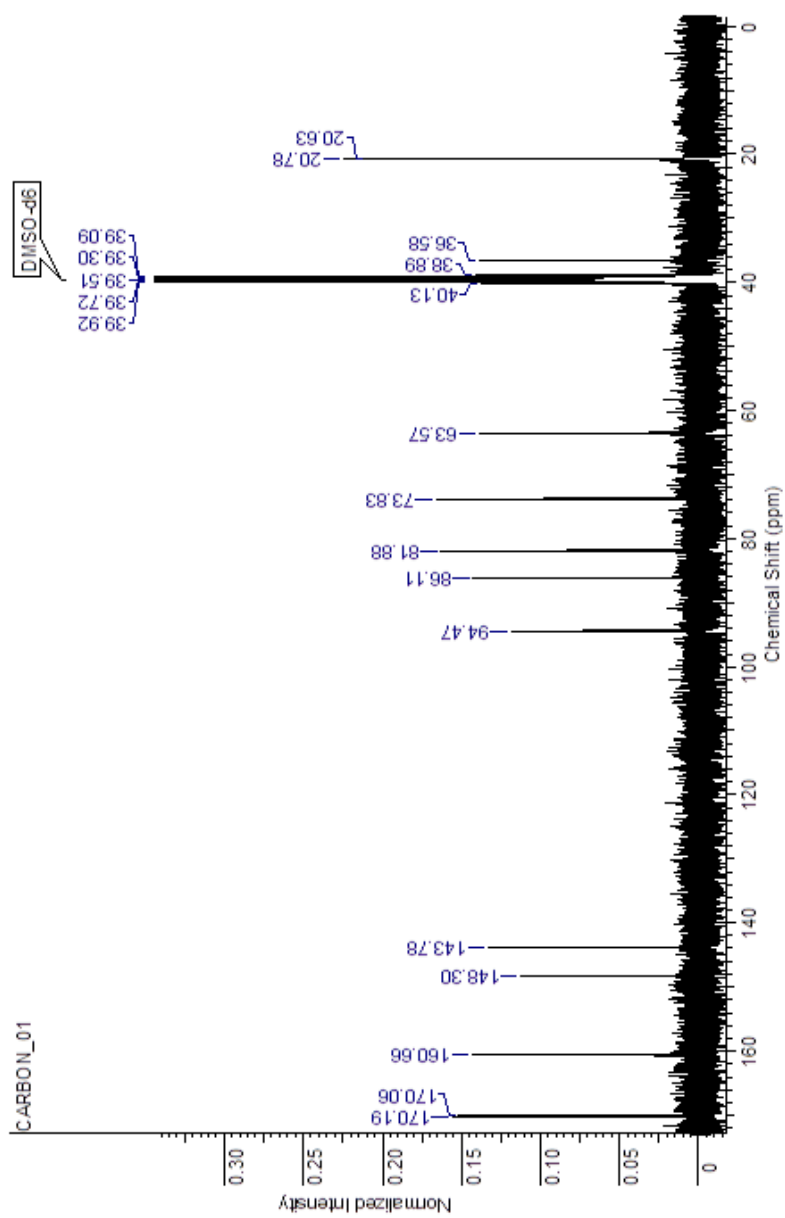
General Remarks.....	68
¹ H NMR (II-7).....	69
¹³ C NMR (II-7).....	70
¹ H NMR (II-8).....	71
¹³ C NMR (II-8).....	72
¹ H NMR (II-9).....	73
¹³ C NMR (II-9).....	74
¹ H NMR (II-10).....	75
¹³ C NMR (II-10).....	76
¹ H NMR (II-11).....	77
¹³ C NMR (II-11).....	78
¹ H NMR (II-12).....	79
¹³ C NMR (II-12).....	80
¹ H NMR (II-13).....	81
³¹ P NMR (II-13).....	82
UPLC Trace (II-14).....	83
UPLC Trace (II-15).....	83

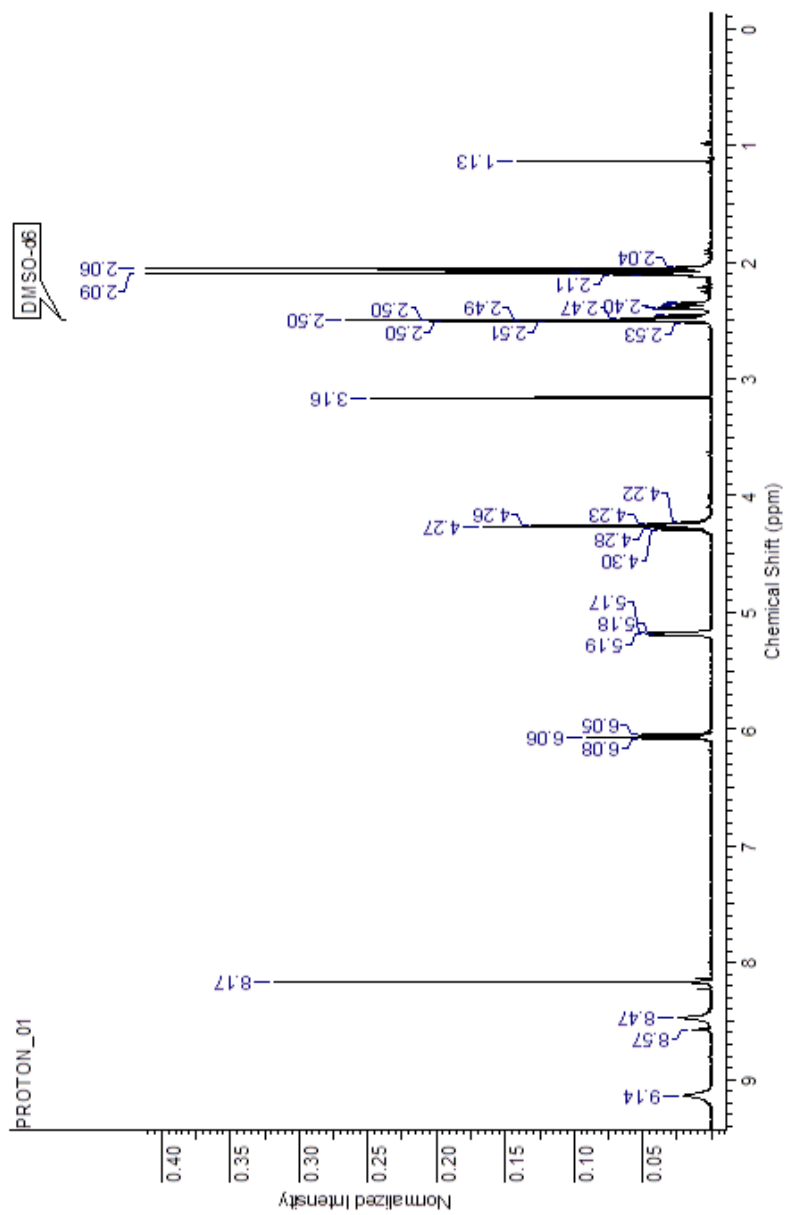
UPLC Trace (II-16).....	84
Thermal Denaturation Curve – Control + Match G.....	85
Thermal Denaturation Curve – CFTR Mod (II-16) + Match G.....	86
Thermal Denaturation Curve – CFTR Mod (II-16) + Mismatch A.....	87
Thermal Denaturation Curve – CFTR Mod (II-16) + Mismatch C.....	88
Thermal Denaturation Curve – CFTR Mod (II-16) + Mismatch T.....	89
UPLC Trace (III-11).....	90
¹ H NMR (III-11).....	91
¹ H NMR (III-7).....	92
¹³ C NMR (III-7).....	93
¹ H NMR (III-8).....	94
¹³ C NMR (III-8).....	95
¹ H NMR (III-9).....	96
UPLC Trace (III-9).....	97

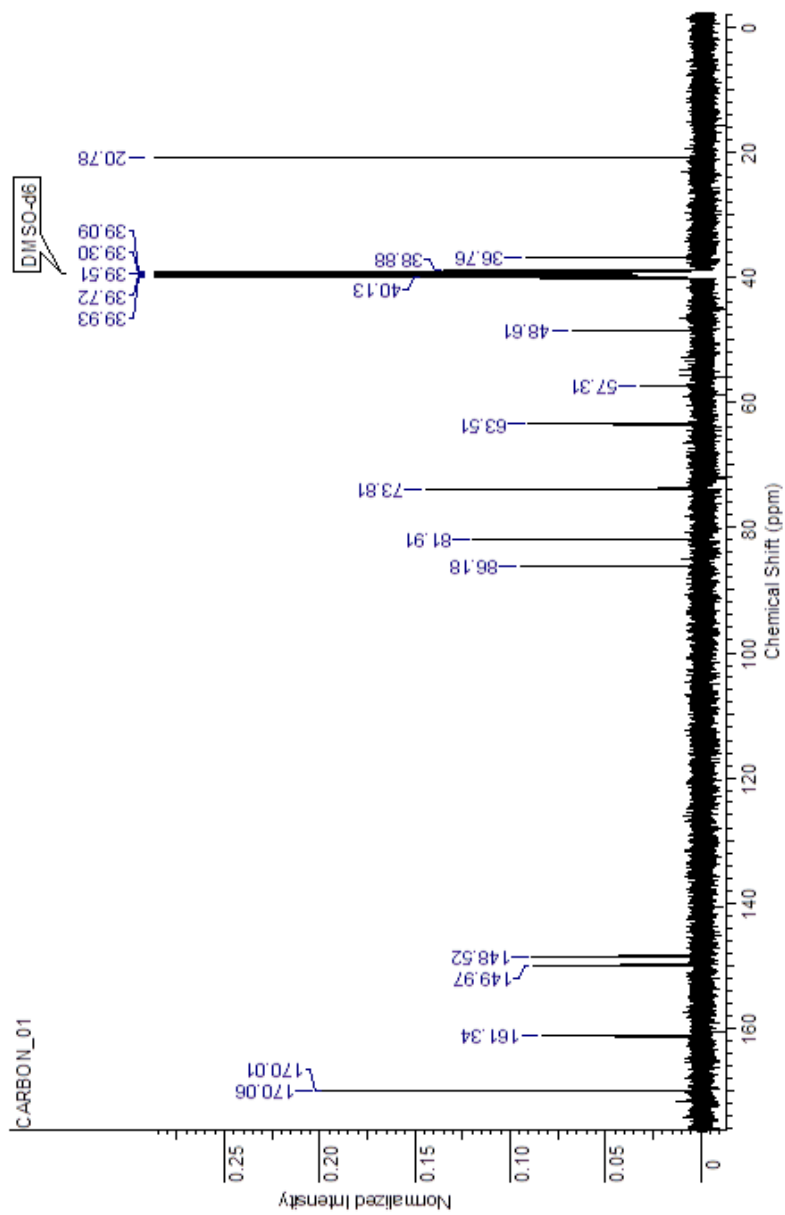
General Remarks

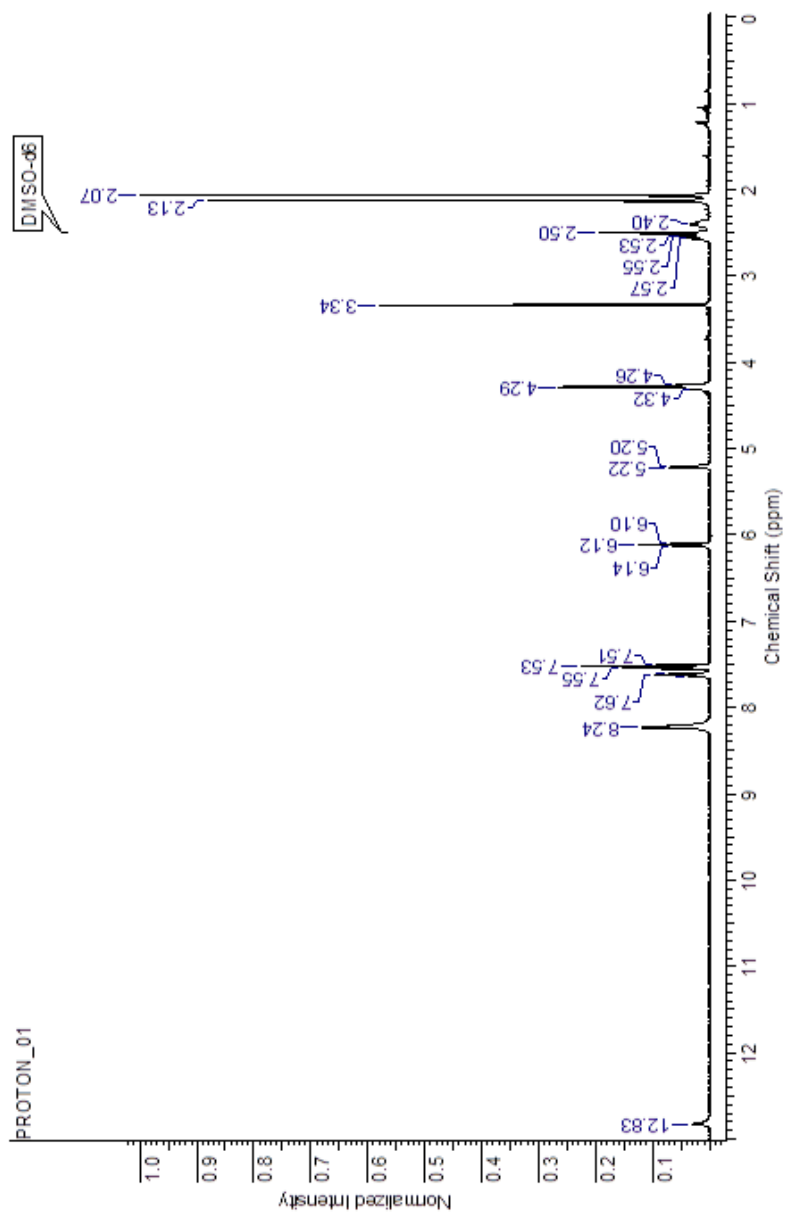
All chemicals were obtained from commercial sources and used without further purification. Flash column chromatography (FCC) was performed on Merck Kieselgel 60 TLC plates. NMR spectra were performed on a Varian Mercury 400 instrument. Chemical Shifts are reported in parts per million (δ), were measured from tetramethylsilane (0 ppm) and are referenced to the residual proton in the deuterated solvent: acetone - d_6 (2.05 ppm), $CDCl_3$ (7.26 ppm), DMSO - d_6 (2.49 ppm) for 1H NMR and acetone - d_6 (29.8, 206.3 ppm), $CDCl_3$ (77.0 ppm), DMSO - d_6 (39.5 ppm) for ^{13}C NMR spectroscopy. Multiplicities are described as s (singlet), d (doublet), t (triplet), q (quartet), p (pentet), m (multiplet), and br s (broad singlet). Coupling constants (J) are reported in Hertz (Hz). High resolution mass spectra (HRMS) and low resolution mass spectra were obtained using electron impact (EI) or electrospray ionization (ESI) methods.

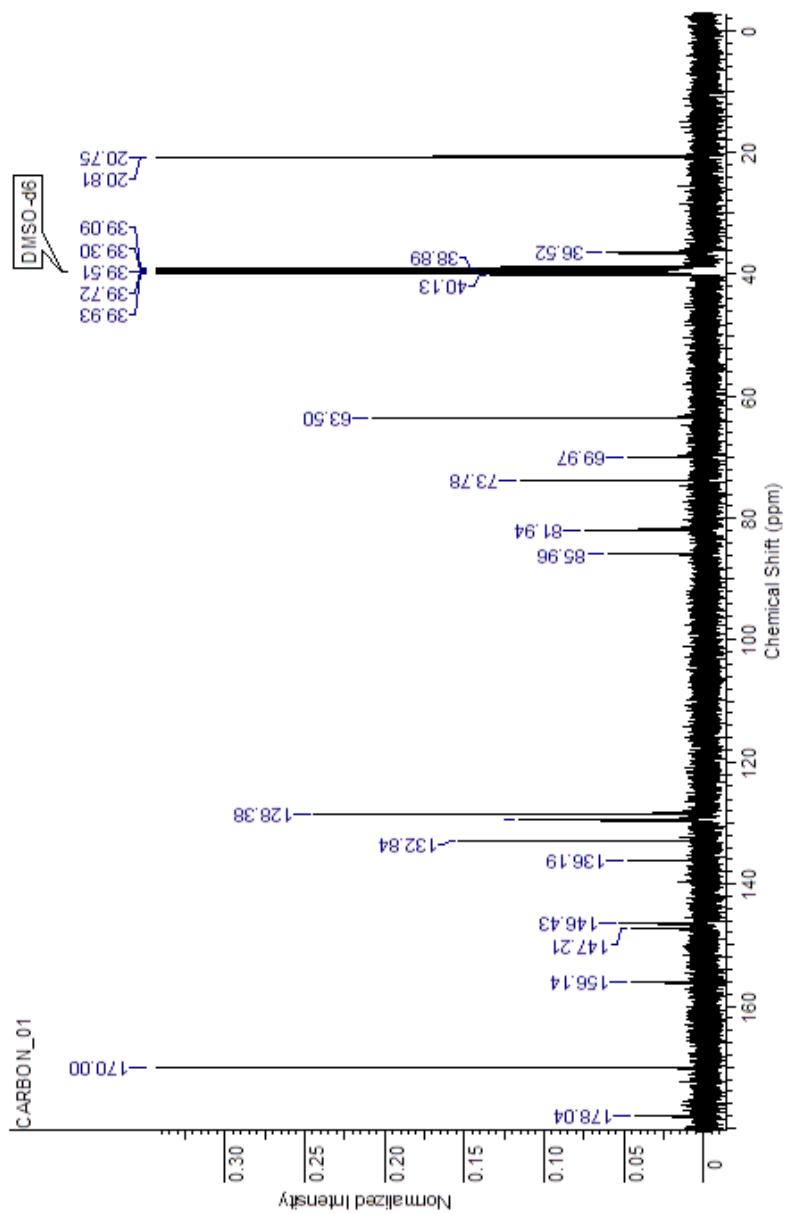
¹H NMR 3',5'-O-acetyl-2'-deoxycytidine (II-7)

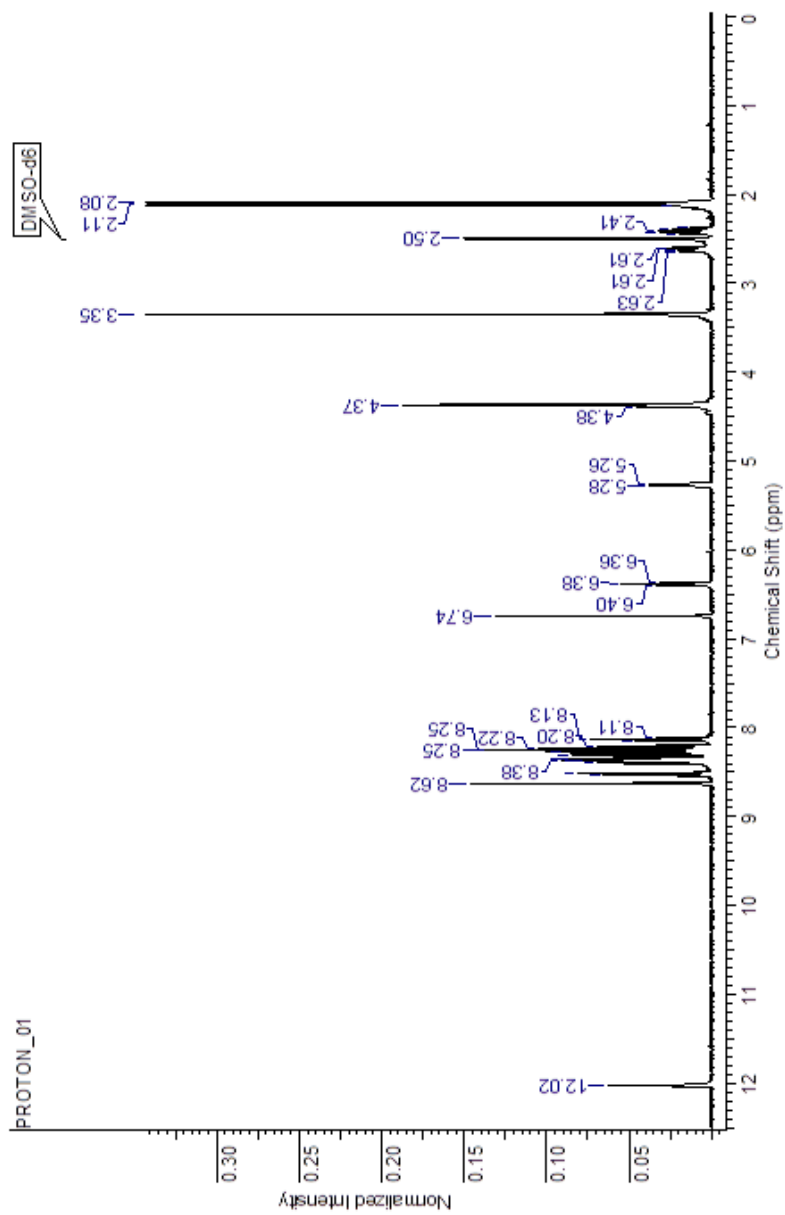
^{13}C NMR 3',5'-O-acetyl-2'-deoxycytidine (II-7)

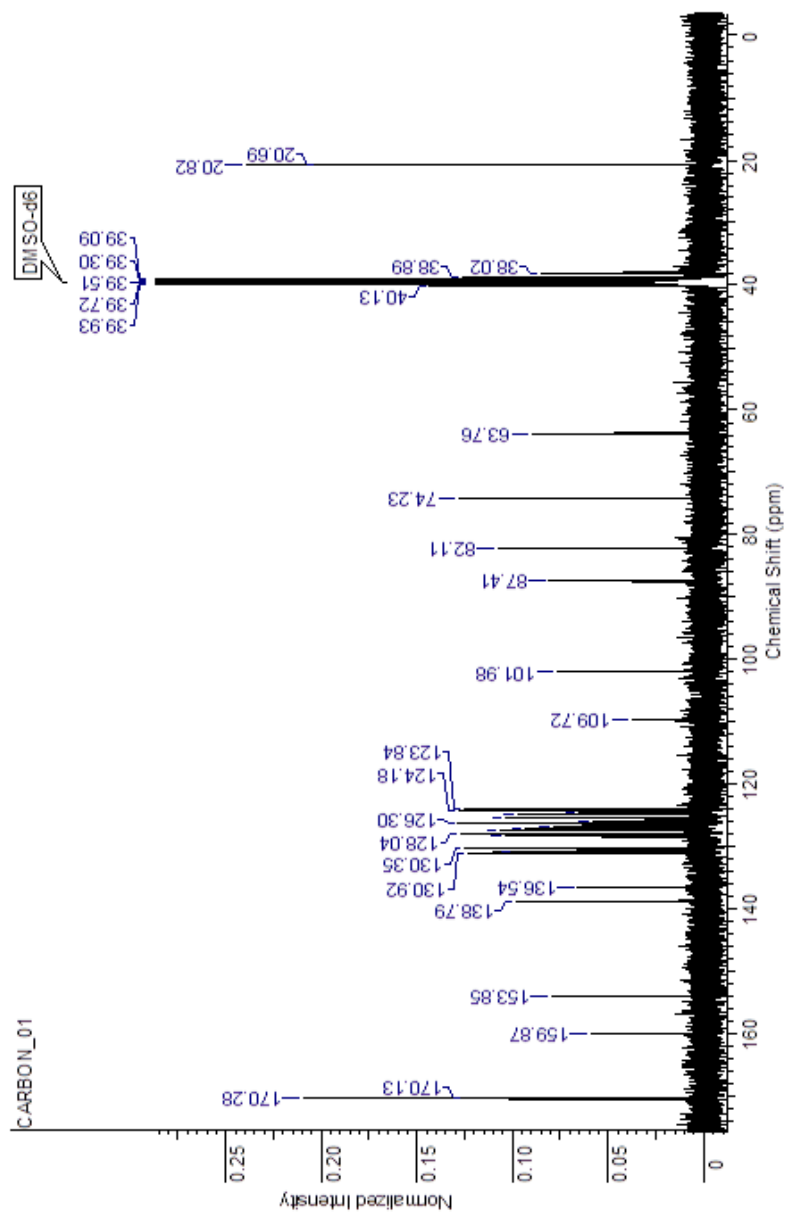
¹H NMR 2'-Deoxy-3',5'-O-acetyl-5-iodocytidine (II-8)

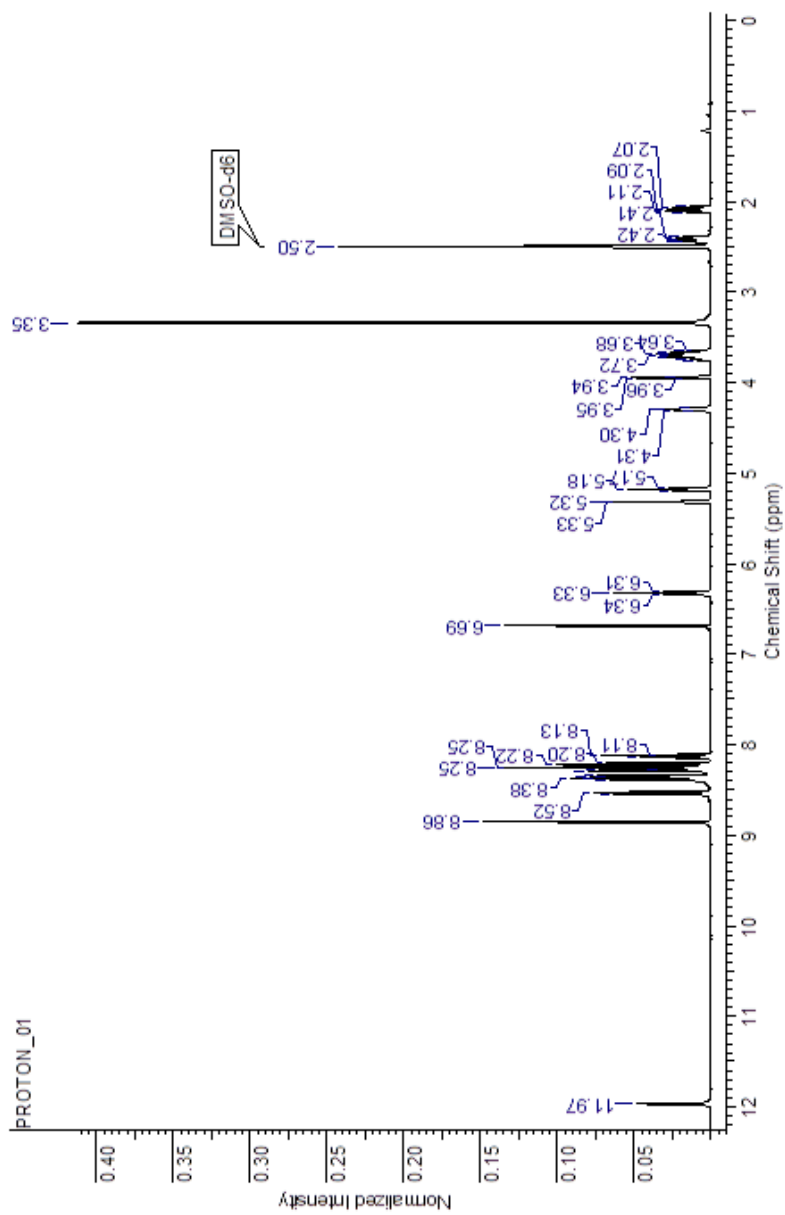
^{13}C NMR 2'-Deoxy-3',5'-O-acetyl-5-iodocytidine (II-8)

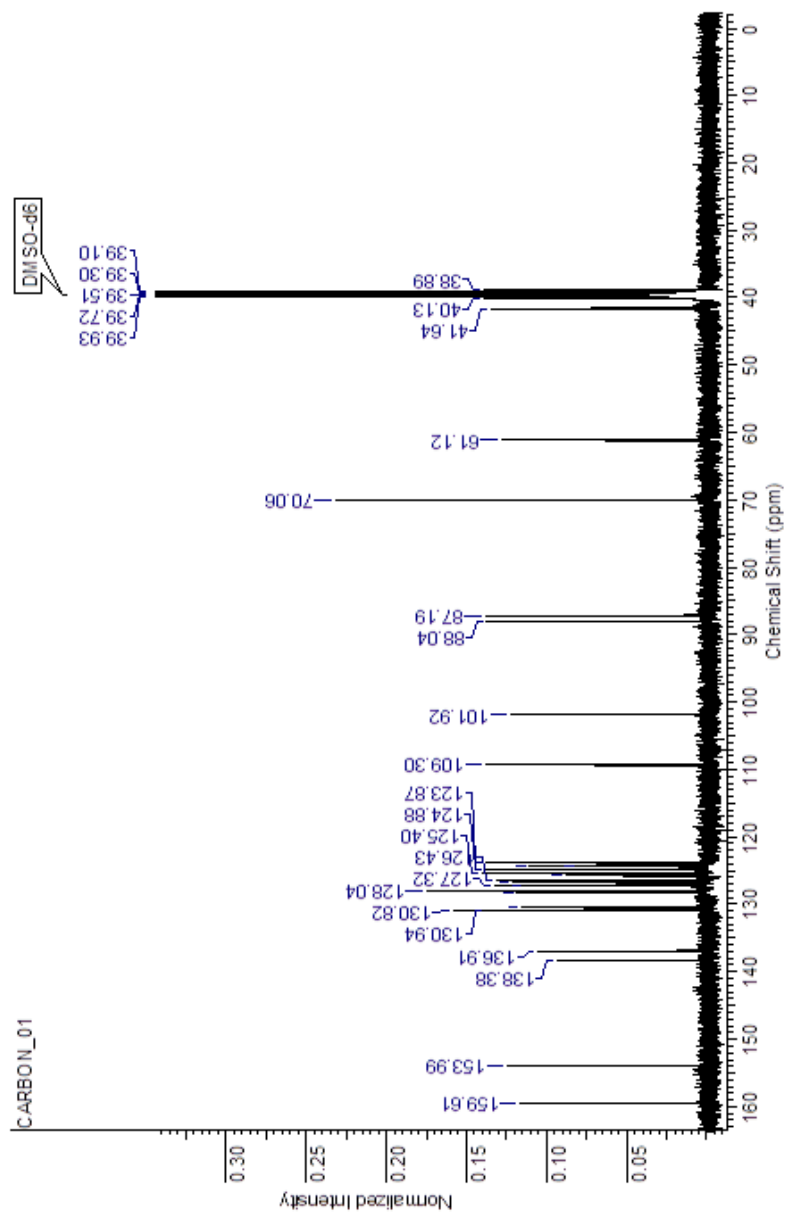
¹H NMR 2'-Deoxy-3',5'-O-acetyl-N⁴-benzoyl-5-iodocytidine (II-9)

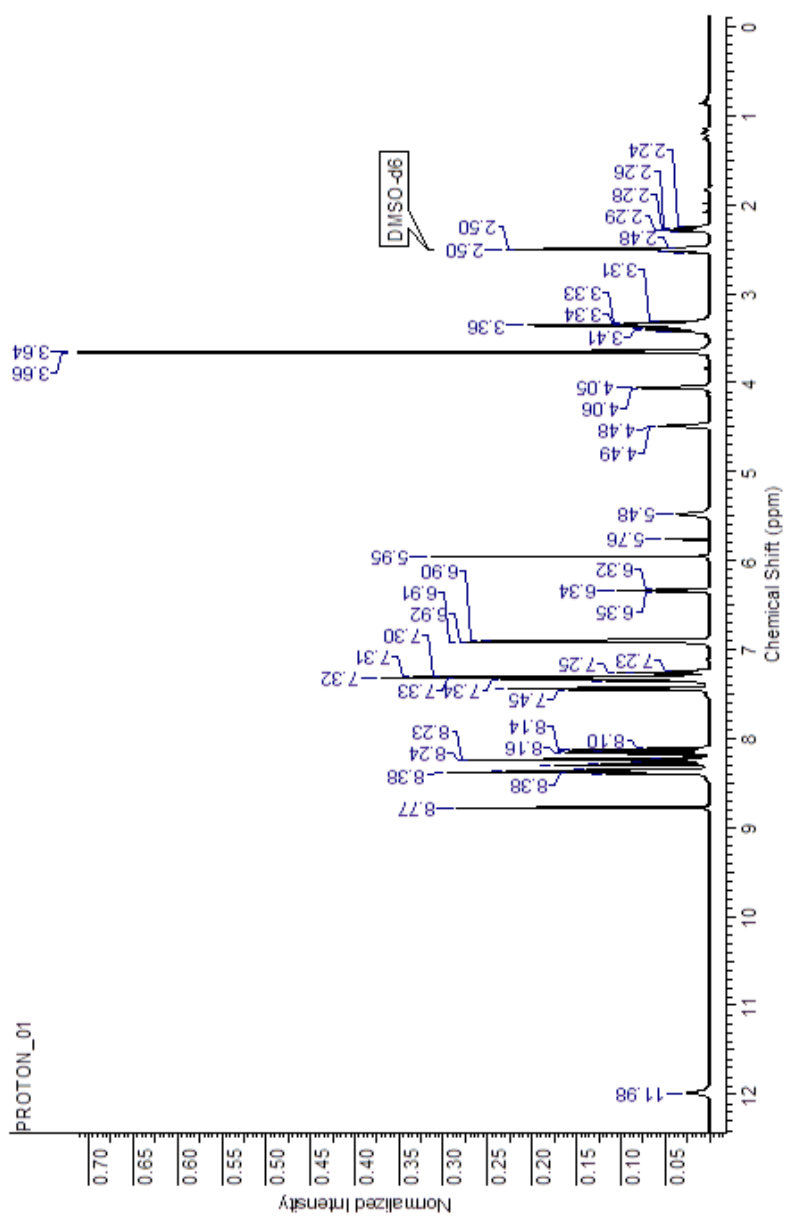
^{13}C NMR 2'-Deoxy-3',5'-*O*-acetyl-*N*⁴-benzoyl-5-iodocytidine (II-9)

¹H NMR 2'-Deoxy-3',5'-O-acetyl-6-(1-pyrenylethynyl)-pyrrolocytidine (II-10)

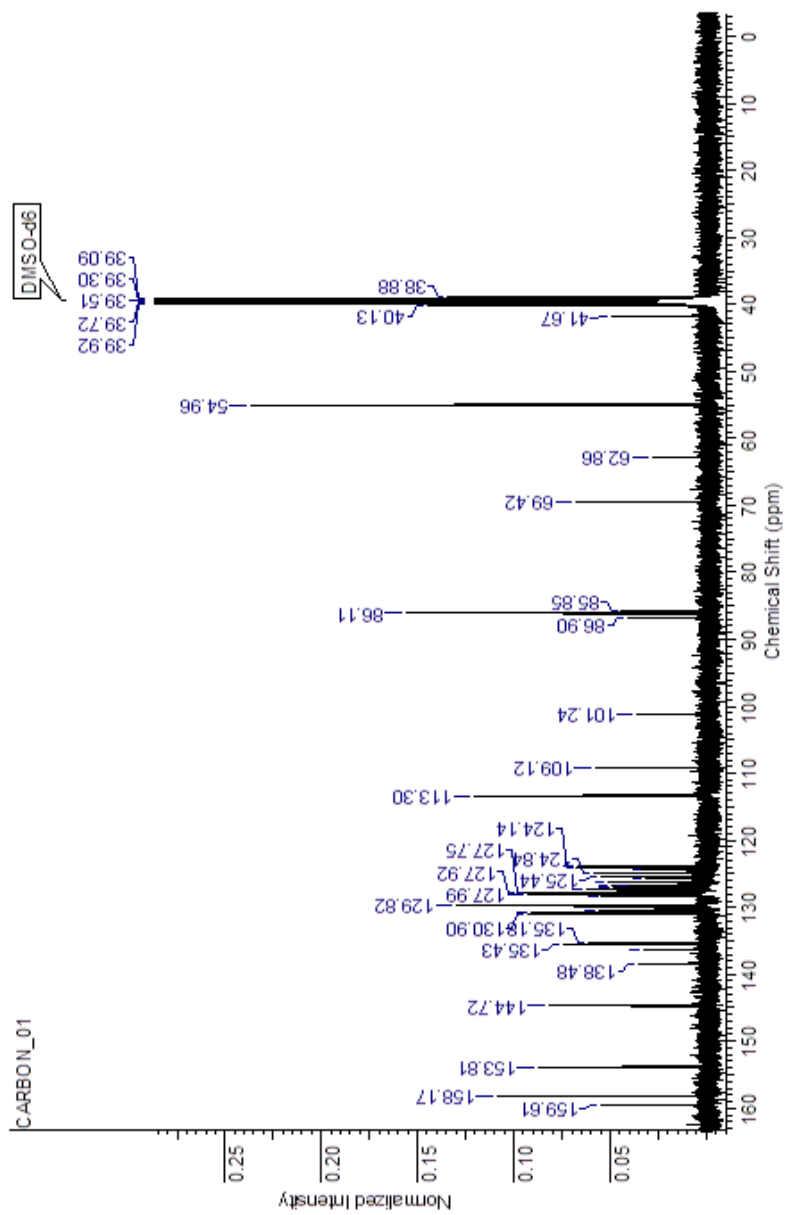
¹³C NMR 2'-Deoxy-3',5'-O-acetyl-6-(1-pyrenylethynyl)-pyrrolocytidine (II-10)

¹H NMR 2'-Deoxy-6-(1-pyrenylethynyl)-pyrrolocytidine (II-11)

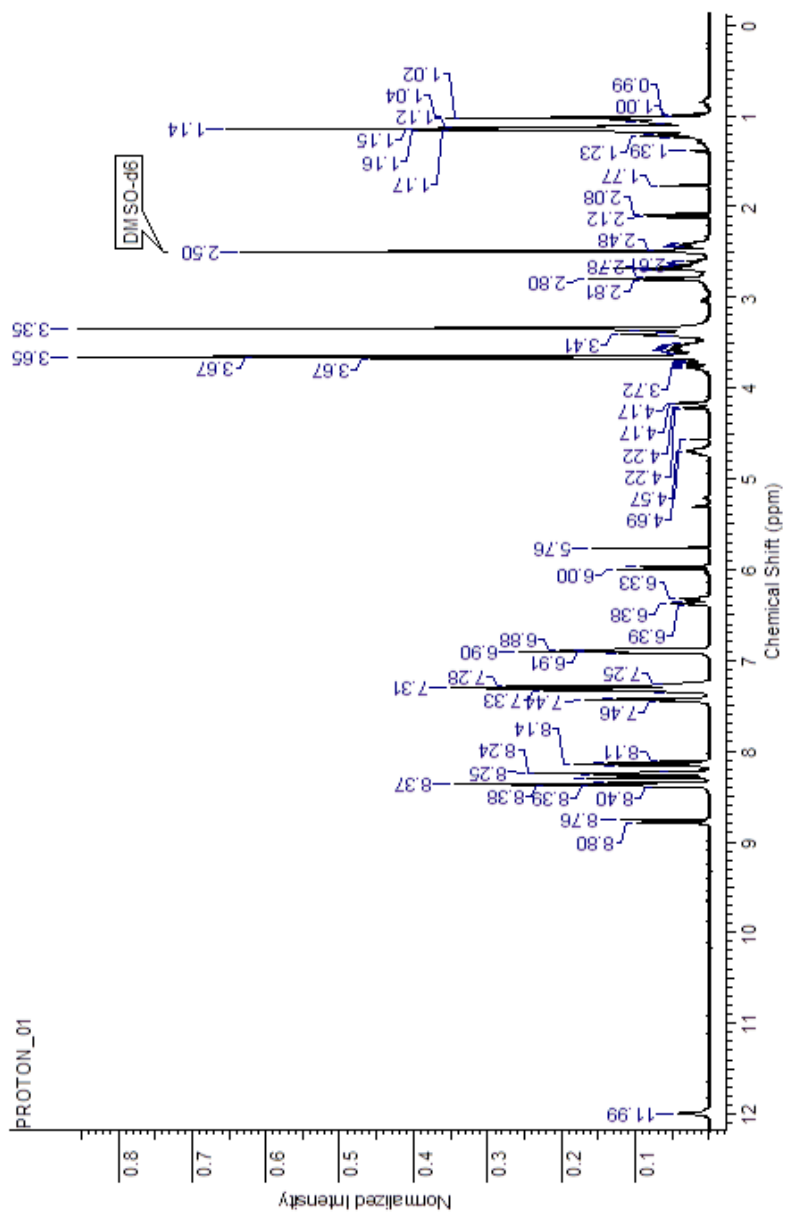
^{13}C NMR 2'-Deoxy-6-(1-pyrenylethynyl)-pyrrolocytidine (II-11)

¹H NMR 2'-Deoxy-5'-O-(4,4'-dimethoxytrityl)-6-(1-pyrenylethynyl)-pyrroloctytidine (II-1).

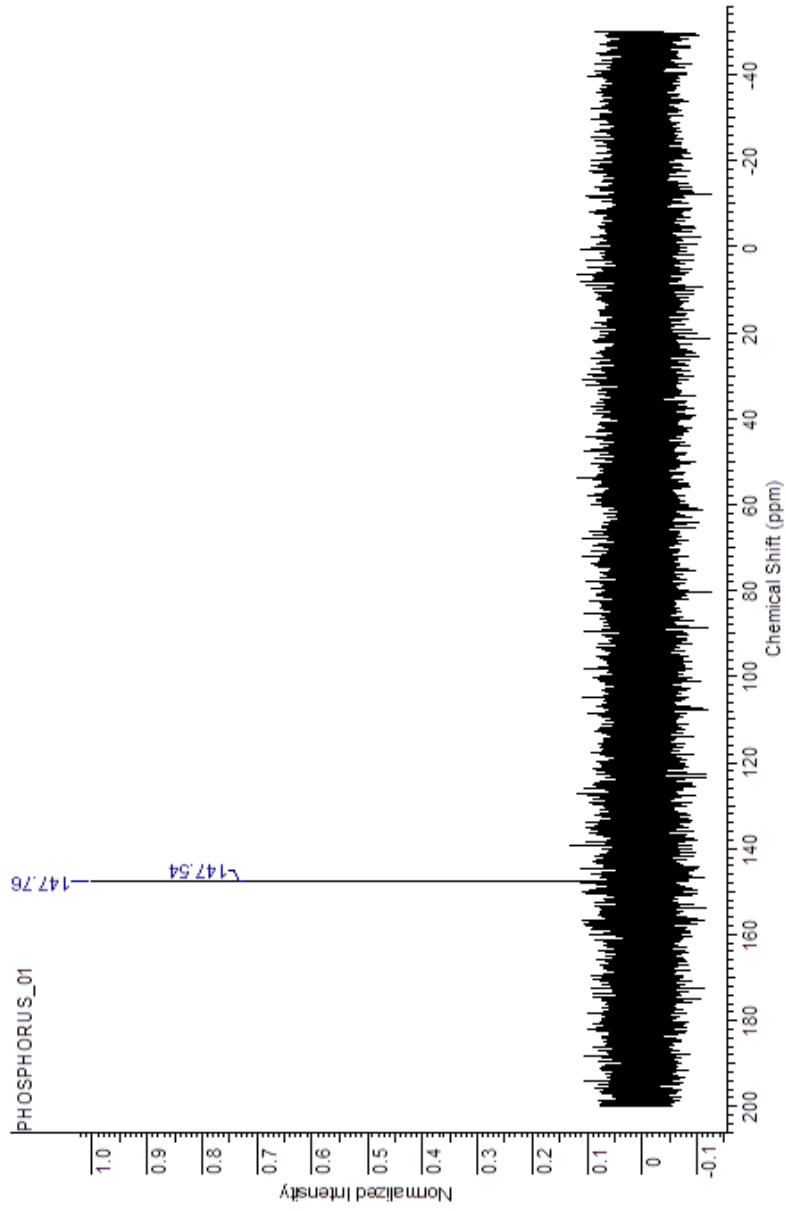
**¹³C NMR 2'-Deoxy-5'-O-(4,4'-dimethoxytrityl)-6-(1-pyrenylethynyl)-pyrrolocytidine
(II-12)**

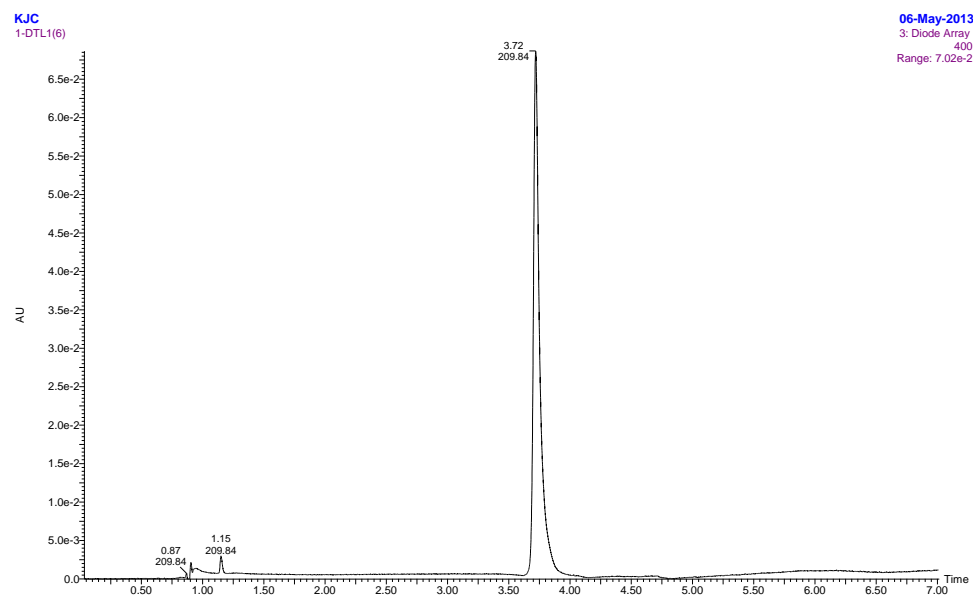
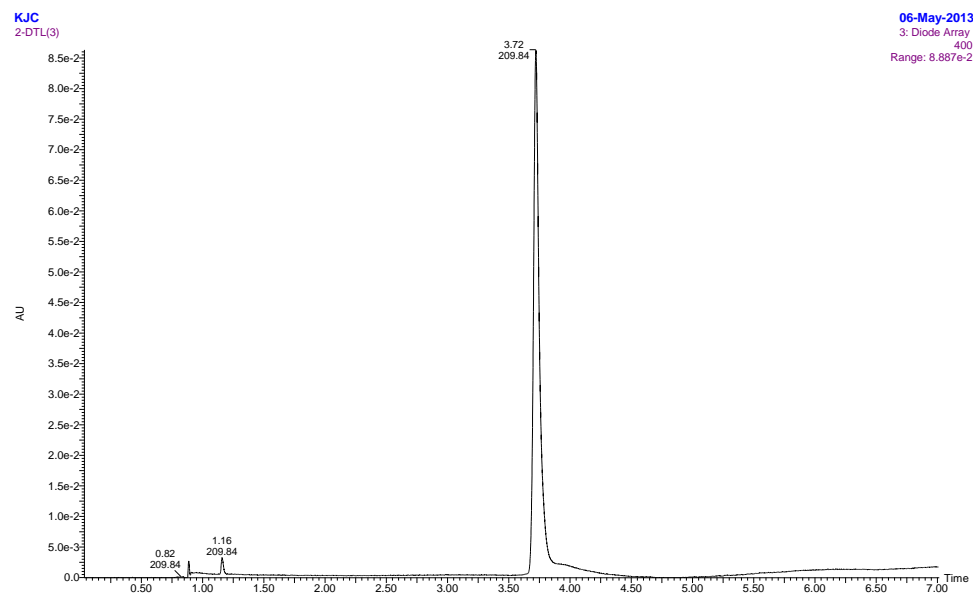


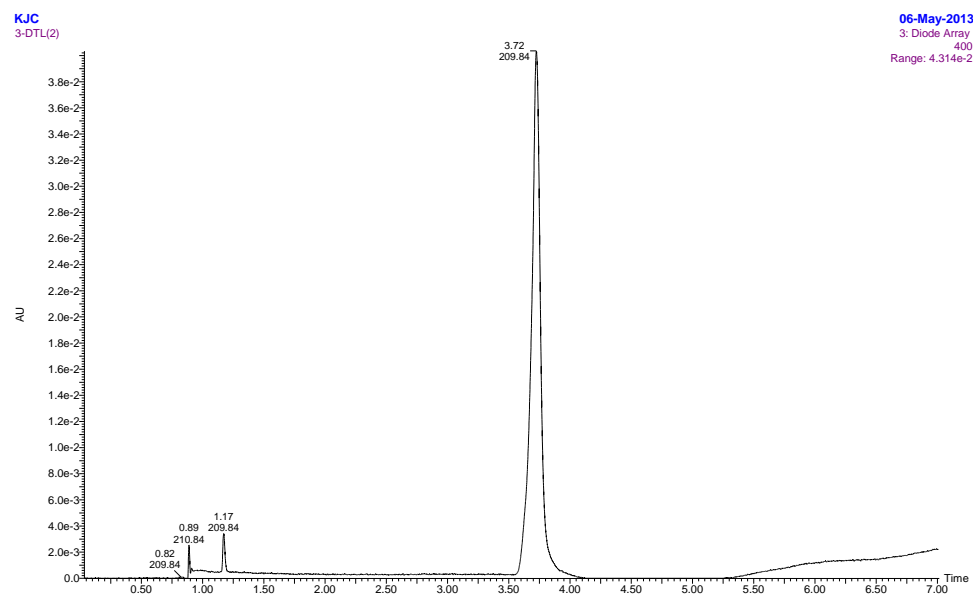
¹H NMR 2'-Deoxy-3'-(2-cyanoethyl)diisopropylphosphoramidite)-5'-O-(4,4'-dimethoxytrityl)-6-(1-pyrenylethynyl)-pyrrolocytidine (II-13)



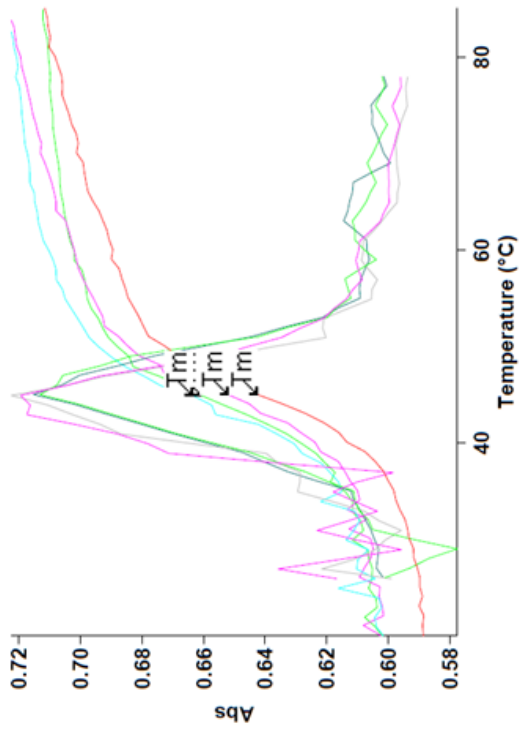
**³¹P NMR 2'-Deoxy-3'-(2-cyanoethyl)diisopropylphosphoramidite)-
5'-O-(4,4'-dimethoxytrityl)-6-(1-pyrenylethynyl)-pyrrolocytidine (II-13)**



(II-14) Mano 1 Mod (5' – GTA GAT PypdC ACT – 3')**(II-15) Mano 2 Mod (5'-GTA GAT C PypdC CT – 3')**

(II-16) CFTR Mod (5'- CTT TCC T PypdC C CAC TGT – 3')

Thermal Denaturation - Control Sequence + Match G



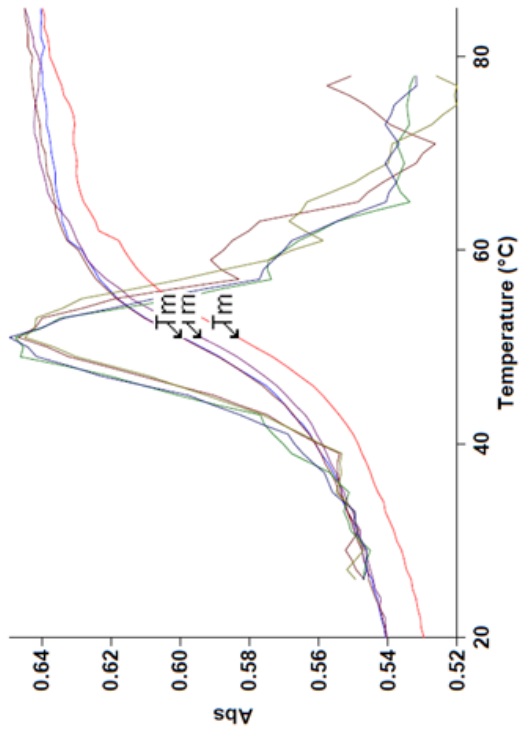
Thermal Tm Results (Derivative Method)

The data was smoothed before calculation
 Smooth Interval 2.00
 Smooth Filter Size 5

Data Name	Tm
C3 20.00-85.00°C Ramp 1	45.02
C3 85.00-20.00°C Ramp 2	44.92
C3 20.00-85.00°C Ramp 3	45.01
C3 85.00-20.00°C Ramp 4	44.92

CFTR Control 5' - CTT TCC TCC CAC TGT - 3'
 Match G 3' - GAA AGG AGG GTG ACA - 5'

Thermal Denaturation – CFTR Mod (II-16) + Match G



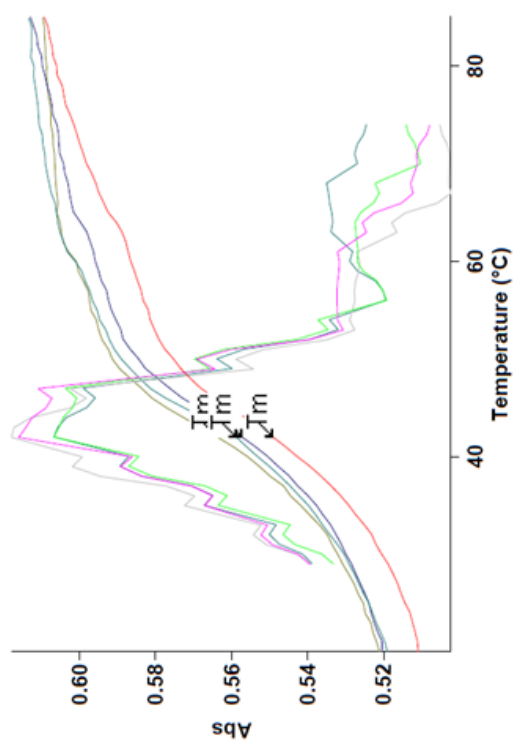
Thermal T_m Results (Derivative Method)

The data was smoothed before calculation
 Smooth Interval 2.00
 Smooth Filter Size 5

Data Name	T _m
m(G) 20.00-85.00°C Ramp 1	51.00
m(G) 85.00-20.00°C Ramp 2	50.99
m(G) 20.00-85.00°C Ramp 3	51.00
m(G) 85.00-20.00°C Ramp 4	51.00

CFTR Mod (II-16) 5' - CTT TCC T**Pypd**CC CAC TGT - 3'
 Match G 3' - GAA AGG A **G** G GTG ACA - 5'

Thermal Denaturation – CFTR Mod (II-16) + Mismatch A



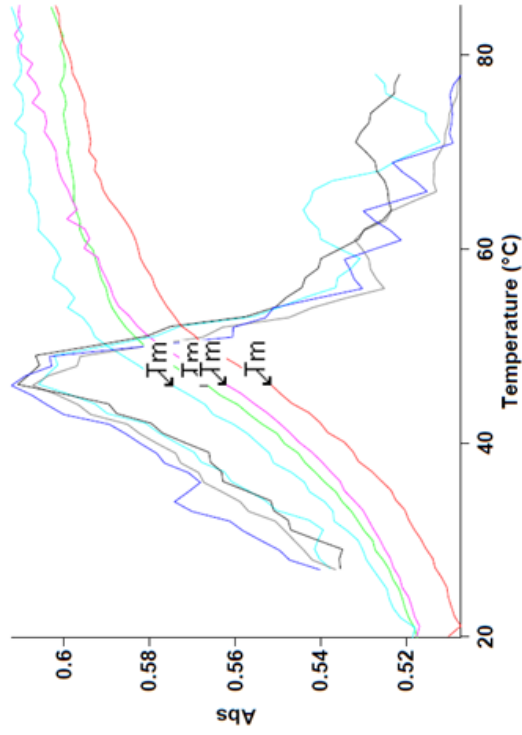
Thermal Tm Results (Derivative Method)

The data was smoothed before calculation
 Smooth Interval 3.50
 Smooth Filter Size 5

Data Name	Tm
A 20.00-85.00°C Ramp 1	42.01
A 85.00-20.00°C Ramp 2	41.96
A 20.00-85.00°C Ramp 3	42.00
A 85.00-20.00°C Ramp 4	41.96

CFTR Mod (II-16) 5' - CTT TCC **TPypdCC** CAC TGT - 3'
 MismatchA 3' - GAA AGG A **A** G GTG ACA - 5'

Thermal Denaturation – CFTR Mod (II-16) + Mismatch C



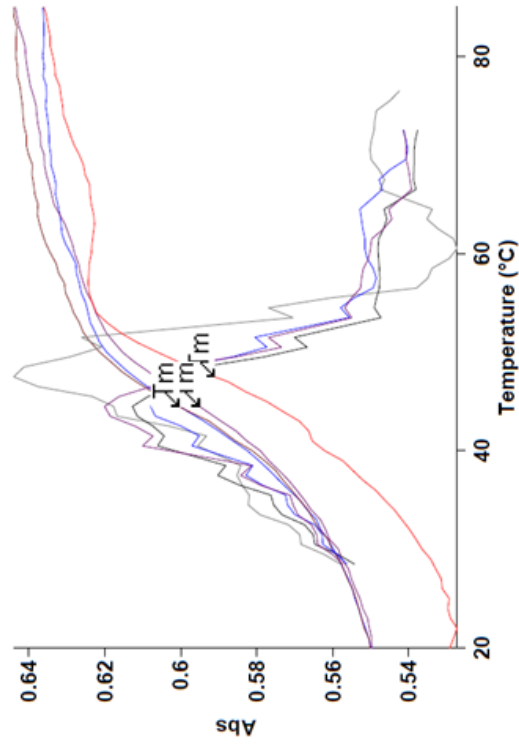
Thermal T_m Results (Derivative Method)

The data was smoothed before calculation
 Smooth Interval 2.50
 Smooth Filter Size 5

Data Name	T _m
C 20.00-85.00°C Ramp 1	46.02
C 85.00-20.00°C Ramp 2	45.92
C 20.00-85.00°C Ramp 3	46.01
C 85.00-20.00°C Ramp 4	45.91

CFTR Mod (II-16) 5' - CTT TCC T**Pypd**CC CAC TGT - 3'
 Mismatch C 3' - GAA AGG A C G GTG ACA - 5'

Thermal Denaturation – CFTR Mod (II-16) + Mismatch T



Thermal T_m Results (Derivative Method)

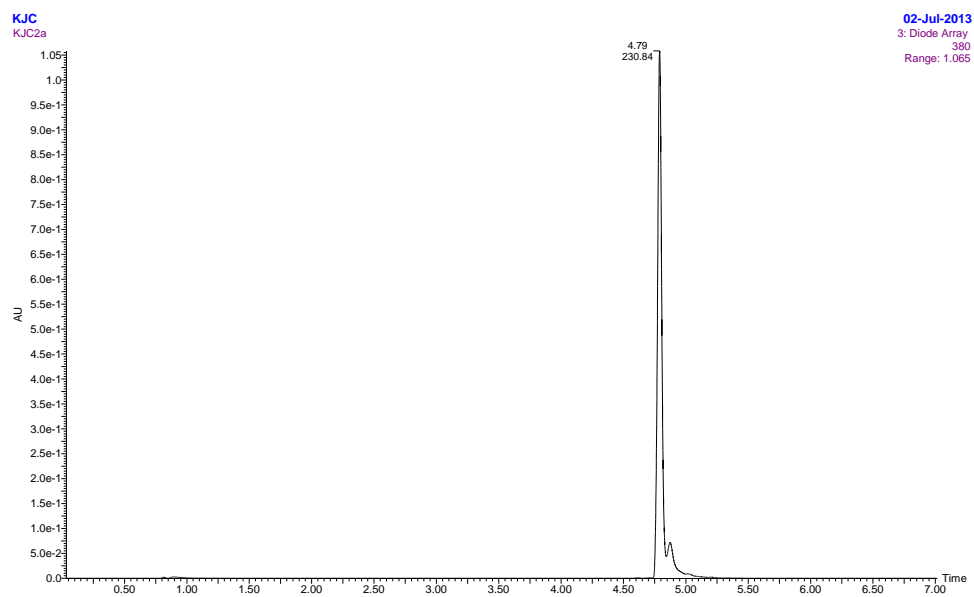
The data was smoothed before calculation
Smooth Interval 3.25
Smooth Filter Size 5

Data Name	T _m
3mmt 20.00-85.00°C Ramp 1	47.50
3mmt 85.00-20.00°C Ramp 2	44.50
3mmt 20.00-85.00°C Ramp 3	44.51
3mmt 85.00-20.00°C Ramp 4	44.49

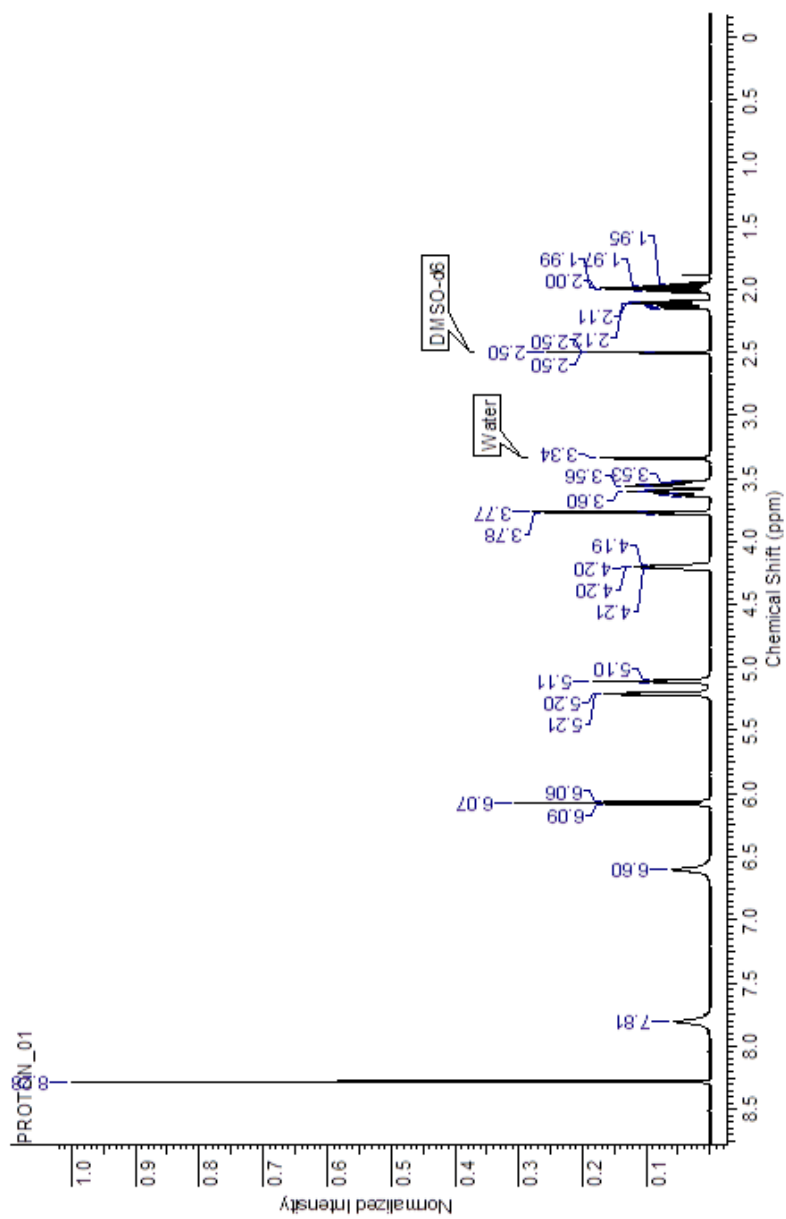
CFTR Mod (II-16) 5' - CTT TCC T**Pypd**CC CAC TGT - 3'

Mismatch T 3' - GAA AGG A **T** G GTG ACA - 5'

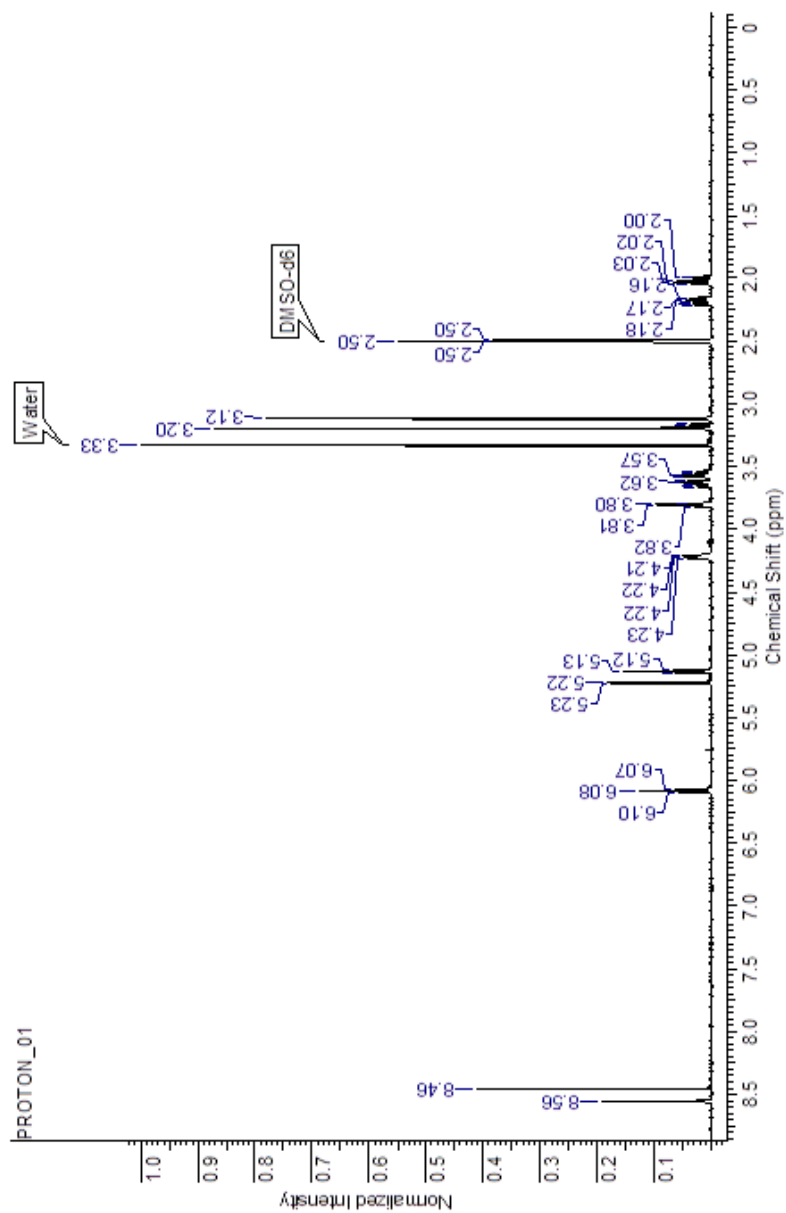
2'-Deoxy-5-(1-pyrenylethynyl)cytidine (III-11)



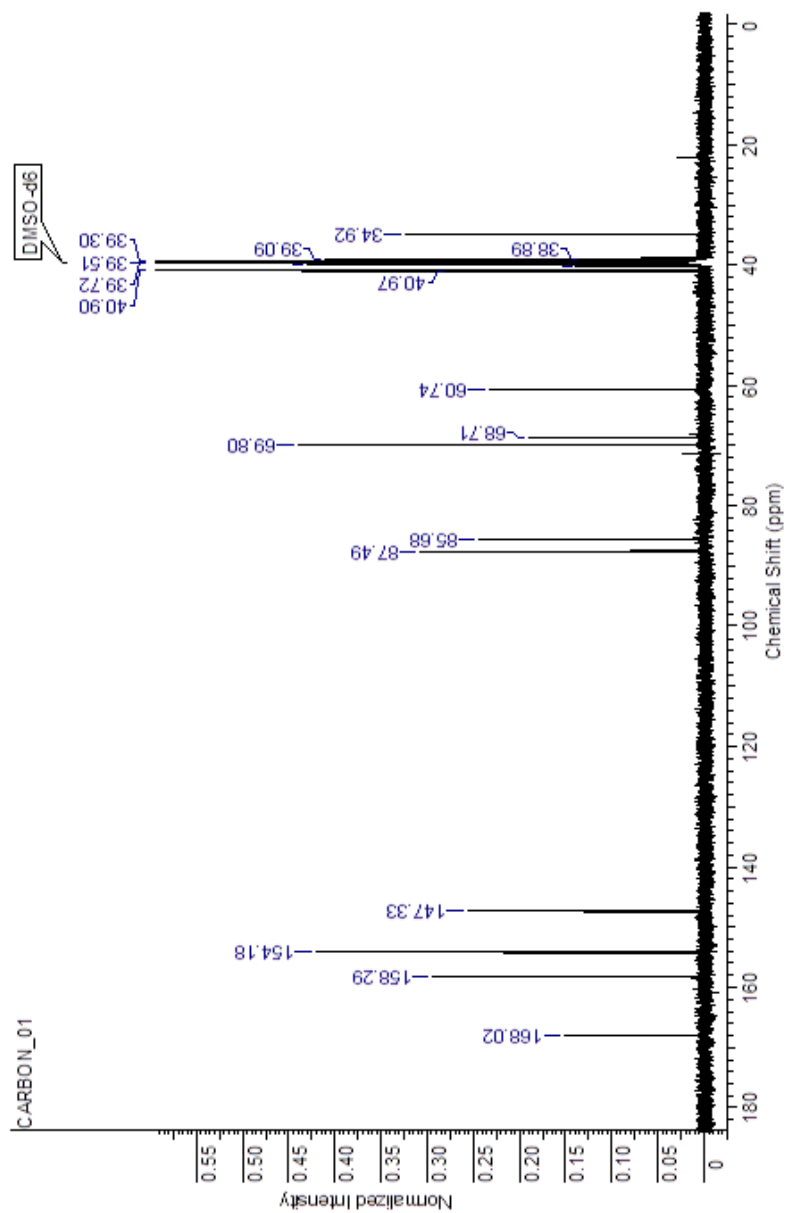
**¹H NMR 2'-Deoxy-5-(1-pyrenylethynyl)-cytidine
(III-11)**



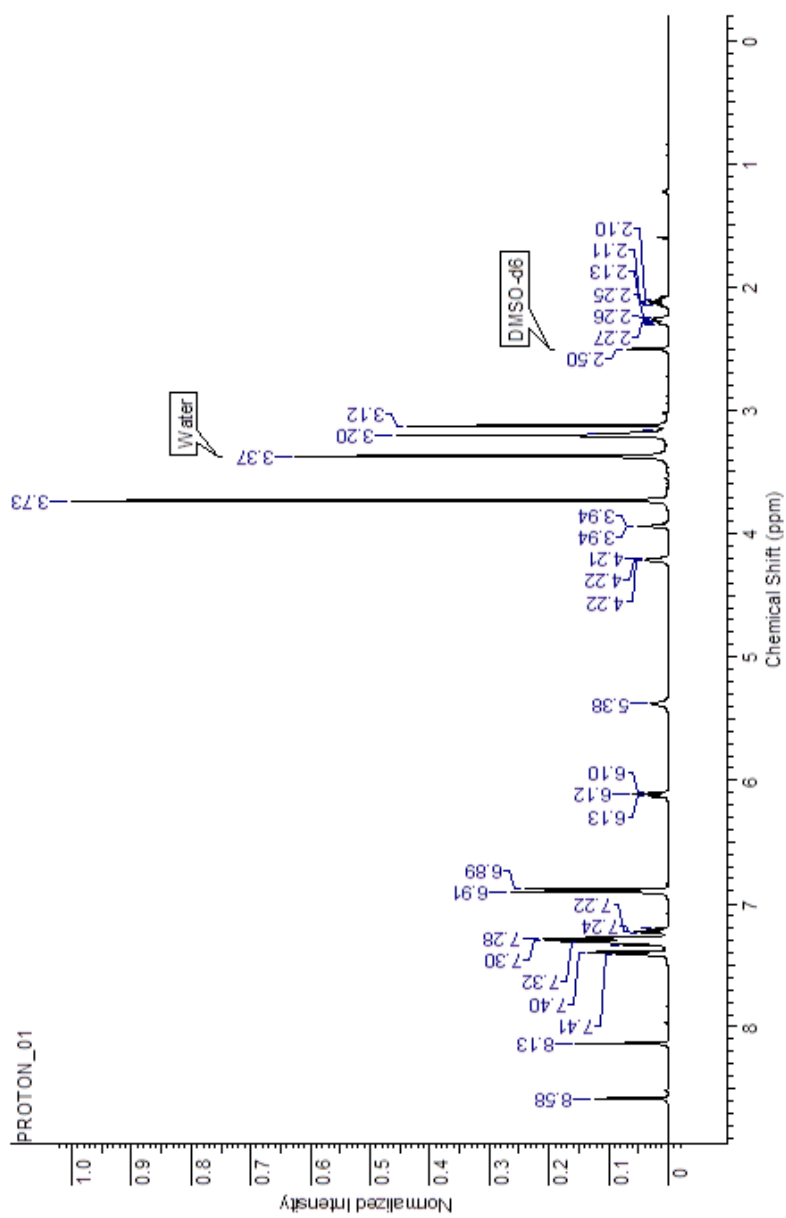
**¹H NMR 2'-Deoxy-N⁴-dimethylformamido-5-iodocytidine
(III-7)**



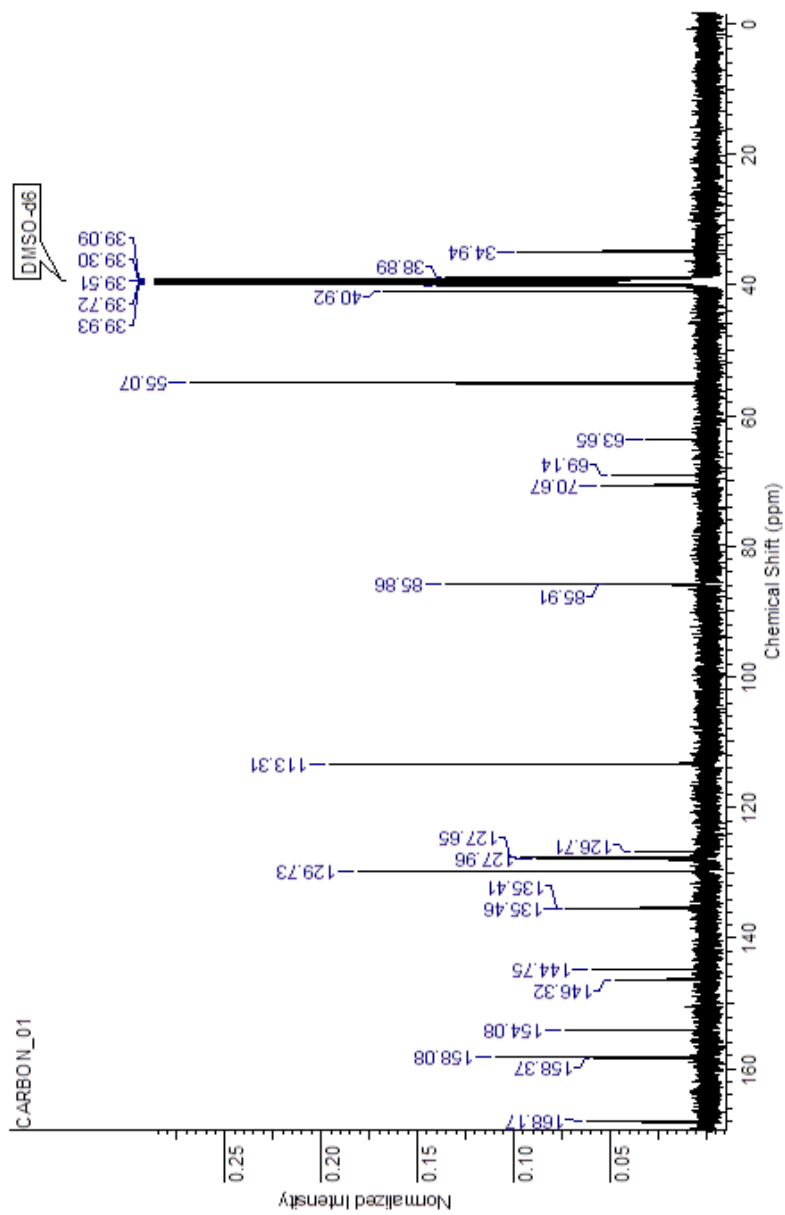
**^{13}C NMR 2'-Deoxy- N^4 -dimethylformamido-5-iodocytidine
(III-7)**



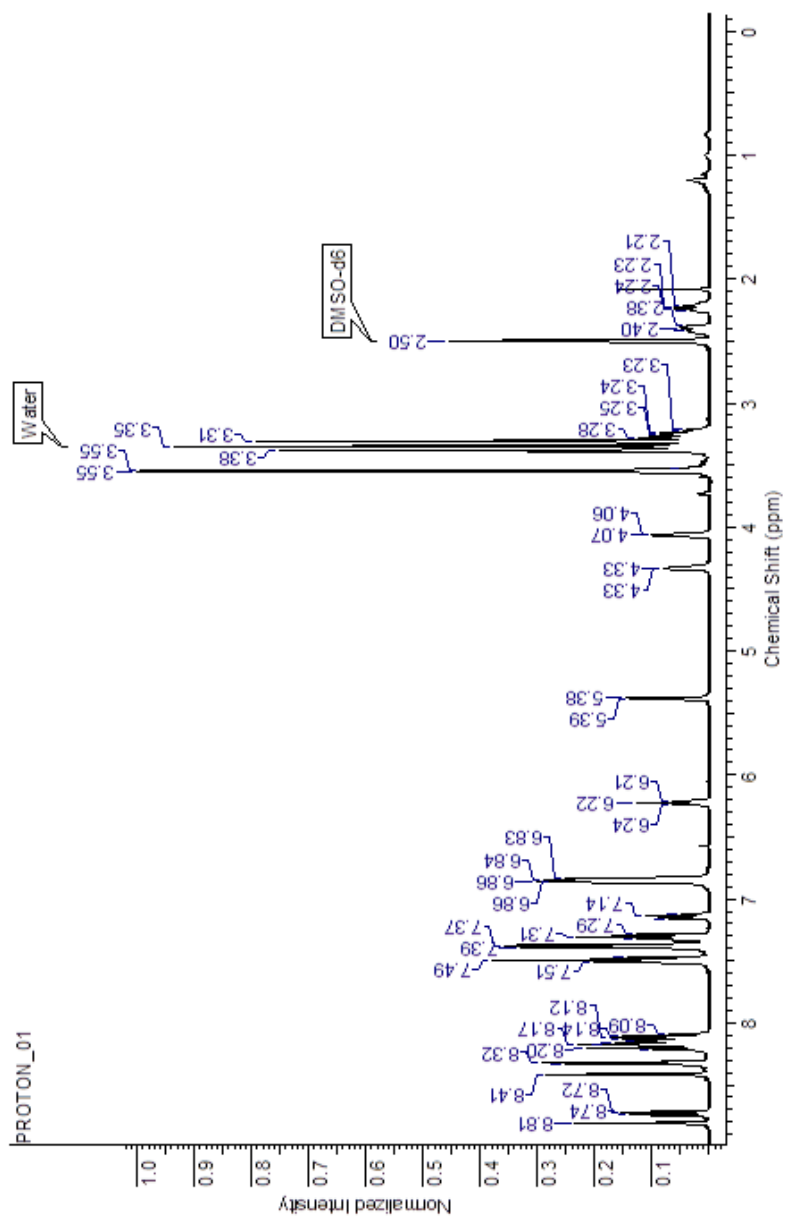
**¹H NMR 2'-Deoxy-5'-O-(4,4'-dimethoxytrityl)-N²-dimethylformamido-5-cytidine
(III-8)**



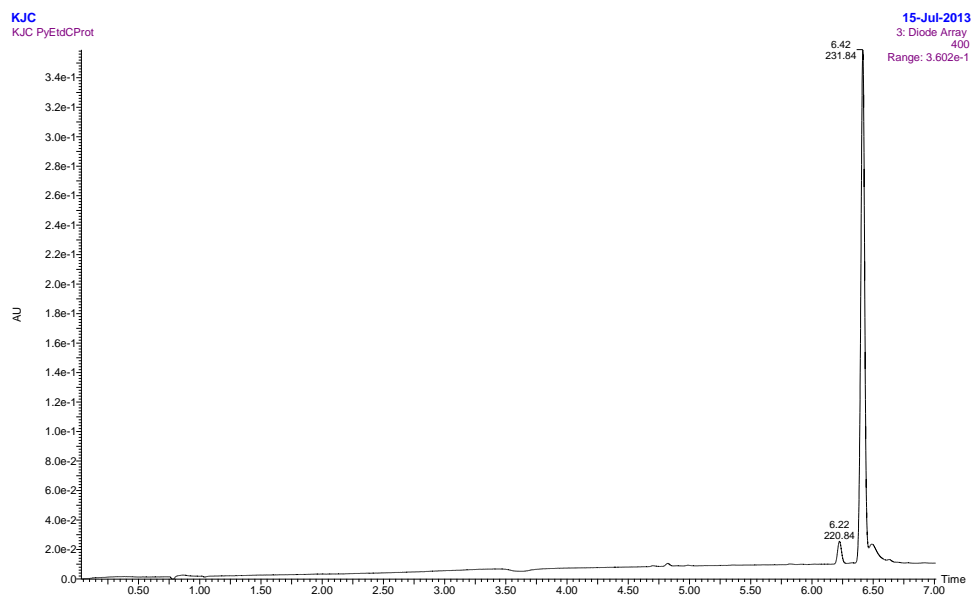
**¹³C NMR 2'-Deoxy-5'-O-(4,4'-dimethoxytrityl)-N^M-dimethylformamido-5-cytidine
(III-8)**



¹H NMR 2'-Deoxy-5'-O-(4,4'-dimethoxytrityl)-N⁴-dimethylformamidino-5-(1-pyrenylethynyl)-cytidine (III-9)



**2'-Deoxy-5'-O-(4,4'-dimethoxytrityl)-N⁴-
dimethylformamidino-5-(1 pyrenylethynyl)-cytidine (III-9)**



Curriculum Vitae

Name: Kirby J. Chicas

Post-secondary Education and Degrees:

2011 – present , M.Sc. Candidate in Chemistry
The University of Western Ontario
London, Ontario, Canada
Supervised by Dr. R.H.E Hudson

2007 – 2011 HBSc., with Specialization in Chemistry
The University of Western Ontario
London, Ontario, Canada
Supervised by Dr. R.H.E Hudson

Honours and Awards:

2013: Western Graduate Research Scholarship

2012: A “best poster” prize XX International Roundtable on Nucleosides Nucleotides
and Nucleic Acids 5-9 August 2012 Québec, Canada

2011: Western Graduate Research Scholarship

2011: University of Western Ontario Dean’s Honour List

2007: Western Scholarship of Distinction

Related Work Experience

2012-2013: Graduate Teaching Assistant

2011-2012: Graduate Teaching Assistant

2011-2012: Mentor for Kelly Firth, Scholars Elective 3303E

2011: Summer Researcher, Supervised by Dr. R.H.E Hudson

2010: Summer Researcher, Supervised by Dr. R.H.E Hudson

Publications:

K. Chicas and R.H.E. Hudson, "Expanding the Nucleic Acid Chemist's Toolbox: New Fluorescent Cytidine Analogues" in *Fluorescent Analogues of Biomolecular Building Blocks: Designs and Applications*, Ed.s. Y. Tor and M. Wilhelmsson, John Wiley and Sons, **2012** (Submitted)

Mark Milne, Kirby Chicas, Alex X Li, Robert Bartha and Robert H.E. Hudson. "ParaCEST MRI contrast agents capable of Derivatization via "click" chemistry" *Org. Biomol. Chem.*, **2012**,10 (2). 287 – 292. DOI: 10 1039/C1OB061622C.